

INFORMATION TO USERS

This manuscript has been reproduced from the microfilm master. UMI films the text directly from the original or copy submitted. Thus, some thesis and dissertation copies are in typewriter face, while others may be from any type of computer printer.

The quality of this reproduction is dependent upon the quality of the copy submitted. Broken or indistinct print, colored or poor quality illustrations and photographs, print bleedthrough, substandard margins, and improper alignment can adversely affect reproduction.

In the unlikely event that the author did not send UMI a complete manuscript and there are missing pages, these will be noted. Also, if unauthorized copyright material had to be removed, a note will indicate the deletion.

Oversize materials (e.g., maps, drawings, charts) are reproduced by sectioning the original, beginning at the upper left-hand corner and continuing from left to right in equal sections with small overlaps.

ProQuest Information and Learning
300 North Zeeb Road, Ann Arbor, MI 48106-1346 USA
800-521-0600

UMI[®]

University of Alberta

Sulfur Concrete Haul Roads at SUNCOR Oil Sands Mines

by

Dawit Gebremeskel Abraha



A thesis submitted to the Faculty of Graduate Studies and Research in partial fulfillment of the requirements for the degree of *Master of Science*

in

Geotechnical Engineering

Department of Civil and Environmental Engineering

Edmonton, Alberta

Spring 2005



Library and
Archives Canada

Bibliothèque et
Archives Canada

0-494-08018-3

Published Heritage
Branch

Direction du
Patrimoine de l'édition

395 Wellington Street
Ottawa ON K1A 0N4
Canada

395, rue Wellington
Ottawa ON K1A 0N4
Canada

Your file *Votre référence*

ISBN:

Our file *Notre référence*

ISBN:

NOTICE:

The author has granted a non-exclusive license allowing Library and Archives Canada to reproduce, publish, archive, preserve, conserve, communicate to the public by telecommunication or on the Internet, loan, distribute and sell theses worldwide, for commercial or non-commercial purposes, in microform, paper, electronic and/or any other formats.

The author retains copyright ownership and moral rights in this thesis. Neither the thesis nor substantial extracts from it may be printed or otherwise reproduced without the author's permission.

AVIS:

L'auteur a accordé une licence non exclusive permettant à la Bibliothèque et Archives Canada de reproduire, publier, archiver, sauvegarder, conserver, transmettre au public par télécommunication ou par l'Internet, prêter, distribuer et vendre des thèses partout dans le monde, à des fins commerciales ou autres, sur support microforme, papier, électronique et/ou autres formats.

L'auteur conserve la propriété du droit d'auteur et des droits moraux qui protègent cette thèse. Ni la thèse ni des extraits substantiels de celle-ci ne doivent être imprimés ou autrement reproduits sans son autorisation.

In compliance with the Canadian Privacy Act some supporting forms may have been removed from this thesis.

Conformément à la loi canadienne sur la protection de la vie privée, quelques formulaires secondaires ont été enlevés de cette thèse.

While these forms may be included in the document page count, their removal does not represent any loss of content from the thesis.

Bien que ces formulaires aient inclus dans la pagination, il n'y aura aucun contenu manquant.


Canada

ABSTRACT

Feasibility of constructing mine haul roads at the oil sands mines using concrete prepared from by-products and mine wastes of the oils sands industry (sulfur, fly ash, coke and tailing sand) is evaluated.

An extensive laboratory test program including unconfined compression, split tensile and freeze thaw durability tests were carried out to characterize the physical and mechanical properties of different mix designs of sulfur concrete. A study of the geochemical interaction of sulfur concrete with the near surface environment included: short term interaction of surface exposed sulfur concrete during the construction and operational life of the haul road and long term interaction of sulfur concrete with ground water following its burial with mine wastes in the mined-out pits.

Haul road test sections were designed based on critical strain and resilient modulus design method. Stress and strain distributions in the haul road cross section induced by the truck tires were calculated using finite element analysis. Required pavement layer thicknesses were then determined on the basis of the truck loads and the resilient modulus and strength of the sulfur concrete and sub-grade material using the critical strain and resilient modulus design method.

ACKNOWLEDGEMENT

The research reported in this thesis was carried out at the University of Alberta under the auspices of Department of Civil and Environmental Engineering. SUNCOR Oil Sands Inc. provided necessary funding for the research. Bursaries and partial teaching assistantships were provided by the University of Alberta and Department of Civil and Environmental Engineering.

I would like to thank my supervisors Dr. David C. Segó and Dr. Robert Donahue for giving me the opportunity to work with you and for your invaluable inspiration and direction throughout the development of this thesis.

Many professors in the Department of Civil & Environmental Engineering contributed to this thesis with advice and moral support. I would particularly like to thank Dr. K. W. Biggar, Dr. H. R. Soleymani and Dr. T. Joseph.

I would like to thank Mrs. Christine Hereygers and Mr. Steve Gamble for their constant support and guidance during the laboratory work. Thanks all fellow students for your advice and moral support.

I wish to express my sincere appreciation for all the help received throughout my stay at the University of Alberta.

Finally, thanks Almighty God for making my dream a reality.

TABLE OF CONTENTS

1	INTRODUCTION	1
1.1	Objective.....	2
1.2	Scope	3
1.3	Thesis Structure.....	3
2	LITERATURE REVIEW	5
2.1	Sulfur and Sulfur Concrete	5
2.1.1	<i>Research on sulfur and sulfur concrete</i>	<i>6</i>
2.1.2	<i>Sulfur concrete mix proportions</i>	<i>9</i>
2.1.3	<i>Advantages and concerns with sulfur concrete.....</i>	<i>10</i>
2.1.4	<i>Modified sulfur cement.....</i>	<i>11</i>
2.2	Characteristics of Sulfur Concrete	14
2.2.1	<i>Compressive strength.....</i>	<i>14</i>
2.2.2	<i>Stress-strain relationships</i>	<i>16</i>
2.2.3	<i>Freeze-thaw durability.....</i>	<i>17</i>
2.2.4	<i>Fatigue behavior</i>	<i>21</i>
2.2.5	<i>The effect of water under constant temperature</i>	<i>22</i>
2.2.6	<i>Creep.....</i>	<i>23</i>
2.2.7	<i>Corrosion resistance</i>	<i>23</i>
2.2.8	<i>Resistance to fire and ultra violet rays.....</i>	<i>25</i>

2.2.9	<i>Resistance to biological attack</i>	25
2.2.10	<i>Recycling</i>	26
2.3	Environmental and Safety Aspects in the Use of Sulfur in Highway Pavements	27
2.3.1	<i>Mix preparation and construction</i>	27
2.3.1.1	Use of sulfur in construction	27
2.3.1.2	Toxicity of sulfur initiated pollutants	28
2.3.1.2.1	<i>Hydrogen sulfide (H₂S)</i>	28
2.3.1.2.2	<i>Sulfur dioxide (SO₂)</i>	29
2.3.1.2.3	<i>Elemental Sulfur</i>	29
2.3.1.3	Conclusions of Phase 1 study (Saylak et al., 1981)	30
2.3.2	<i>Post construction exposure</i>	30
2.3.2.1	Weathering studies	31
2.3.2.2	Simulated in service conditions	32
2.3.2.2.1	<i>Temperature, actinic light and run-off effects</i>	32
2.3.2.2.2	<i>Freeze-thaw</i>	32
2.3.2.2.3	<i>Chemical weathering</i>	32
2.3.2.2.4	<i>Biological weathering</i>	33
2.3.2.2.5	<i>Simulated traffic effects</i>	33
2.3.2.2.6	<i>Simulated fire test</i>	34

2.3.2.3	Conclusions of phase 2 study (Deuel and Saylak, 1981)	34
2.4	Batching, Transporting, Placing and Finishing of Sulfur Concrete.	34
2.4.1	<i>Floor construction</i>	36
3	LABORATORY TESTS	38
3.1	Materials and Proportion	39
3.1.1	<i>Oil sands processes</i>	40
3.1.2	<i>Sulfur</i>	41
3.1.3	<i>Tailing sand</i>	42
3.1.4	<i>Coke</i>	42
3.1.5	<i>Fly ash</i>	43
3.1.6	<i>Sulfur and aggregates proportions</i>	44
3.2	Test Specimen Preparation and Measurement	44
3.2.1	<i>Sample preparation procedure</i>	46
3.2.2	<i>Measurements of specimen dimensions and unit weight.</i>	47
3.3	Uni-axial Compression Test	48
3.3.1	<i>Test procedure and equipments</i>	49
3.3.2	<i>Test results</i>	50
3.4	Sonic Velocity Measurement	55
3.4.1	<i>Test equipment and specimen</i>	56
3.4.1.1	Sonic pulse generator	56

3.4.1.2	Pulsing and sensing heads	57
3.4.1.3	Test specimens.....	57
3.4.2	<i>Test procedure</i>	57
3.4.3	<i>Test results</i>	59
3.5	Optimum Mix Designs	60
3.6	Split Tensile Test.....	61
3.6.1	<i>Test procedure and equipments</i>	61
3.6.2	<i>Test results</i>	63
3.7	Freeze Thaw Durability Test.....	63
3.7.1	<i>Test procedure and equipments</i>	64
3.7.2	<i>Test results</i>	68
3.8	Geochemical Investigation.....	70
3.8.1	<i>Potential geo-environmental impact associated with sulfur concrete haul roads</i>	70
3.8.2	<i>pH and electrical conductivity (EC) measurement</i>	71
3.8.2.1	pH	71
3.8.2.2	Electrical conductivity.....	71
3.8.2.3	Test equipment	72
3.8.3	<i>Geo-chemical interaction studies</i>	73
3.8.3.1	Sulfur concrete weathering tests.....	73
3.8.3.2	Long term geochemical stability of sulfur concrete mixtures	75

4	HAUL ROAD CROSS-SECTION DESIGN.....	80
4.1	Geometrical Cross Section Design Parameters	80
4.1.1	<i>Road width.....</i>	<i>80</i>
4.1.2	<i>Safety berm, side ditch and cross slope.....</i>	<i>81</i>
4.2	Structural Design of Haul Road Cross-Section	82
4.2.1	<i>Haul road construction materials</i>	<i>84</i>
4.2.1.1	Surface course materials.....	85
4.2.1.1.1	<i>Compacted gravel and crushed rock</i>	<i>87</i>
4.2.2	<i>Cross section design.....</i>	<i>90</i>
4.2.2.1	Cross-section design based on critical strain and resilient modulus	92
4.2.2.1.1	<i>Tire pressure and foot print area.....</i>	<i>93</i>
4.2.2.1.2	<i>Design procedure.....</i>	<i>95</i>
4.2.2.1.3	<i>Critical strain limit</i>	<i>97</i>
4.2.2.1.4	<i>Resilient modulus test</i>	<i>98</i>
4.2.2.1.5	<i>Finite element analysis</i>	<i>100</i>
5	CONCLUSION AND RECOMMENDATION.....	110
5.1	Summary of Findings	110
5.2	Recommendations.....	113
5.2.1	<i>Sample preparation.....</i>	<i>113</i>
5.2.2	<i>Sulfur concrete placement during construction.....</i>	<i>113</i>

5.2.3	<i>Geochemical interaction studies</i>	113
5.2.4	<i>Future work</i>	114
	REFERENCES	115
	APPENDIX A LABORATORY TEST RESULTS	123
	APPENDIX B LABORATORY TEST PROCEDURES	140

LIST OF TABLES

Table 2.1 Some properties of elemental sulfur	5
Table 2.2 Compositions of modified sulfur cements used in North America, taken from ACI 548.2R (1988).....	13
Table 2.3 Range of physical and mechanical properties of sulfur concrete after Raymont (1978).....	15
Table 2.4 Chemical resistance at room temperature, after Crick and Whitmore (1998)	24
Table 2.5 Effect of Thiobacillus thiooxidans on sulfur concrete, modified from Laishly and Tyler (1978), (1 psi = 6.895 kPa).....	26
Table 2.6 Strength of original and recycled sulfur concrete, Lee et al. (1978) (1 psi = 6.895 kPa)	27
Table 2.7 Effects of H₂S on humans, after Saylak et al. (1981).....	28
Table 2.8 Effects of SO₂ on humans, after Saylak et al. (1981).....	29
Table 3.1 Sulfur and aggregate proportions.....	44
Table 3.2 Unit weight statistics of the mix designs.....	48
Table 3.3 Peak strength statistical data.....	54
Table 3.4 Young's modulus statistical data	54
Table 3.5 Summary of the sonic velocity measurement test.....	59
Table 3.6 Split tensile test summary	63
Table 3.7 Rapid freeze-thaw test summary	69
Table 3.8 Weathering test results.....	75
Table 4.1 Strength and deformation properties of road building materials ...	84
Table 4.2 Advantages and disadvantages of various road surface materials (after Monenco 1989).....	86
Table 4.3 Grading requirements for soil aggregate materials for surface course (after AASHTO 1993a).....	88
Table 4.4 Recommended grading for granular surface course (Monenco 1989)	88

Table 4.5 Recommended material properties for a haul road surface material (after Thompson & Visser 2000)	89
Table 4.6 Michelin radial tire specifications (after Doyle, 1999)	95
Table A-1 Density of sulfur concrete mixes	124
Table A-2 Peak compressive strength of sulfur concrete mixes.....	131
Table A-3 Young's modulus of sulfur concrete mixes	132
Table A-4 Sonic velocity measurement results	133
Table A-5 Split tensile test results.....	134
Table A-6 Sulfur concrete porosity calculation	139

LIST OF FIGURES

Figure 3.1 SUNCOR tailing sand grain size curve.....	42
Figure 3.2 SUNCOR coke grain size curve	43
Figure 3.3 Compression test set up	49
Figure 3.4 Stress-strain curves of coke and sulfur mixes	51
Figure 3.5 Stress-strain curves of coke, sulfur, and 2.3 to 4.6 % fly ash mixes.....	52
Figure 3.6 Stress-strain curves of coke, sulfur, and 10 to 33.3% fly ash mixes.....	52
Figure 3.7 Stress-strain curve of tailing sand, sulfur, and fly ash mix.....	53
Figure 3.8 Sonic velocity measurement test set up.....	58
Figure 3.9 Stress-strain curves of optimum mix design samples	61
Figure 3.10 Split tensile test set up	63
Figure 3.11 Sand sulfur concrete specimens during thawing in water	67
Figure 3.12 Construction joint on 35S2.3FA62.7C sample	68
Figure 3.13 30S2.3FA67.7C sample failed after 24 cycles	68
Figure 3.14 Effect of freeze thaw cycle on peak strength, yield strength and Young's modulus.....	69
Figure 3.15 Weathering test set up	74
Figure 3.16 pH vs. time for DI water overlaid samples	77
Figure 3.17 EC vs. time for DI water overlaid samples	77
Figure 3.18 pH vs. time for CT recycled water overlaid samples.....	78
Figure 3.19 EC vs. time for CT recycled water overlaid samples.....	78
Figure 4.1 Optimal and sub-optimal range of values for the shrinkage product and grading coefficient for a granular surface course material (after Thompson & Visser 2000)	90
Figure 4.2 Method to obtain resilient modulus (after Bowles 1984).....	93
Figure 4.3 Major steps of the resilient modulus haul road design method (modified from Kumar 2000).....	96

Figure 4.4 Cyclic stress vs. time plot.....	99
Figure 4.5 Axial deformation vs. time plot.....	100
Figure 4.6 Typical axisymmetric model used in a Sigma/W analysis.....	102
Figure 4.7 Schematic diagram for positions of tires on back axle of CAT 797 haul truck.....	103
Figure 4.8 Vertical strains beneath single tire (in micro-strain) using E = 9750 MPa	105
Figure 4.9 Vertical strains beneath two adjacent tires (in micro-strain) using E = 9750 MPa	105
Figure 4.10 Vertical strains beneath four rear tires (in micro-strain) using E = 9750 MPa	106
Figure 4.11 Vertical stress distribution beneath four rear tires (in kPa) using E = 9750 MPa	106
Figure 4.12 Vertical strains beneath single tire (in micro-strain) using E = 3925 MPa	107
Figure 4.13 Vertical strains beneath two adjacent tires (in micro-strain) using E = 3925 MPa	108
Figure 4.14 Vertical strains beneath four rear tires (in micro-strain) using E = 3925 MPa	108
Figure 4.15 Vertical stress distribution beneath four rear tires (in kPa) using E = 3925 MPa	109
Figure A-1 30S70C stress-strain curve.....	125
Figure A-2 35S65C stress-strain curve.....	125
Figure A-3 40S60C stress-strain curve.....	126
Figure A-4 30S2.3FA67.7C stress-strain curve	126
Figure A-5 30S4.6FA65.4C stress-strain curve	127
Figure A-6 35S2.3FA62.7C stress-strain curve	127
Figure A-7 35S4.6FA60.4C stress-strain curve	128
Figure A-8 30S20FA50C stress-strain curve	128
Figure A-9 40S10FA50C stress-strain curve	129

Figure A-10 33.3S33.3FA33.3C stress-strain curve	129
Figure A-11 30S2.3FA67.7C stress-strain curve	130
Figure A-12 30S2.3FA67.7C tensile stress-vertical strain curve.....	134
Figure A-13 35S2.3FA62.7C tensile stress-vertical strain curve.....	135
Figure A-14 30S2.3FA67.7Sa tensile stress-vertical strain curve	135
Figure A-15 Compressive stress-strain curve of original sample (0 freeze- thaw cycle)	136
Figure A-16 Compressive stress-strain curve after 50 freeze-thaw cycles	136
Figure A-17 Compressive stress-strain curve after 100 freeze-thaw cycles	137
Figure A-18 Compressive stress-strain curve after 200 freeze-thaw cycles	137
Figure A-19 Compressive stress-strain curve after 300 freeze-thaw cycles	138

1 INTRODUCTION

The mining of oil sands in the Fort McMurray area of Northern Alberta is a significant part of Alberta's economy. Over the last 20 years, mining methods have evolved from bucket wheel and dragline excavators to shovel and truck operation. Transportation of overburden and oil sands ore is one of the critical mining operations in the shovel and truck mining method. Mine productivity mainly depends on the performance of the haul trucks, which in turn are highly dependent on the quality of the haul roads they travel on. Thus one of the key elements of the shovel and truck mining method is the haul road.

Economics of scale and expansion of the mining activity has led to the use of ultra large mining trucks with a payload capacity of more than 320 tons. The gross vehicular weight of these trucks reaches about 550 tons and they are expected to be even larger in the near future. Efficient utilization of these ultra large haul trucks demands the construction of well-designed haul roads. Presently used empirical design methods and designs based on past experience have been proven to be inadequate for these large haul trucks. A good haul road ensures low vehicle operating and maintenance costs, low road maintenance cost, and reduced truck cycle time and full loading of trucks to maximize productivity.

Presently the haul roads at SUNCOR are constructed using crushed limestone, gravel, lean oil sand, sandy till and clayey till (Kumar V., 2001). These roads severely deteriorate during summer months due to material softening. Haul road performances have been below the desired standard and are having a negative impact on mine productivity. In addition, the use of these low strength and low stiffness construction materials require road sections to be built with thick layers of gravel to sustain the very large truck loads. Handling of these large construction volumes by itself is costly. Moreover the good construction materials available at the site, limestone and gravel, will become scarce over the next few years. All these highlight the necessity to find an

alternative road construction material, which can overcome the constraints and provide smooth rut free riding surface to ensure an efficient mining operation.

Sulfur concrete is a relatively new construction material being used in the construction of civil works. It is a thermoplastic material prepared by hot mixing sulfur cements and mineral aggregates. Upon cooling it solidifies and gains its strength rapidly. At SUNCOR Oil Sands mines there are abundant supplies of materials such as sulfur, coke, fly ash and tailing sand, which are by-products and wastes of the oil sands extraction and upgrading processes. Sulfur concrete produced from these wastes can be a potential construction material for the mine haul roads. The sulfur concrete produced from these waste materials will have superior physical performance when compared to the existing road building materials. Thus haul roads can be built with reduced pavement thickness compared to the existing haul roads built using compacted gravel and/or crushed limestone.

Apart from the benefits associated with building high quality haul roads which enhances mine productivity, utilization of these waste products reduces the need for onsite waste storage or costly offsite transport or disposal of the waste products. Also it may reduce the greenhouse gas emissions associated with the offsite truck and rail delivery of the sulfur to distant customers. The use of sulfur concrete as a road construction material will also reduce the use of the diminishing aggregate supply near the SUNCOR Oil Sands mines.

1.1 Objective

The purpose of this research is to evaluate the technical feasibility of construction of mine haul roads using sulfur concrete prepared from the mine wastes (sulfur, coke, fly ash and tailing sand), as the mine wastes are readily available at SUNCOR Oil Sands mines. The use of sulfur concrete to build the haul roads may provide an economic and environmental solution to the mine operation and mine waste disposal.

1.2 Scope

The construction of mine haul roads using sulfur concrete requires an understanding of the physical, mechanical and chemical properties of the material. An extensive laboratory testing program consisting of unconfined compression test, sonic velocity measurement, split tensile test and freeze-thaw durability test was carried out to characterize the strength properties and deformation characteristics of different mix designs of sulfur concrete prepared from oil sands mine by-products and mine wastes such as sulfur, fly ash, coke and tailing sand. The potential geochemical interactions of sulfur concrete with the near surface environment were also studied in the laboratory for its use as road building material.

Based on the laboratory test results, optimum mix designs were selected and preliminary design evaluation of a haul road test section was carried out.

1.3 Thesis Structure

In chapter 1, general background information is provided on the mining methods, existing condition of mine haul roads and haul road construction materials at SUNCOR Oil Sands mines in Fort McMurray. The objective of the thesis and the scope of the thesis required to achieve its objectives are also summarized in this section.

In chapter 2, an extensive literature review of sulfur and sulfur concrete is presented. The basic chemistry of sulfur is presented. The characteristics of sulfur concrete and its developments are also addressed. Environmental and safety aspects in the use of sulfur in highway pavements are addressed.

In chapter 3, the laboratory tests performed in order to characterize the physical, mechanical and chemical properties of different mix designs of sulfur concrete for

their use in haul road construction are addressed. Results of all the tests conducted are presented.

In chapter 4, preliminary haul road test section design using critical strain and resilient modulus method is presented. The material properties obtained in chapter 3 coupled with results of resilient modulus test carried out in the laboratory were used in modeling the sulfur concrete haul road cross section. Finite element analysis of stress and strain distributions in haul road cross section imposed by the truck tires was evaluated using Sigma/W finite element program.

In chapter 5, summary of findings and recommendations related to the use of sulfur concrete in haul road construction and its impact on the environment are provided. Topics for further research are identified and discussed.

2 LITERATURE REVIEW

2.1 Sulfur and Sulfur Concrete

Pure solid sulfur is a tasteless, odorless, brittle solid that is pale yellow in color, and a poor conductor of electricity. It weighs between 2000 and 2100 kg/m³. At normal temperatures, it has an orthorhombic crystalline structure, upon heating it inverts slowly at 96⁰C to a monoclinic less dense allotrope which melts at about 119⁰C. When hot molten sulfur is cooled suddenly (as by pouring it into cold water), it forms a soft, sticky, elastic, non-crystalline mass called amorphous or plastic sulfur. The liquid ranges in color from transparent straw yellow to dark reddish brown depending on its temperature, and its viscosity changes markedly, particularly above 159⁰C. Some sulfur properties summarized by Malhotra (1979) are presented in Table 2.1.

Viscosity	@ 120 ⁰ C	11.8 x 10 ⁻³ Pa.S
	@ 159 ⁰ C	6.6 x 10 ⁻³ Pa.S
	@ 188 ⁰ C	100 Pa.S
Specific gravity	of solid	1.96 – 2.07
	of liquid @ 120 ⁰ C	1.80
Compressive strength	on 75 x 150 mm cylinders	28 MPa
Thermal coefficient of expansion	@ 25 ⁰ C	74 x 10 ⁻⁶ / ⁰ C

Table 2.1 Some properties of elemental sulfur

Sulfur concrete is a relatively new material, and although similar in final appearance to Portland cement concrete, its manufacture, handling, use, and testing is different. Sulfur concrete is a thermoplastic material prepared by hot-mixing sulfur cements and mineral aggregates. Sulfur concrete solidifies and gains strength rapidly after cooling. As with other concrete materials, such as Portland cement and asphalt concrete, sulfur concrete is a generic term for a range of products that vary with aggregates, sulfur cements and proportions used. By using sulfur cement binders and aggregates that are

not attacked by many mineral acid and salt solutions, high strength corrosion resistant sulfur concrete can be produced for use in certain applications where other construction material deteriorate rapidly. Sulfur concretes are generally not resistant to alkalis or oxidizers but exhibit excellent performance in many acidic and salt environments (ACI 548.2R, 1988).

Early sulfur concrete products, prepared with unmodified sulfur as binder, were plagued with durability problems. While materials with excellent mechanical properties were produced, in actual use they deteriorated and failed after a relatively short period of time. The development of modified sulfur cements, however, increased the durability of sulfur concrete and made its use as construction material more feasible. When modified sulfur cement is used as a binding agent with appropriate aggregates, the resulting sulfur concrete has shown some unique properties such as: high strength and fatigue resistance, excellent corrosion resistance against most acids and salts, and extremely rapid set and strength gain (ACI 548.2R, 1988).

2.1.1 Research on sulfur and sulfur concrete

Antoine Lavoisier first classified sulfur as an element in 1777. It is estimated to be the ninth most abundant element in the universe. In the form of sulfides, sulfates, and elemental sulfur, the element constitutes about 0.03 percent of the earth's crust. After oxygen and silicon, it is the most abundant constituent of minerals (<http://www.c-f-c.com>).

The earliest known use of sulfur in construction was in the 17th century in Latin America where it was employed to anchor metal to stone (Rybezynski et al., 1974). Wright (1859) referred to the cementing property of sulfur in a USA patent. For the next 60 years there was little reported on the possible uses of sulfur in construction. At the end of World War I, sulfur was in oversupply in North America and this gave impetus to research for new uses. Bacon and Davis (1921) reported the development

of acid resistant mortars containing 60% sand and 40% sulfur for use in chemical industry.

Kobbe (1924) reported on the acid-resistant properties of materials prepared from sulfur and coke. Duecker (1934) and Payne and Duecker (1940) reported the development and use of additives to overcome the instability of sulfur sand mortars in thermal cycling. The reasons for this instability are that molten sulfur on cooling below 95.5⁰C transforms from the monoclinic S_β form to orthorhombic S_α crystalline form, the latter being denser, occupying less volume and being subjected to disintegration on thermal cycling.

Duecker (1934) found that the 60 % sand and 40 % sulfur product of Bacon and Davis increased in volume on thermal cycling with a loss in flexural strength. Duecker was able to retard both the tendency for volume increases and the resulting loss of strength on thermal cycling by modifying the sulfur with an olefin polysulfide. The use of additives to prepare more stable cements and products led to more industrial acceptance and more research and development on means of improving sulfur products for use as acid-resistant mortars and grouts. McKinney (1940) outlined testing methods for sulfur materials that had been found satisfactory at the Mellon Institute. Many of these methods have been adopted and are found in ASTM specifications for chemical-resistant sulfur mortar.

In the late 1960's Dale and Ludwig (1966 and 1968) pioneered the work on sulfur-aggregate systems, pointing out the need for well-graded aggregates to obtain optimum strength. This was followed up by the investigations of Crow and Bates (1970) on the development of high strength sulfur-basalt concretes. The United States Department of the Interior's Bureau of Mines and The Sulfur Institute (Washington, D.C.) launched a cooperative program in 1971 to investigate and develop new uses for sulfur. At about the same time, the Canada Center for Mineral and Energy Technology (CANMET), and the National Research Council (NRC) of Canada initiated a research

program in the development of sulfur concrete (Malhotra, 1973 and 1974; Beaudoin and Sereda, 1973). This was followed by work at the University of Calgary (Loov, 1974).

In 1973, the Sulfur Development Institute of Canada (SUDIC), jointly founded by the Canadian Federal Government, the Alberta Provincial Government, and the Canadian sulfur producers was established to develop new markets for the increasing Canadian sulfur stockpiles. In 1978, CANMET and SUDIC sponsored an international conference focusing on sulfur in construction (Malhotra et al. 1978). Also during this period, a number of investigators published papers and reports dealing with various aspects of sulfur and sulfur concrete: Malhotra (1974), Loov (1974), Sullivan et al. (1975), Sullivan and McBee (1976), Vroom (1977 and 1981), McBee and Sullivan (1979 and 1982), McBee et al. (1981, 1983, and 1986), Funke and McBee (1982), and Sullivan (1986). All of these activities led to an increased awareness of the potential use of sulfur as a construction material.

While sulfur concrete material could be prepared by hot-mixing unmodified sulfur and aggregate, durability of the resulting product was a problem. Unmodified sulfur concretes failed when exposed to repeated cycles of freezing and thawing, humid conditions, or immersion in water (ACI 548.2R, 1988). It was necessary to develop an economical means of modifying the sulfur so that the sulfur concrete product would have good durability. While olefinic polysulfide additives had shown promise in these applications, their costs were deemed prohibitive for use in preparing sulfur concrete for large scale construction uses (ACI 548.2R, 1988).

Following the work of Duecker (1934) and Payne and Duecker (1940), considerable effort was devoted to develop plasticizers/modifiers for sulfur (Raymont, 1978). Almost all of the materials used as modifiers for sulfur were either polymeric polysulfides or chemicals, which react with elemental sulfur to form polymeric polysulfides insitu (Blight et al., 1978). For the reaction to take place the sulfur must

be molten, and on cooling, the modified sulfur contains polysulfides and elemental sulfur in a variety of forms, mostly S_β , S_μ and S_8 (liquid). These forms were found to be stable and there didn't appear to be crystallization to S_α . In modifying sulfur it is important to take into account the reaction time and temperature.

Vroom (1977 and 1981) modified sulfur by reacting it with olefinic hydrocarbon polymers. It was also discovered that a similar reaction would yield a sulfur soluble polymer concentrate. Other researchers have reported various methods for treating sulfur to produce modified sulfur concretes, they include: Leutner and Diehl (1977), Gillott et al. (1980), Schneider and Simic (1981), McBee et al. (1981), McBee and Sullivan (1982), Woo (1983) and Nimer and Campbell (1983).

The increasing demand since 1976 for corrosion resistant sulfur concrete has led to the installation of precast and/or cast in place sulfur concrete in industrial plants, where Portland cement concrete material fail from acid and salt corrosion. The typical installations, as described by Pickard (1983), included floors, slabs on grades, overlays, curbs, walls, trench drains, sump pits, tanks, electrolytic cells, pump bases, column piers, foundations, and pipes.

2.1.2 Sulfur concrete mix proportions

According to Malhotra, 1979, as sulfur concrete contains no water or cement, the mix proportions are primarily concerned with achieving the highest strength properties with a minimum amount of sulfur, and with the provision that the resulting mixture is workable. Published data indicate sulfur content of the order of 20% by weight of total mix for concrete made with 19-mm maximum size aggregate. The percentage of sulfur may further be reduced by selecting aggregate grading which result in minimum void content. The best proportions of sulfur, fine aggregate and coarse aggregate will greatly vary depending on the surface texture, size and gradation of the aggregates (Loov, 1974).

2.1.3 Advantages and concerns with sulfur concrete

The main advantage of sulfur concrete is its use as a highly durable replacement for construction materials, especially Portland cement concrete, in locations within industrial plants or other locations where acid and salt environments result in premature deterioration and failure of Portland cement concrete. Other advantages of sulfur concrete are its fast setting time and rapid gain of high strength. Since it achieves most of its mechanical strength in less than a day, forms can be removed and the sulfur concrete placed in service without a long curing period. Generally sulfur concrete has the following useful characteristics:

- Sulfur concrete's tensile, compressive, and flexural strengths (McBee et al., 1986) and fatigue life (Lee and Klaiber, 1981) are greater than those obtained with normal Portland cement concrete.
- Sulfur concrete shows excellent resistance to attack by most acids and salts, some at very high concentrations (McBee et al., 1983).
- Sulfur concrete sets very rapidly and achieves a minimum of 70 to 80 percent of ultimate compressive strength within 24 hours (McBee et al., 1986).
- Sulfur concrete can be placed year round, in below-freezing temperatures.
- Sulfur concrete exhibits very low water permeability (McBee et al., 1983).

Because of the above characteristics sulfur concrete could be used advantageously in the following (Smith, 1980):

- In piping, where the greater strengths and corrosion resistance offer many opportunities.
- In floor construction, where the corrosion resistance of sulfur concrete makes it ideal for new floors and repairs in hostile environments

- In structural applications, where its superior strengths could reduce the size and spacing of structural elements
- In the repair of Portland cement highways, bridge decks and airfield runways where its high early strength would allow the sooner return of facilities to service.
- In rail road ties due to its high fatigue resistance
- In marine applications such as sheet piling, where its impermeability and resistance to salts are of high value

As with any other construction material, certain measures must be taken with sulfur concrete to ensure safe handling in its preparation and use. Sulfur concrete should be produced within its recommended mixing temperature range of 127 to 141⁰C to minimize emissions. Adequate ventilation during construction operations and normal precautions for handling hot fluid materials (proper protective clothing, eye protection, gloves, and hard hats) should be observed. Practices for safe handling of both solid and liquid sulfur have been established by the National Safety Council (1978 and 1979) in Chicago and should be observed when preparing and handling sulfur concrete.

2.1.4 Modified sulfur cement

The need for using modified sulfur cements in sulfur concrete manufacture has been recognized since the 1930s. Sulfur cements are modified by introducing additives to improve stability and durability and reduce the expansion-contraction of sulfur concrete during thermal cycling. Duecker (1934) was able to retard the tendency for volume increases and the resulting loss of strength of sand-sulfur mortars on thermal cycling, by modifying the sulfur with an olefin polysulfide.

In 1973, A. H. Vroom developed a process, with assistance from the National Research Council of Canada and A. Ortega of McGill University, Montreal. This

process involved modifying sulfur by reacting it with olefinic hydrocarbon polymers (Vroom 1977, and 1981). It was also discovered that a similar reaction would yield a sulfur soluble polymer concentrate. The resulting sulfur concrete was first produced for commercial use in Calgary, Alberta, in 1975.

Modification of sulfur by reaction with dicyclopentadiene (DCPD) has been investigated by many researchers, but its practical use in commercial applications has been limited because the reaction between sulfur and DCPD is exothermic and requires close control. Also, the DCPD modified sulfur cement is unstable when exposed to higher temperatures (greater than 140⁰C), such as when mixing with hot aggregates, and may react further to form an unstable sulfur product which reverts back from the S_β to the S_α form (McBee et al., 1981). McBee and Sullivan (1982) solved this problem through the development of a process for preparing modified sulfur cement that is stable in the S_β form and is not temperature sensitive in the mixing temperature range for producing sulfur concrete. This process utilized a controlled reaction of cyclopentadiene (CPD).

Other researchers have reported various methods for treating sulfur to produce modified sulfur concretes. Leutner and Diehl (1977) introduced the use of dicyclopentadiene (DCPD), Gillott et al. (1980) used crude oil and polyol additives, Schneider and Simic (1981), used DCPD or glycol, Woo (1983), used phosphoric acid to improve freeze-thaw resistance and Nimer and Campbell (1983), used organosilane to improve water stability. In addition, Gregor and Hack (1978) have reported on laboratory design tests for DCPD modified sulfur concrete products, Bright et al. (1978) on modified sulfur systems, and Bordoloi and Pierce (1978) on stabilizing sulfur with DCPD.

Although several methods exist, two methods are widely used in North America to produce modified sulfur cements that are marketed under different trade name. The compositions of the modified sulfur cements are shown in Table 2.2.

Material	Method 1 (% by weight)	Method 2 (% by weight)
Sulfur	95 ± 1	80
Carbon	5 ± 0.5	18
Hydrogen	0.5 ± 0.05	2

Table 2.2 Compositions of modified sulfur cements used in North America, taken from ACI 548.2R (1988)

Method 1 shown in Table 2.2 is based on the polymeric reaction, in which 100 % of the sulfur reacts with a modifier containing equal parts of cyclopentadiene oligomer and dicyclopentadiene (DCPD) (McBee and Sullivan, 1982). DCPD is a hydrocarbon in the form of a colorless liquid with double bonds suitable for reacting with sulfur, and it also retards and prevents the crystallization of sulfur (Sullivan and McBee, 1976). This process is known as the Chempruf® Process and uses a proprietary composition called “Chement 2000” (Crick and Whitmore, 1998).

Method 2, also shown in Table 2.2, uses a modified sulfur concrete prepared by combining sulfur with olefinic hydrocarbon polymers such as Escopol (Vroom, 1981). This concentrate is then mixed with locally available pure sulfur in the ratio of 10 parts of sulfur to 1 part of concentrate, by weight. This process is used commercially to produce the concrete product named STARcrete™. Its predecessor Sulfurcrete® was first marketed in Canada in 1976.

Both methods of modifying sulfur give extremely long shelf life in the solid state. If stored in the molten state, both modifiers may continue to react and produce inferior concretes.

Although various additives are available to enhance the properties of sulfur concrete, this thesis focuses on unmodified sulfur concrete (pure elemental sulfur concrete) because of its abundance in the oil sands mines.

2.2 Characteristics of Sulfur Concrete

2.2.1 Compressive strength

Sulfur concrete develops about 70 % of its ultimate strength within a few hours of cooling, and usually 75 to 85 % after 24 hours at 20⁰C, however, it attains its ultimate strength after 180 days at 20⁰C (McBee et al., 1983). The rate of strength development depends on the temperature at which the material is aged. Strength gain is slower at elevated temperatures and faster at lower temperatures. Since larger masses of sulfur concrete cool more slowly, they gain strength more slowly but in the end attain the same ultimate strength as smaller masses (McBee and Sullivan, 1979). Johnston (1979) emphasized that there is no evidence of strength retrogression during a six-month period following placement of sulfur concrete.

As with normal Portland cement concrete, strength properties of sulfur concrete are affected by the type of aggregate used. Gregor and Hack (1978) have shown that sulfur concretes had about 30 % higher compressive strength when crushed basaltic aggregate was used than when the concrete was made with smooth aggregate with the same grain size distribution. This is because crushed stone have rough surfaces that provide higher frictional resistance to shear than the smooth round aggregate particles.

Malhotra (1974) has investigated the effect of specimen size on compressive strength of sulfur concrete. The compressive strength of 100 x 200 mm concrete cylinders was considerably higher than those of 150 x 300 mm cylinders. For a typical sulfur concrete mix containing about 20 % sulfur, the 28-day compressive strengths of 100 x 200 mm cylinders ranged from 32.8 to 46.2 MPa, whereas the corresponding strengths of 150 x 300 mm cylinders ranged from 26.1 to 34.4 MPa. However density of the smaller cylinders was only slightly higher than the larger cylinders. The decrease in strength of large specimens is probably due to the combined effect of specimen size and slower rate of cooling while they are still in the moulds (Malhotra, 1974).

Abel-Jawad and Al-Qudah (1994) found that sulfur concrete prepared using three different types of aggregates, namely, limestone, sandstone, and basalt developed much of their strength within few hours after casting and that no significant strength was gained afterwards. Therefore, the sulfur concrete strength may be considered independent of time.

Raymont (1978) summarized the range of physical and mechanical properties of sulfur concrete as given in Table 2.3.

Physical and mechanical properties	Range
Compressive strength, MPa	28 - 70
Modulus of rupture, MPa	3 - 10
Ratio, modulus of rupture to compressive strength, %	12 - 20
Tensile strength, MPa	3 - 8
Ratio, tensile strength to compressive strength, %	10 - 20
Modulus of elasticity, GPa	20 - 45
Coefficient of thermal expansion per $^{\circ}\text{C}$ ($\times 10^{-6}$)	8 - 35
Thermal conductivity, W/m. $^{\circ}\text{C}$	0.4 to 2
Water absorption, %	0 - 1.5

Table 2.3 Range of physical and mechanical properties of sulfur concrete after Raymont (1978)

Lee et al. (1978) showed that the addition of fly ash in a proportion of 7.3 % by weight of the total mix to the unmodified sulfur concrete improved the compressive strength by 73 %.

Czarnecki and Gillott (1989) studied the effect of different admixtures on the strength of sulfur concrete. Their conclusions included the following:

- The strength of sulfur concrete didn't depend entirely on the amount of sulfur binder
- The strongest rock aggregate didn't produce the strongest sulfur concrete. Moreover the aggregate particle shape and texture played a major role in the overall strength and density of concrete.
- The addition of crude oil resulted in lower strengths
- Sulfur concrete continuously immersed in water developed lower strengths than that exposed to normal laboratory air.
- Saline admixtures affected positively the moisture durability and strength in air and water.

2.2.2 Stress-strain relationships

Sulfur concrete is a relatively brittle material. This is quite evident during the testing of specimens in compression. Loov (1975) has published stress-strain relationship for sulfur concrete and has shown that in the testing of sulfur concrete specimens there was no gradual reduction in stiffness when the ultimate load was approached. Moreover failure occurred at a strain of approximately 0.0014. The brittleness of the material is a disadvantage but it may be overcome by using fibrous materials. Shrive et al. (1977) reported that sulfur, sulfur mortars, and sulfur concrete are extremely brittle materials, far more so than Portland cement mortars and concretes.

Young's modulus of sulfur concrete and Portland cement concrete are comparable, at approximately 30 GPa for a sulfur concrete with strength of 40MPa (Loov, 1974, Malhotra, 1979). Moreover, after one day of cooling, the ACI 548.2R (1988) reported that for sulfur concrete with a compression strength of 27.6 MPa, the Young's modulus ranged from 20.7 to 27.6 GPa.

Lee et al. (1981) found that admixtures such as olefins and thiocols stabilized the bonding structure and converted the sulfur concrete into a more ductile material.

However, the effect of these admixtures was time dependent and the ductility disappeared with time.

Gillott et al. (1980) studied another type of admixture that they believed could alter the bond characteristics between the sulfur mix and the aggregate and between the sulfur crystals within the matrix. Petroleum additives and some polyols improved the strain capacity, and the effect remained for long periods of time (Gillott et al., 1982 and 1983).

Lee and Klaiber (1981) found that modulus of elasticity of plasticized sulfur concrete, prepared by modifying the sulfur cement using oligomers of cyclopentadiene, was lower than that of unmodified sulfur concrete. However, the ductility of the concrete was improved, as indicated by the larger strains at failure.

2.2.3 .Freeze-thaw durability

The durability of sulfur concrete subjected to freeze-thaw cycles has been studied extensively (Malhotra, 1973, Beaudoin and Sereda, 1974, Loov, 1975, Sullivan and McBee, 1976). Their laboratory results showed sulfur concrete to have poor freeze-thaw durability.

Duecker (1934) proposed a theory explaining the deterioration of sulfur concrete under freeze-thaw cycles, and it has been supported by many published works such as Vroom (1977), Sullivan and McBee (1978), and Malhotra (1979). Duecker suggested that since sulfur has a low thermal conductivity, large internal temperature gradients develop when the ambient temperature changes externally by few degrees. These temperature gradients, when coupled with the unusually high coefficient of thermal expansion of sulfur ($\sim 55 \times 10^{-6}/^{\circ}\text{C}$), generate high thermal stresses. These stresses were thought to be responsible for the development of fissures or fractures within the material (Shrive et al., 1981). The factors that were thought to contribute to the failure

includes, residual stresses resulting from the crystallographic reversion of sulfur from monoclinic to the denser orthorhombic form, differential stresses within the sulfur matrix, and between the sulfur matrix and aggregates due to the different expansion and contraction behaviors of the materials (Shrive et al., 1981).

As sulfur concrete contains no water or cement, its performance in freeze-thaw cycling is principally a problem of resistance to thermal cycling. This is further compounded by the fact that sulfur has a very high thermal coefficient of expansion. Malhotra (1973) has shown that sulfur concrete produced with crushed gravel aggregate is not durable under freeze-thaw cycling. This investigation indicated that the prisms had been extensively damaged after exposure to less than 75 cycles; the dynamic modulus of elasticity was generally less than 30 % of original.

Shrive et al. (1977) remarked that many sulfur concretes can support many temperature thaw cycles, although these concretes fail in the presence of water at constant temperatures. This phenomenon was attributed to the presence of expansive clays in the aggregate. Shrive et al. (1977) also found that sulfur concrete specimens which did not break up at constant temperature in the presence of water and did not lose strength when subjected to temperature cycles in the absence of water, did however fail laboratory tests of cyclic freezing and thawing in the presence of water. Thus they concluded that the lack of freeze-thaw durability of sulfur concrete was due to some mechanism involving the freezing and thawing of water in the specimen.

Shrive et al. (1981) suggested that freeze-thaw failure mechanism of sulfur concrete was similar to that proposed for Portland cement concretes under freeze-thaw cycles and involved the effect of moisture in the material. It was thought that moisture migration associated with the growth of ice crystals was the principal factor in the creation of cracks and fractures. Powers (1975) remarked that pressure great enough to exceed the tensile strength of the material has been attributed to an osmotic type

mechanism. In addition, Litvan (1976) suggested that differences in vapor pressure between the more stable ice and unfrozen water absorbed on internal surfaces also increased the pressure. Therefore the ice is understood to form in large voids or cracks. This failure mechanism is controlled by entraining an air and void system, which is created such that the distance between voids within the matrix is sufficiently small (on average) to avoid development of large internal pressures. Shrive et al. (1981) showed that moisture reaches the interior of the samples despite the low permeability of the sulfur concrete. They inferred that both the mechanism of failure and the potential solution could be the same as Portland cement concretes.

The air content and the void spacing factor are important parameters considered in Portland cement concretes for freeze-thaw durability and are measured by the ASTM C-457. An air content of at least 7 % and a void spacing factor of at most 0.2 mm are considered necessary to provide an adequate durability for severe exposure conditions in Portland cement concretes. However, no consistent trend was found in sulfur concrete specimens studied by Shrive et al. (1981). They argued that the durability of sulfur concrete must also be a function of the permeability, tensile strength, stress strain behavior, and water absorption properties of the concrete.

Cohen (1987) performed an investigation to evaluate the freeze-thaw durability of sulfur concrete based on the mechanism proposed by Shrive et al. (1981). A total of twelve 2 x 2 x 12 inch mortar bars of commercial grade were used for testing. Six of the bars were cut into 2 x 2 x 2 inch cubes. The cubes and the bars were immersed either in water, a petroleum base oil, or air (in sealed plastic containers) and stored in a freeze-thaw apparatus with a temperature range from -12 to 32⁰C at 27 cycles per week.

From the test, it was observed that the oil stored specimens showed severe weight loss and scaling, whereas the water and air stored samples didn't. The main reason for these was attributed to deleterious chemical reactions between the oil and sulfur

concrete specimens leading to disintegration. The freeze-thaw action also didn't cause significant harm to the relative compressive strength of water and air stored specimens. The decreasing values for oil-stored specimens were attributed to chemical disintegration. If the freeze-thaw mechanism of sulfur concrete is similar to that of Portland cement concrete, then it would be expected that water stored specimens would show more damage than their air stored counterparts. The fact that this was not the case suggested that moisture migration mechanism is not the dominant damaging source.

Interpretation of the relative modulus data according to ASTM C 666 would indicate that all specimens failed because the relative moduli had decreased to 60 % at 300 cycles. However, analyses of the relative compressive strengths, surface conditions, and weight loss data of the water and air stored samples seemed to indicate good freeze-thaw resistance. Moreover there were no appreciable differences in the frequency and strength behavior of the water and air stored samples. Consequently, Cohen (1987) suggested that the mechanism by Duecker (1934) should not be dismissed from consideration. In other words, cyclic freezing and thawing in sulfur concrete may be equivalent to thermal cycling, in which case water does not have any significant role. Furthermore, the fact that mortar bars failed the ASTM C-666, when at the same time the cube strength showed satisfactory resistance, showed that the ASTM C-666 test cannot be used effectively for sulfur concrete (Cohen, 1987).

Studies by Beaudoin and Sereda (1973) have shown that the freeze-thaw resistance of mortars may be improved by the addition of pyrites. The best freeze-thaw performance was obtained with mortars containing 20 % or more of pyrite by weight.

McBee and Sullivan (1978) modified sulfur with 5 % dicyclopentadiene to improve the freeze-thaw resistance of sulfur concrete. Two types of concrete were investigated: for one type the coarse and fine aggregate were crushed quartz and for the other type coarse aggregate was crushed limestone and fine aggregate was manufactured

limestone sand. The test result indicated a marginal improvement in the freeze-thaw resistance of sulfur concrete.

Lee and Klaiber (1981) found that while the resistance of plasticized sulfur concrete (modified using oligomers of cyclopentadiene) to freeze-thaw cycles and to water action was lower than that of conventional Portland cement concrete, there appeared to be considerable improvement over unmodified sulfur concretes.

2.2.4 Fatigue behavior

A material is said to fail in fatigue if failure takes place after a number of repeated loads, each smaller than the static strength of the material. This characteristic is important in structures such as highway pavements, which are subjected to many repetitive traffic loads during their service lives. Lee and Klaiber (1976) and Lee et al. (1978) investigated the fatigue properties of unmodified and laboratory modified sulfur concretes. They found out that sulfur concrete exhibited much higher fatigue lives than did conventional Portland cement concrete. They also noticed slightly higher fatigue life for plasticized sulfur concrete than for the unmodified sulfur concrete. Lee and Klaiber (1981) showed that plasticized sulfur concrete withstood repeated loadings at much higher percent of the modulus of rupture than conventional concrete. These findings mean that for pavements of the same thickness and of equivalent compressive strengths, sulfur concrete is able to carry many more applications of traffic loads than Portland cement concrete.

Furthermore, Lee et al. (1978) indicated that sulfur concrete with fly ash as an additive had higher fatigue life and improved considerably the compressive strength. All sulfur concrete mixes studied by Lee et al. (1978) showed better fatigue behavior than Portland cement concrete. The behavior of the fly ash modified sulfur concrete is far better than that of the dicyclopentadiene (DCPD) modified sulfur concrete.

2.2.5 The effect of water under constant temperature

The immersion in water under constant temperature also affects the durability of the sulfur concrete. Gillott et al. (1983) and Czarnecki and Gillott (1989 and 1990) showed that sulfur concrete is subject to excessive expansion, cracking, strength loss, and decrease in dynamic modulus of elasticity as a result of continuous immersion in water at room temperature. Their results indicated that sulfur concrete made with good quality aggregates may show poor durability in the presence of water. The durability of sulfur concretes containing glycerin and crude oil admixtures was slightly improved, but expansions were still unacceptably high. However, silane admixtures were found to significantly reduce the moisture expansion and improve durability of sulfur concrete by changing the surface characteristics at the aggregate-sulfur interface (Czarnecki and Gillott, 1990). Their effectiveness depends on the type of admixture and the type of aggregate.

Czarnecki and Gillott (1989) also found no correlation between the expansion of the rocks and the expansion of the concretes made with these rocks. They observed much greater expansion in the concretes than in the rocks, leading to the conclusion that the expansion resulted from a physical phenomenon within the sulfur.

Abdel-Jawad and Al-Qudah (1994) studied the combined effect of water and temperature on the compressive strength and microstructure of sulfur concrete prepared using three different types of aggregates: limestone, sandstone, and basalt. The results showed that sulfur concrete immersed continuously in water at different temperatures developed lower strength than samples exposed to normal laboratory air conditions. The reduction in strength ranges from 42 % to 75 %, depending on the types of aggregates and water temperature. The highest reduction in strength was obtained in the case of basalt aggregate and water temperature of 20⁰C. Most of the strength loss, at all temperatures, took place during the first three days of immersion in water.

As well, visible cracks and surface cavities appeared in the samples prepared with aggregates of crushed limestone and basalt, possibly because of the presence of clay minerals. Sandstone aggregate concrete showed no sign of visible cracks because it was free of clay minerals.

2.2.6 Creep

Loov (1975) and Malhotra (1979) indicated that sulfur concrete exhibited considerably more creep than Portland cement concrete, which can be a serious disadvantage for structural concrete members. Gamble and Shrive (1978) suggested several mechanisms of creep in sulfur and also mentioned that the creep in elemental sulfur was greatly affected by the methods of preparation and curing.

2.2.7 Corrosion resistance

Sulfur concrete is a desirable material for use in construction in the fertilizer and metal refining industries because of its resistance to attacks by a wide range of acids and corrosive materials. McBee and Sullivan (1978) showed that concretes prepared with silica aggregates and modified sulfur binder were superior to those made with unmodified sulfur binder. The effects on the mechanical properties of modified sulfur concrete test specimens immersed in water, and in 1, 5, and 10 % by weight of H_2SO_4 for up to one year showed no change in compressive and tensile strengths though some loss in flexural strength, which may be explained by a loss in plasticity of the modified sulfur with time. Investigations by McBee and Sullivan (1978) also showed that sulfur concrete prepared from silica or limestone aggregates and modified sulfur were not affected by exposure to 5 % NaCl, 5 % $CaCl_2$ or 5 % Na_2SO_4 salt solutions. The test specimens did not show any loss in weight and there was only negligible gain in weight ranging from zero to 0.3 %.

Dielhl (1976) presented some data showing the resistance of elemental sulfur and dicyclopentadiene-modified sulfur to aggressive chemical attacks. More recently,

Crick and Whitmore (1998) presented a list of the sulfur concrete's chemical resistance to various solutions at room temperature as shown in Table 2.4.

Acids	Concentration* (%)	Chemicals	Concentration* (%)
Boric acid	100	Ammonium sulfate	100
Hydrochloric acid	32	Calcium chloride	100
Nitric acid	50	Copper sulfate	100
Phosphoric acid	85	Ferric chloride	100
Sulfuric acid	93	Magnesium chloride	100
		Magnesium sulfate	100
		Potassium chloride	100
		Nickel chloride	100
		Nickel sulfate	100
		Sodium chloride	100
		Sodium sulfate	100
		Zinc chloride	100
		Zinc sulfate	100

* Maximum concentration resisted by sulfur concrete

Table 2.4 Chemical resistance at room temperature, after Crick and Whitmore (1998)

Malhotra (1975) mentioned that unmodified sulfur is attacked or dissolved by strong oxidizing agents such as concentrated sulfur, nitric, and chromic acids, sodium hypochlorite, strong alkalis at pH 10, polysulfide solutions, and certain organic chemicals like carbon disulfide, phenols and others. Sulfur also reacts with a number of metals in solutions like copper and beryllium to form insoluble sulfides.

Okamura (1998) studied the performance of sulfur concrete floors, which have been used in industrial and acid plants in British Columbia and Calgary. The sulfur concretes consisted of elemental sulfur, sulfur polymer stabilizer (Sulfurcrete[®]), fine filler material, and aggregate. Core samples from the facilities with sulfur concrete

were taken to obtain details about mix proportions used, placing of the material, compressive strength, and general performance. The findings showed that sulfur concretes were in good conditions after years of service in these highly corrosive environments. The quality control in mix design, production, and placing of sulfur concrete were paramount for success against chemical attacks.

2.2.8 Resistance to fire and ultra violet rays

Sulfur melts at about 119⁰C, and sulfur concrete subjected to this or higher temperature will melt and lose all its strength. Because of the low melting point of sulfur the use of sulfur concrete is limited to applications where temperature does not exceed about 80⁰C (Malhotra, 1979). In spite of the development of fire retardants, sulfur concrete cannot be considered stable in fire. In addition, sulfur combustion is self-sustaining and, thus once ignited, will continue to burn until extinguished. In the presence of oxygen, sulfur will burn to sulfur dioxide, a toxic gas (Malhotra, 1979).

Kemp et al. (1971) have shown that the oxidization of sulfur in the presence of moisture is accelerated by ultraviolet light. It may be speculated that large surfaces of sulfur concrete when exposed to moisture and ultraviolet light may result in the formation of sulfuric acid (Malhotra, 1979).

2.2.9 Resistance to biological attack

Loov (1974) and Malhotra (1979) pointed out that sulfur mortars and sulfur concretes are susceptible to attack by bacteria, primarily *Thiobacillus thiooxidans*, resulting in the production of sulfurous and sulfuric acids. Thus a drop in pH indicates growth of this organism.

Frederick and Starkey (1948) reported that the oxidation of elemental sulfur by *Thiobacillus thiooxidans* was dependent upon particle size. The smaller the sulfur particle, the faster is its rate of oxidation in pure culture experiments. Fjerdningstad

(1960) pointed out that the optimum growth temperature for *Thiobacillus thiooxidans* is between 28 and 30°C, therefore the attack would be more severe on soils in countries with hot climate.

Investigations have been reported on the use of bactericides to counter the attack caused by bacteria (Duecker et al. 1948, Laishly and Tyler, 1978). Laishly and Tyler (1978) indicated as shown in Table 2.5 the effect of *Thiobacillus thiooxidans* on sulfur concrete.

Sulfur limestone concrete bars	Cell count of <i>Thiobacillus thiooxidans</i> /ml		pH		SO ₄ (mg/ml)		Length of bars*** (inches)		Flexure test (psi)
	Initial	Final	Initial	Final	Initial	Final	Initial	Final	
Inoculated*	3.1x10 ⁶	7x10 ⁷	3.3	1.8	0.5	9.5	10.06	10.06	384(±37)
Un-inoculated*			4.5	4.8	0.5	1.6	10.08	10.08	381(±35)
Dry control**							10.07	10.06	481(±36)

* Average of 4 different experiments

** Average of 3 different experiments

*** Measured with Demec extensometer

() Standard deviation of the mean

Table 2.5 Effect of *Thiobacillus thiooxidans* on sulfur concrete, modified from Laishly and Tyler (1978), (1 psi = 6.895 kPa)

2.2.10 Recycling

One attractive feature of sulfur concrete is that, if needed, sulfur concrete can be melted to recover the sulfur and aggregates and the recycled materials can be used again for concrete (Malhotra, 1979). Limited data by Lee et al. (1978) showed that the strength properties of concrete made with recycled sulfur are comparable to the original strength values (Table 2.6).

Series	Original		Recycled			
	Compressive Strength (psi)	Mod. of Rupture (psi)	Compressive Strength (psi)	Percent change	Mod. of Rupture (psi)	Percent change
I	4510	533	4286	-5.0	466	-12.6
II	4410	497	5506	+24.8	466	-6.2
III	2610	486	4516	+73.0	479	-1.4

Table 2.6 Strength of original and recycled sulfur concrete, Lee et al. (1978) (1 psi = 6.895 kPa)

2.3 Environmental and Safety Aspects in the Use of Sulfur in Highway Pavements

The material presented in this section is extracted from the works of Saylak et al. (1981) and Deuel and Saylak (1981). Their studies were sponsored by the Federal Highway Association (FHWA), and were performed at the Texas Transportation Institute (TTI). The first part of these studies dealt with the pollution from mix preparation and construction (Saylak et al., 1981). The second part investigated those aspects related to post construction exposures to the elements, and to the problems that can occur while the pavement is in use (Deuel and Saylak, 1981).

2.3.1 *Mix preparation and construction*

2.3.1.1 Use of sulfur in construction

One of the major concerns throughout the development of sulfur/asphalt concrete in construction applications has been the potential hazards created at the construction site due to the evolution of toxic gases such as: Hydrogen sulfide (H₂S), Sulfur Dioxide (SO₂) and Elemental Sulfur.

A Federal Highway Association (FHWA) sponsored research program at Texas Transportation Institute (TTI) by Saylak et al. (1980), with the objective of assessing the environmental and safety implications of using sulfur as a highway paving

material, has concluded that as long as the temperature of the mix is maintained below 149°C, the concentrations of the pollutants (H₂S, SO₂ and S) remain below the maximum allowable concentrations (MAC) suggested by the American Conference of Governmental Industrial Hygienists (ACGIH). Similar studies sponsored by other organizations like Sulfur Institute (Izatt, 1977), Gulf (Kennepohl et al., 1975), Shell (Deme, 1974), and SUDIC (Rennie, 1978) also supported this claim.

2.3.1.2 Toxicity of sulfur initiated pollutants

The three most common sulfur initiated pollutants are Hydrogen sulfide (H₂S), Sulfur Dioxide (SO₂) and particulate sulfur. The safety problems of each of these contaminants are discussed here.

2.3.1.2.1 Hydrogen sulfide (H₂S)

Hydrogen sulfide is known for its characteristic “rotten egg” odor. Although this odor is noticeable at concentrations as low as 0.02 ppm, odor is not a good indicator of concentration level. Hydrogen sulfide can have a paralyzing effect on the sense of smell. Therefore, high concentrations cannot be noticed. During the TTI research project, the toxicity of H₂S was established based on the relationships between its concentration and the effects on humans, as specified by the ACGIH. Those concentrations and their effects are given in Table 2.7

H ₂ S concentration, ppm	Effect
0.02	Odor threshold
0.1	Eye irritation
5 – 10	Suggested MAC for prolonged exposure
70 – 150	Slight symptoms after exposure of several hours
170 – 300	Maximum concentration which can be inhaled
400 – 700	Danger after exposure for half to one hour
600	Fatal with half hour's exposure

Table 2.7 Effects of H₂S on humans, after Saylak et al. (1981)

On the basis of these effects a MAC value of 5 ppm is normally specified as the upper threshold limit for continuous exposure to H₂S emissions in areas expected to be normally occupied by construction or plant personnel.

2.3.1.2.2 Sulfur dioxide (SO₂)

Sulfur Dioxide is a colorless gas with a pungent odor, which unlike H₂S gives ample warning of its presence. The principal health hazard from SO₂ comes from inhalation of excessive quantities above its MAC. The National Institute for Occupation Safety and Health, and the Manufacturing Chemists Association have established the relative toxicity of SO₂ emissions on the basis of its effects on humans (Table 2.8)

SO ₂ concentration, ppm	Effect
0.3 – 1	Detected by taste
1	Injurious to plant foliage
3	Noticeable odor
5	MAC (ACGIH)
6 – 12	Immediate irritation of nose and throat
20	Irritation to eyes
50 – 100	MAC for 30 – 60 minute exposures
400 – 500	Immediately dangerous to life

Table 2.8 Effects of SO₂ on humans, after Saylak et al. (1981)

A concentration of 5 ppm is the MAC specified as the upper threshold limit for SO₂ emissions in areas expected to be normally occupied by construction and plant personnel.

2.3.1.2.3 Elemental Sulfur

Vapors emitted during mixing and dumping operations contain a certain amount of undissolved and unreacted sulfur. As the vapors come in contact with air and cool, the

sulfur crystallizes into small particles that are carried by wind. Since there is no practical way to eliminate this pollutant, its effect on both the environment and personnel must be considered.

Saylak et al. (1981) pointed out that the principal problem related to sulfur dust is the irritation of the eyes after contact. Sulfur is capable of irritating the inner surfaces of the eyelids. Sulfur dust may rarely irritate the skin. Sulfur is virtually non-toxic, and no evidence has been found that systematic poisoning results from the inhalation of sulfur dust. The primary hazard in handling solid sulfur results from the fact that sulfur dust suspended in air may be ignited. This problem is limited to enclosures and unventilated areas such as storage silos and hoppers (Saylak et al., 1981).

2.3.1.3 Conclusions of Phase 1 study (Saylak et al., 1981)

Six mix designs representing four types of sulfur-asphalt pavement materials; sand-asphalt-sulfur, sulfur extended asphalt, sulfur recycled system, and sulfur concrete were evaluated to assess their potential environmental impact during mix preparation and construction. The evolution of sulfur based pollutants, primarily H₂S, SO₂, and particulate sulfur was investigated from the mix preparation stages through construction. In the formulation phase the influence of sulfur in seven mix designs was examined against mix temperature, humidity, and oxygen content of air. The results generated from this study tend to support the data generated by others in the laboratory as well as the field that, as long as the mix temperature is kept below 149⁰C, evolved gases and pollutants can be maintained within safe limits. However, the conclusion does not apply when sulfur-asphalt mixtures are processed or stored for prolonged periods of time in closed environments such as silos and hoppers.

2.3.2 Post construction exposure

The second part of the study performed by the TTI (Deuel and Saylak, 1981), dealt with post construction aspects while the pavements are in use. Nine mix designs

which included, five sulfur-asphalt systems, two sulfur concretes, and two control asphalt concretes, were subjected to a variety of simulated in service weathering traffic conditions including hot temperatures, actinic light (ultra violet radiation), rainfall, freeze-thaw, biological activities, chemical spills and fire. Pollutants in the form of dust, fumes and run-off products were collected and analyzed for their safety and environmental impact assessment.

2.3.2.1 Weathering studies

The combined effects of temperature, actinic light, and rainfall conditions on emissions and run-off products were achieved by exposing slabs of six selected mix designs of asphalt, sulfur asphalt, and sulfur concrete to natural daily and seasonal weathering.

Their result showed that the discharge of H₂S and SO₂ from the sulfur concrete and sulfur concrete modified with dicyclopentadiene were approximately equal in magnitude to that of the lower sulfur-asphalt pavement materials, although they contained more than 10 times of total sulfur than the sulfur-asphalt mixes. To put the magnitude of the flux values in perspective, the maximum value of H₂S measured during the test was 955 µg/m²/hour (reported for the high sulfur asphalt blend). This value corresponded to a concentration in air of 2.6 ppm, which was half of the maximum allowable concentration recommended in section 2.3.1.2.1. Moreover, the maximum values measured for the sulfur concrete mix was 159 µg/m²/hour of H₂S and 201 µg/m²/hour of SO₂, and for the sulfur concrete modified with dicyclopentadiene were 164 µg/m²/hour of H₂S and 232 µg/m²/hour of SO₂. These values were well below the recommended maximum allowable concentrations.

2.3.2.2 Simulated in service conditions

2.3.2.2.1 *Temperature, actinic light and run-off effects*

Compacted specimens of sulfur asphalt, asphalt and sulfur concrete were exposed to actinic light and temperature. After 6 months of exposure, the outer edges were chipped away and grounded in an ore crusher for subsequent total sulfur analysis. Total sulfur values obtained were utilized to determine the potential weathering effect of a combination of high temperature and UV light with potential loss as run off from rain. The most relevant results were that UV radiations from full sunlight did not affect the total sulfur measured and that the conservation of sulfur suggested no losses from a rainfall run-off mechanism.

2.3.2.2.2 *Freeze-thaw*

Compacted specimens of sulfur asphalt, asphalt and sulfur concrete were subjected to the weathering impact of freeze-thaw cycling following ASTM C-666 test procedure. After the final thaw, the water used as the surrounding matrix was filtered and extracted. Initial analysis of the water showed contents of organic leachate. However, further analysis demonstrated that these leachates were not constituents of the samples and also did not contain sulfur.

Chips taken from the outer edges of beam samples for total sulfur analysis suggested no loss of sulfur from the sample following the multiple freeze-thaw weathering sequence.

2.3.2.2.3 *Chemical weathering*

Deuel and Saylak (1981) analyzed for hydrolysates by using gas chromatographic techniques on both weathered specimens and laboratory control materials. This analysis revealed that organic material was not solubilized by hydrolysis reaction in either pH=2 or pH=10 water at a reaction temperature equivalent to the maximum

surface temperature. Much more acidic or basic reactions at the pavement surface were required to induce chemical hydrolysis of sulfur asphalt pavements. The total sulfur lost as H₂S was small in magnitude, suggesting that hydrolysis reactions would at best be significant in the weathering of sulfur asphalt pavements over a long term. The chemical oxidation of sulfur was an exceedingly slow reaction at ambient temperatures of the natural environment.

2.3.2.2.4 *Biological weathering*

The different mix designs mentioned above were ground to pass through a 1mm mesh sieve, and 10 grams of samples were incorporated into 100 grams of fresh soil matrix, at field capacity moisture level, to determine the potential biological degradation. The data suggested that the sulfur tended to increase the biological activity of the soil. A mechanism of weathering was not reported for the sulfur concrete mixes. The study also revealed that no significant levels of sulfur were lost from the specimens exposed to a natural weathering environment over a relatively short period of time. However, the results suggested that soil-born microbes might be important in the long term. All soils contain microorganisms, which can utilize sulfur as an energy source, with potential for deposition on in service pavements.

2.3.2.2.5 *Simulated traffic effects*

Deuel and Saylak (1981) studied the following factors, which result from traffic and could impact the environment by affecting the road surface: skidding, snow low friction, tire pavement interaction, and exhaust fumes. With the exception of the exhaust fumes, the other three factors produced dust from either friction or erosion. This dust could be transported by wind or rain to adjacent stream and ground surfaces. Elemental sulfur was detected in dusts created by grinding the test samples, however it was believed that the test exaggerated the mechanism of degradation.

2.3.2.2.6 *Simulated fire test*

Deuel and Saylak (1981) showed that putting compacted specimens of sulfur asphalt and sulfur concrete mixes in direct contact with a natural gas flame resulted in significant sulfur losses as H₂S and SO₂. Compared with the sulfur losses (in the form of SO₂) of the asphalt sulfur mixes, those of the concrete mixes were extremely high. The SO₂ emissions of sulfur concrete and sulfur concrete modified with DCPD were 2800 ppm and 3400 ppm respectively compared with the highest sulfur asphalt emissions of 750 ppm. However, the H₂S emissions of the sulfur concrete mix was nil, and the emissions of mix modified with DCPD was 25 ppm, comparable with the lower emissions from the sulfur asphalt mix. Another important issue was that only the DCPD modified sulfur concrete systems remained on fire once the burner flame was removed.

2.3.2.3 Conclusions of phase 2 study (Deuel and Saylak, 1981)

From the studies it was found that exposure to the elements had negligible effects on the paving materials studied and run-off either by wind or rain produced little or no effect on the immediate environment. It should be noted that both mix preparation and simulated weathering experiments were designed to maximize the test conditions and thus the results generated may be considered conservative.

The possibility of accidental events such as fires and chemical spills were investigated and revealed some possible short-term undesirable effects. These effects were essentially obnoxious fumes and/or short-term pollution. Virtually all of the sulfur paving materials were difficult to ignite and were self-extinguishing.

2.4 Batching, Transporting, Placing and Finishing of Sulfur Concrete

The ACI 548.2R (1988) guideline provides recommendations for batching, transporting, placing and finishing sulfur concrete. The minimum and maximum

temperatures of a sulfur concrete mixture are controlled because: 1) the sulfur cement melts at 119⁰C and 2) above 149⁰C, the viscosity of sulfur cement rapidly increases to an unworkable consistency. For these reasons, 132 to 141⁰C has been found to be an optimum temperature range to allow time for transportation, placement and finishing of sulfur concrete before solidification. The ACI 548.2R (1988) indicated that the keys to successful placing and finishing of sulfur concrete are: 1) having the sulfur concrete mass heated from 132 to 141⁰C at the moment of the placement, and 2) speed in placing and finishing.

The ACI 548.2R (1988) pointed out that if sulfur concrete has a stiff, dry appearance when is heated above 149⁰C, additional sulfur cement should not be added. When this happens, the temperature should be checked to determine whether the mixture is too hot. If it is, the mix temperature should be quickly reduced below 149⁰C. If the right amount of sulfur cement was originally added, the sulfur concrete will return to more fluid and workable consistency.

Equipment and techniques from both the concrete and asphalt technologies are used to batch, transport, place, and finish sulfur concrete. The typical equipment for a cast in place sulfur concrete operation would include the following: aggregate drying system, weigh hopper/scale for proportioning mixture materials, mixing/transporting equipment, and typical concrete hand-placing and finishing tools.

Yarbrough (1983) examined the use of conventional asphalt and concrete equipments for batching, mixing, and placing sulfur concretes in production of precast concrete items, and parking pad and pavement patch construction. The findings showed that very little difficulty was encountered in manufacturing sulfur concretes with a conventional asphalt batch plant. The modified redi-mix truck used for transporting concrete has worked well with the only apparent problem being the inability to keep the discharge chute hot enough to prevent the sulfur concretes from solidifying on the

chute. The relatively simple Portland cement concrete placing equipment worked reasonably well in placing and finishing the sulfur concretes.

2.4.1 Floor construction

ACI 548.2R (1988) guideline also added that in floor construction, compaction, strike off, and finishing of sulfur concrete can be done with conventional Portland cement concrete hand tools. Sulfur concrete should be worked in as large a mass as possible to maintain heat. The maximum dimensions for slabs are normally limited by the ability of the finishing crew to finish the concrete while it is sufficiently hot.

Once a placement section is filled with sulfur concrete it should be struck off with a simple screed. With a properly designed mixture, probe vibrators are generally not necessary. A vibrating screed is effective in achieving a relatively smooth sealed finish. After the slab is struck off, there are only a few minutes available to finish the surface (depending upon the ambient conditions). High quality wood and metal floats are recommended for the finishing. One pass over the slab surface while it is still molten to smooth and seal the surface is all that is required. If the finisher continues to work the surface as it starts to crust, the crust will tear and the finish will be destroyed. If this happens, a propane torch can be used to quickly remelt that area so that it can be refinished.

When sulfur concrete is unintentionally spilled, it should be left in a mass to solidify. No attempt should be made to quickly shovel and scrape it up because this will leave a thin film bonded to the surface, which is difficult to remove. A solidified mass of sulfur concrete can be removed more easily with a crowbar or shovel. Sulfur concrete's final (as screeded) finished texture and skid resistance are generally desirable in most industrial environments. The surface of the slab is dense, washes down easily, and provides good abrasion resistance.

Sulfur concrete floors should be poured on a dry compacted base material. If there is any moisture in the base, a vapor barrier, such as plastic sheeting, must be used over the base to prevent hot sulfur concrete from vaporizing the moisture in the base. It is best to pour sulfur concrete floors in small sections. Since sulfur concrete is poured hot and will contract on cooling to ambient temperatures, expansion joints must be provided between adjacent pours of a floor (McBee et al., 1981)

3 LABORATORY TESTS

The construction of mine haul roads using sulfur concrete requires an understanding of the physical, mechanical and chemical properties of the material. An extensive laboratory testing program consisting of unconfined compression test, sonic velocity measurement, split tensile test and freeze-thaw durability test was carried out to characterize the strength properties and deformation characteristics of different mix designs of sulfur concrete prepared from oil sands mine by-products and amine wastes such as sulfur, fly ash, coke and tailing sand. The potential geochemical interactions of sulfur concrete with the near surface environment were also studied in the laboratory for its use as road building material.

Different mix proportions were selected to produce laboratory test specimens taking into consideration the strength, workability of the mixes and production rate of waste materials at the SUNCOR oils sands mines site in Fort McMurray. The test samples were prepared either from sulfur and coke with or without fly ash addition or sulfur mixed with tailings sand and fly ash. The sulfur in all mixes was the binder while the coke, fly ash and tailings sand were aggregates.

Uni-axial compressive loading testing was performed to fully characterize the strength and deformation properties of cylindrical sulfur concrete specimens when subjected to compressive loading. From the compression test the peak compressive strength, Young's modulus and the strain at peak stress of different mix designs of sulfur concrete were evaluated. Moreover the full ranges of stress strain curves of these mixes were also obtained. Sonic velocities through cylindrical sulfur concrete samples were measured to determine elastic material properties such as Young's modulus, bulk modulus, shear modulus and Poisson's ratio of different mix designs of sulfur concrete.

Based on the uni-axial compression testing and sonic velocity measurements results and the production rate of waste materials at SUNCOR oils sands mines in Fort McMurray, three optimum mix designs were selected for further testing. Two of the optimum mixes contained coke, sulfur and fly ash and one mix contained sand, sulfur and fly ash. Split tensile test, freeze-thaw durability studies and geochemical investigation of the use of sulfur concrete in a road were studied on laboratory test samples prepared based on the optimum mix designs.

The resistance of sulfur concrete to multiple freeze-thaw cycles is very important for its application in northern locations where there are significant fluctuations of temperatures throughout a year. Rapid freeze-thaw testing was carried on sulfur concrete specimens prepared using the optimum mix designs to evaluate the effect of multiple freeze/thaw cycles on the strength and deformation characteristics of the material. The parameters measured to evaluate the freeze thaw durability differed from those recommended in the standards for Portland cement concrete. However, they were consistent with the observations found in section 2.2.3.

Geo-environmental impacts of sulfur concrete haul roads on the near surface environment were also studied. The study of geochemical interaction of sulfur concrete with the near surface environment included: short term interaction of surface exposed sulfur concrete during the construction and operational life of the haul road and long term interaction of sulfur concrete with ground water following its burial with mine wastes in the mined-out pits. These chemical (environmental) interactions were studied separately to understand the potential environmental impact of using sulfur concrete for haul roads.

3.1 Materials and Proportion

According to Environment Canada (1984), the primary source of elemental sulfur is from sour natural gas (containing hydrogen sulfide), with smaller amounts from sour

petroleum. Other sources include sulfuric acid and sulfur dioxide recovered from smelter gases, and sulfuric acid from pyrites concentrates, and minor amounts from direct mining operations. Meyer (1977) pointed out that one way to produce sulfur is from the extraction of ores mined primarily for lead, zinc, and copper. In Alberta, particularly, sulfur is recovered from hydrocarbons as a by product of the oil and gas industry. Near Fort McMurray sulfur is produced as by product of the oil sands bitumen upgrading process. Environment Canada (1984) remarked that Alberta accounts for 90 percent of the total sulfur production in Canada, with the various oil industry facilities distributed throughout the province.

Alberta's oil sands contain the biggest known reserve of oil in the world. An estimated 1.7 to 2.5 trillion barrels of oil are trapped in a complex mixture of sand, water and clay. The most prominent theory of how this vast resource was formed suggests that light crude oil from southern Alberta migrated north and east with the same pressures that formed the Rocky Mountains. Over time, the actions of water and bacteria transformed the light crude into bitumen, a much heavier, carbon rich, and extremely viscous oil. The percentage of bitumen in oil sand can range from 1% -20%. The oil saturated sand deposits left over from ancient rivers in three main areas, Peace River, Cold Lake and Athabasca. The Athabasca area is the largest and closest to the surface, accounting for the large-scale oil sands development around Fort McMurray (<http://www.oilsandsdiscovery.com>).

3.1.1 Oil sands processes

Mined oil sand, which is a mixture of bitumen (a thick sticky form of crude oil), sand, water and clay, is mined using shovels with buckets and is delivered to the ore preparation plant using large haul trucks. Crushers and sizers in the ore preparation plants prepare the ore for delivery to primary extraction plants via hydro-transport pipelines. The primary extraction plants on both sides of the Athabasca River separate raw bitumen from the sand in giant separation cells. After the bitumen is extracted

from the oil sands ore, the sand and water is disposed of into settling ponds. The settled sand is known as tailing sand.

The extracted bitumen is a complex hydrocarbon made up of a long chain of molecules. In order for the bitumen to be processed in refineries, this chain must be broken up and reorganized. Unlike smaller hydrocarbon molecules, bitumen is carbon rich and hydrogen poor. Thus, the bitumen is upgraded by removing some carbon while adding additional hydrogen to make more valuable hydrocarbon products. The bitumen is heated in furnaces and sent to drums where petroleum coke, the heavy bottom material, is removed. Coke, which is similar to coal, is used as a fuel source for the utilities plant. The fly ash is a waste product from power plants as a result of burning coke and it is collected from Electrostatic Precipitators. Depending on the requirement of the final product sulfur is removed by hydro-treating the hydrocarbon products.

3.1.2 Sulfur

Sulfur is a by-product of bitumen upgrading process. The sulfur used to produce laboratory specimens for testing was shipped from SUNCOR Oil Sands mines at Fort McMurray inside sealed barrels to University of Alberta.

Pure solid sulfur is yellow in appearance and the specific gravity ranges between 1.96 and 2.07. At normal temperatures, it has an orthorhombic crystalline structure. Upon heating, it inverts slowly at 96⁰C to a monoclinic less dense allotrope which melts at about 119⁰C. The liquid ranges in color from transparent straw yellow to dark reddish brown depending on its temperature. Viscosity changes markedly with temperature, particularly above 159⁰C. The specific gravity of liquid sulfur at 120⁰C is about 1.8.

3.1.3 Tailing sand

Tailing sand is a waste material from the extraction of oil sands. The tailing sand was transported from the tailing dams located at the SUNCOR Oil Sands mines in Fort McMurray in sealed barrels to the University of Alberta. A washed sieve analysis was performed at the University of Alberta, and the grain size distribution is presented in Figure 3.1. The tailing sand is classified as poorly graded sand (SP) under the unified soil classification system.

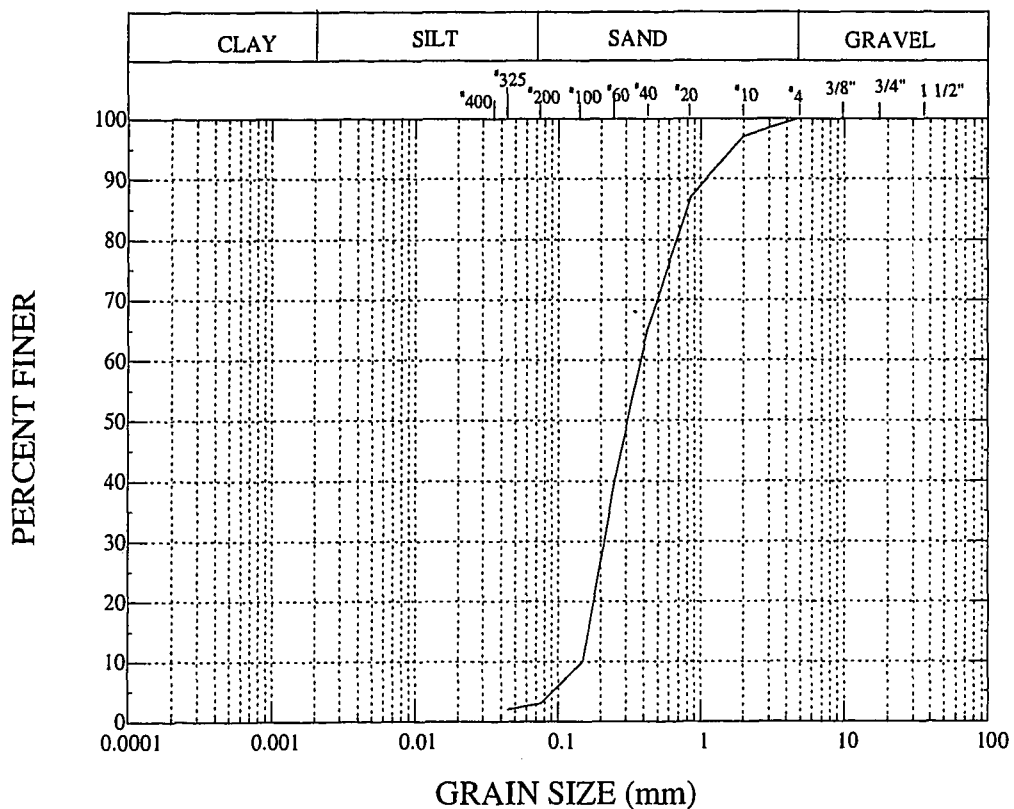


Figure 3.1 SUNCOR tailing sand grain size curve

3.1.4 Coke

Coke is a waste product of the bitumen upgrading process. Coke was transported from the SUNCOR Oil Sands mines in Fort McMurray inside sealed barrels to the

University of Alberta. Originally, the coke delivered contained large amount of coarse particles. These coke chunks were crushed to 3/8 inch minus, in the laboratory, which was required to prepare test specimens. Sieve analysis was carried out on the crushed coke samples. The grain size distribution of the coke used to produce laboratory test specimens is shown in Figure 3.2. Specific gravity of the coke ranges from 1.3 to 1.6. The coke is classified as poorly graded (SP) under the unified soil classification system.

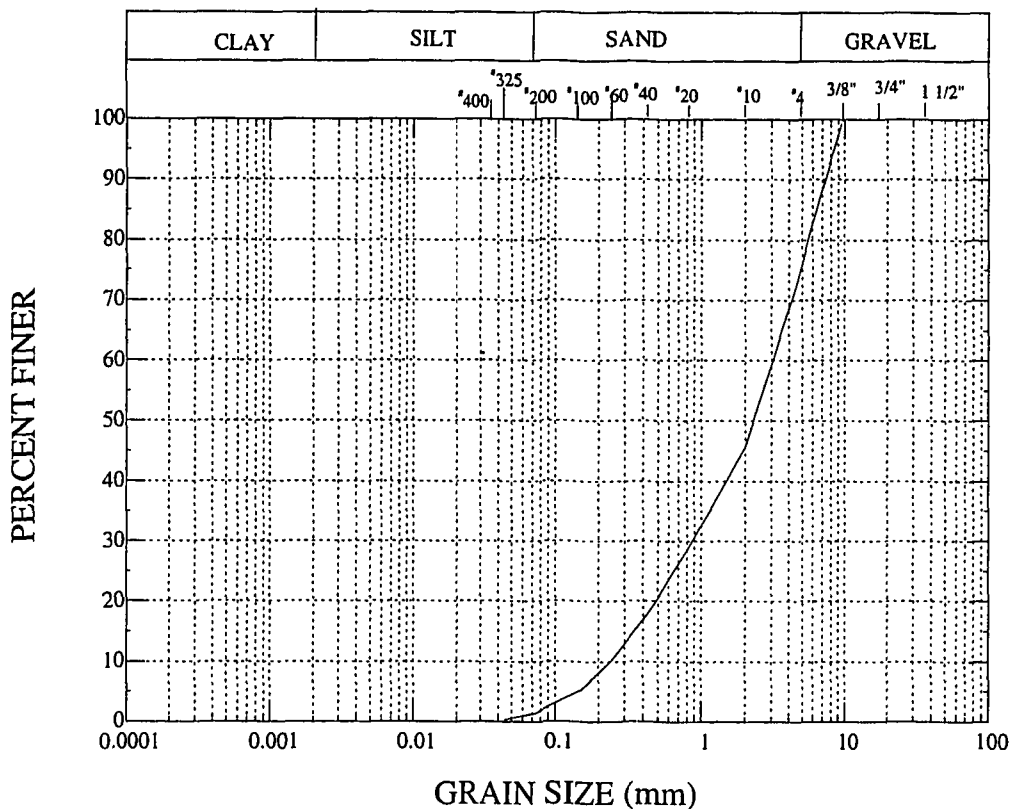


Figure 3.2 SUNCOR coke grain size curve

3.1.5 Fly ash

The fly ash is a waste material, collected from the electrostatic precipitators as a result of burning coke, in the power plant at the SUNCOR Oil Sands mine site in Fort McMurray, Alberta. The fly ash can be described as a fine grayish brown powder with

similar appearance to Portland cement. The solid particles have a specific gravity of 2.34.

3.1.6 Sulfur and aggregates proportions

Sulfur concrete test specimens were prepared in the laboratory using different mix proportions by weight of sulfur, fly ash, coke, and tailing sand. Different mix proportions were selected taking into consideration strength, workability of mixes and production rate of waste materials at the SUNCOR site. Proportions of materials used along with abbreviations used to designate each mix design are presented in Table 3.1. These abbreviations are used throughout this thesis when discussing the results.

Percentage by weight				Consistency	Key
Sulfur	Fly Ash	Coke	Tailing sand		
30	-	70	-	Sticky	30S70C
35	-	65	-	Sticky-soupy	35S65C
40	-	60	-	Sloppy	40S60C
30	2.3	67.7	-	Sticky	30S2.3FA67.7C
35	2.3	62.7	-	Sticky-soupy	35S2.3FA62.7C
30	4.6	65.4	-	Sticky	30S4.6FA65.4C
35	4.6	60.4	-	Sticky-soupy	35S4.6FA60.4C
30	20	50	-	Dry	30S20FA50C
40	10	50	-	Sticky-soupy	40S10FA50C
33.3	33.3	33.3	-	Very dry	33.3S33.3FA33.3C
30	2.3	-	67.7	Sticky	30S2.3FA67.7Sa

Table 3.1 Sulfur and aggregate proportions

3.2 Test Specimen Preparation and Measurement

Sulfur concrete is a thermoplastic material produced by hot mixing aggregate and sulfur as the binder. For it to be prepared all components of the mix have to be heated

above the melting point of sulfur, which is about 119⁰C. The sulfur needs to be molten in order to mix well with the aggregates. The aggregates also need to be heated to prevent the sulfur from quickly solidifying when in contact with the aggregates during the mixing process. After the components are mixed well the resulting mixture is cast inside a mold to produce test specimens. Upon cooling the sulfur quickly solidifies and binds the aggregates into hard concrete mass. Two mixing techniques have been used, namely the open hot mix and the dry post heating mix.

The open hot mix process requires the sulfur to be molten and the aggregates to be heated before mixing. This process produces toxic gases such as Hydrogen Sulfide (H₂S) and Sulfur Dioxide (SO₂). However, as long as the temperature of the mix is maintained below about 149⁰C, the concentrations of these gases remain below the Maximum Allowable Concentrations (MAC) suggested by the American Conference of Governmental Industrial Hygienists (ACGIH) (Saylak et. al., 1981).

In the dry mix post heating process, granular sulfur and aggregates are mixed before heating, and then enough heat is applied for the sulfur to melt. The mixing process could be performed at room temperature, and the temperature is increased in a sealed container controlling the emission of gases, but even then, avoiding some exposure to fumes is difficult.

Because of the simplicity of the equipment required the open hot mix process was used to produce the test specimens in the laboratory. A respirator, goggles and gloves were worn at all times during the sample preparation process, and the specimens were prepared in a fume hood to vent gas emissions.

The materials used to prepare the concrete for testing (sulfur, coke, fly ash and tailing sand) were shipped from SUNCOR Oil Sands in Fort McMurray inside sealed barrels to University of Alberta. Different mix proportions were selected taking into consideration strength, workability of mixes and production rate of waste materials at

the SUNCOR site. Samples were prepared either from sulfur and coke with or without fly ash or sulfur mixed with tailings sand and fly ash. The sulfur in all mixes was the binder while the coke, fly ash and tailing sand were aggregates.

3.2.1 Sample preparation procedure

The ACI 548.2R (1988) requires that sulfur concrete test specimens be cast in steel molds in the mixing and working temperature range of 132⁰C to 141⁰C. The molds need to be preheated to approximately 138⁰C before adding the mixture. The specification also requires compacting the sulfur concrete as it is added to the mold by tamping with a heated 16 mm hemispherical tipped rod. The samples should be cast in an upright position and the specimen surfaces are finished and allowed to cool to room temperature before being removed from the molds. This procedure was followed during the preparation and casting of all samples reported in this thesis.

The minimum and maximum temperatures of sulfur concrete mixture is controlled because: a) the sulfur cement melts at 119⁰C, b) above 149⁰C there might be a potential evolution of toxic gases such as Hydrogen Sulfide and Sulfur Dioxide, and c) above 159⁰C the viscosity of sulfur concrete rapidly increases to an unworkable consistency. For all these reasons 132⁰C to 141⁰C was found to be an optimum temperature range for sulfur concrete production, casting and finishing before solidification.

The test specimens for unconfined compression test, sonic velocity measurement, split tensile test and freeze-thaw durability tests were approximately 76 mm in diameter by 152 mm high, with height to diameter ratio of 2. This dimension is appropriate to facilitate the investigation of the stress-strain curve of the materials and determine the Young's modulus (ACI 548.2R, 1988). Also Malhotra (1978) and ACI 548.2R (1988) pointed out that small cylinders gained strength faster; thus to investigate the compressive strength this size was convenient. Test specimens for geochemical

investigation studies were 152 mm in diameter by 76 mm high prepared inside 152 mm by 305 mm plastic cylinders.

Laboratory ovens were used to melt the sulfur and heat the aggregates to the required mixing temperature ranging from 140⁰C to 145⁰C. A preheated mixing pot was used to mix the heated aggregate and the molten sulfur until a homogeneous fluid mixture was obtained. Samples were cast in preheated molds and were compacted in two or three layers using a heated flat circular tamper. After each tamping, the tamper was returned to the oven to be heated for compaction of the next layer. The sample was tamped to a height above the top of the mold and trimmed with a preheated steel trimmer. Care was taken during trimming to maintain the compaction and provide a finished surface. After the samples were cast in the molds, they were cured in air at room temperature (20⁰C) in an upright position. The molds were removed after the specimens cooled to room temperature and samples were ready for testing. The mixing spoon, tamper, and trimming tool were all preheated to the same temperature range as mentioned above.

The 35S65C, 35S2.3FA62.7C, 35S4.6FA60.4C, 40S10FA50C, and 40S60C mixtures were easy to mix. Their consistency varied from the very sticky-soupy 35S65C mix to the sloppy 40S60C. The 30S70C, 30S2.3FA67.7C, 30S2.3FA67.7Sa, and 30S4.6FA65.4C, mixtures were slightly difficult to mix. They were slightly thicker with sticky consistency. The 30S20FA50C mix was dry, while the 33.3S33.3FA33.3C mix was very dry, and both were very difficult to mix during sample preparation.

3.2.2 Measurements of specimen dimensions and unit weight

The diameter and height of the cylindrical samples were measured, following a minimum of 24 hours after curing in air at room temperature, using a digital caliper. Diameter readings were taken at three locations, top and bottom ends and at the middle of the sample. At each location two measurements were taken at right angles to each other. Two sample height measurements were taken at right angles to each other.

The average of these readings was used in the calculation of cross sectional area and volume of sample.

The weight of the samples was taken by using laboratory scales with a precision of 0.1 g. The unit weights of triplicate samples of the different mixes were calculated and the statistical results are given in Table 3.2. Density of individual samples tested is presented in Table A-1 (Appendix A).

Mix Type	Density (kg/m ³)			
	Mean	Minimum	Maximum	Standard Deviation
30S70C	1040	1036	1045	3.68
35S65C	1158	1129	1187	23.68
40S60C	1222	1198	1253	23.1
30S2.3FA67.7C	1064	1040	1078	16.86
35S2.3FA62.7C	1193	1151	1223	30.59
30S4.6FA65.4C	1080	1060	1093	14.52
35S4.6FA60.4C	1217	1152	1250	46.18
30S20FA50C	1358	1310	1386	34.3
40S10FA50C	1462	1431	1493	25.32
33.3S33.3FA33.3C	1303	1290	1327	16.78
30S2.3FA67.7Sa	2170	2079	2261	91

Table 3.2 Unit weight statistics of the mix designs

3.3 Uni-axial Compression Test

Uni-axial compression test was carried out by loading different mix designs of 76 mm x 152 mm cylindrical sulfur concrete specimens to failure to determine their strength and deformation characteristics under compressive loading. The compressive load and axial displacements were measured throughout the test. The peak compressive strength, the Young's modulus, the strain at peak stress and the full range of the stress - strain curve were determined from this test.

3.3.1 Test procedure and equipments

The test was carried out following ASTM C 39 test procedure as recommended in ACI 548.2R (1988). Details of the testing procedure are given in Appendix B. Figure 3.3 shows the compression test set up. The sulfur concrete samples were capped with sulfur mortar before testing (ASTM C 617).

Triplicate samples prepared using the mix designs shown in Table 3.1 were tested to failure, and measurements of axial deformations and loads were recorded. Load controlled hydraulic compression machine was used during the test. The machine was a Baldwin manufactured by Southwark Tate-Emery Testing Machines, with a maximum capacity of 1350 KN. The Baldwin testing machine had been calibrated prior to carrying out the tests. The machine has two dial gauges, one for reading up to 220 KN and the other for up to 1350 KN of applied load. Two control valves are used in its operation, one for loading and another one for unloading. It has two steel bearing blocks. The upper block is spherically seated and fixed, whereas the bearing block at the bottom moves vertically up applying the compressive load to the specimens or down to release the applied load.

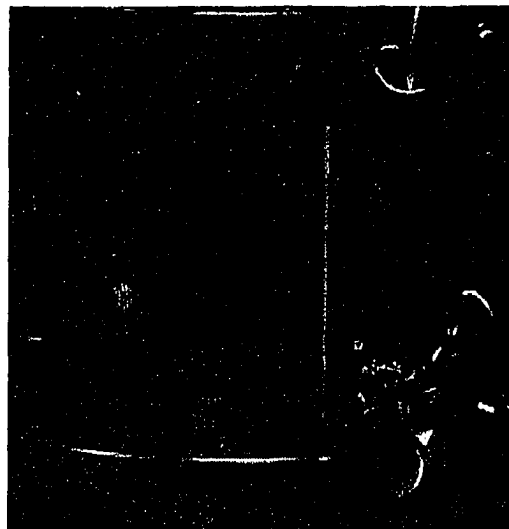


Figure 3.3 Compression test set up

The vertical displacements of the test specimens were measured using the average of two displacement transducers located at diametrically opposite positions approximately at the same distance from the center of the specimen. These transducers were linear variable differential transducers (LVDT) with a built in 24 Volt DC excited carrier oscillator and phase sensitive demodulator systems. The transducer's model was the 24DCDT-250, manufactured by Hewlett-Packard, with ± 0.25 inch displacement range and proportioned with a scale factor of 28 Volt/inch (1.1 Volt/mm). The full scale output of these displacement transducers was 7 Volts, with a maximum non linearity of $\pm 0.5\%$ of the full scale. This type of transducer provides high accuracy and sensitivity. Figure 3.3 shows the compression test set up. An acrylic casing was used to protect the LVDT transducers from danger of sample breakage.

The applied compressive load was measured using a load cell (not shown in Figure 3.3), at the same interval of time as the LVDT transducers were measured. The readings of the transducers and the load cell were recorded through a data logger (Data Dolphin DD-124 manufactured by Optimum Instruments, Inc.) in 3 to 5 seconds interval. The reading precision of this device was about 1×10^{-7} Volts. The maximum load applied on the samples was read from the machine dial gauge. The loading rate used was between approximately 75 and 150 kPa/sec, which is about half of the specified range to obtain accurate readings as failure is approached. The failures were usually sudden and noisy, characteristic of failure of brittle material and sometimes were explosive. It was not possible to record a post peak response for most of the specimens tested.

3.3.2 Test results

The results of the compression test are summarized in Figures 3.4 to 3.7 and Tables 3.3 and 3.4. Figure 3.4 presents the typical stress strain curves of sulfur concrete specimens produced from coke and sulfur. Figure 3.5 depicts the typical stress strain curves of sulfur concrete specimens produced from coke, sulfur, and small amounts of

fly ash (2.3 and 4.6% by weight). Figure 3.6 presents the typical stress strain curves of sulfur concrete specimens produced from coke, sulfur, and larger amounts of fly ash (10 to 33.3 % by weight). Figure 3.7 shows the typical stress strain curve of sulfur concrete specimen produced from tailing sand, sulfur, and fly ash. Stress-strain curves of all samples tested are presented in Figures A-1 to A-11(Appendix A).

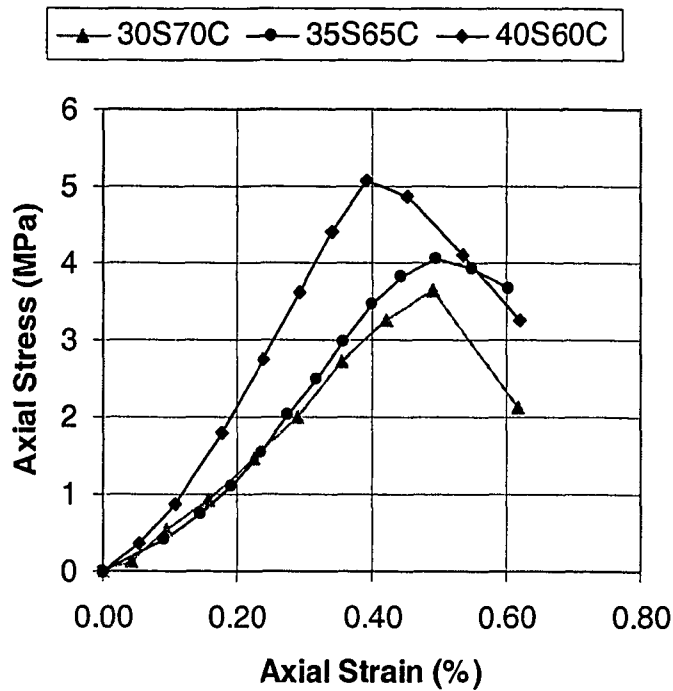


Figure 3.4 Stress-strain curves of coke and sulfur mixes

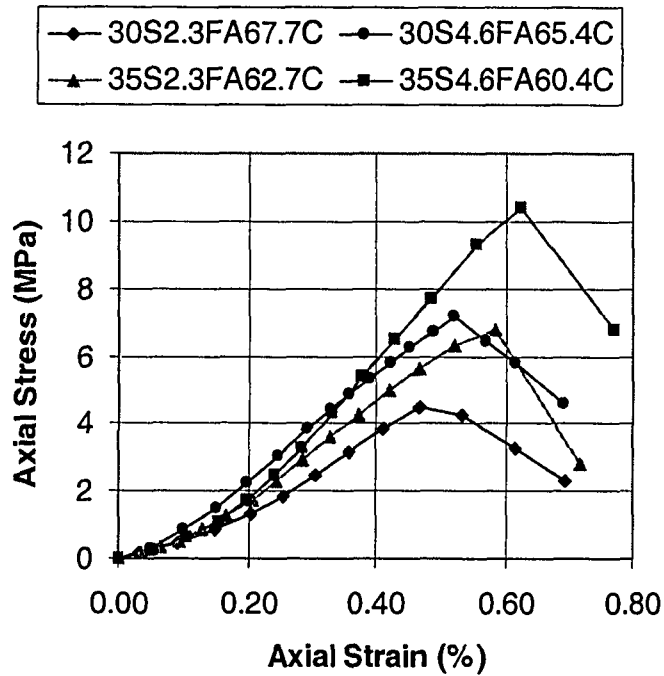


Figure 3.5 Stress-strain curves of coke, sulfur, and 2.3 to 4.6 % fly ash mixes

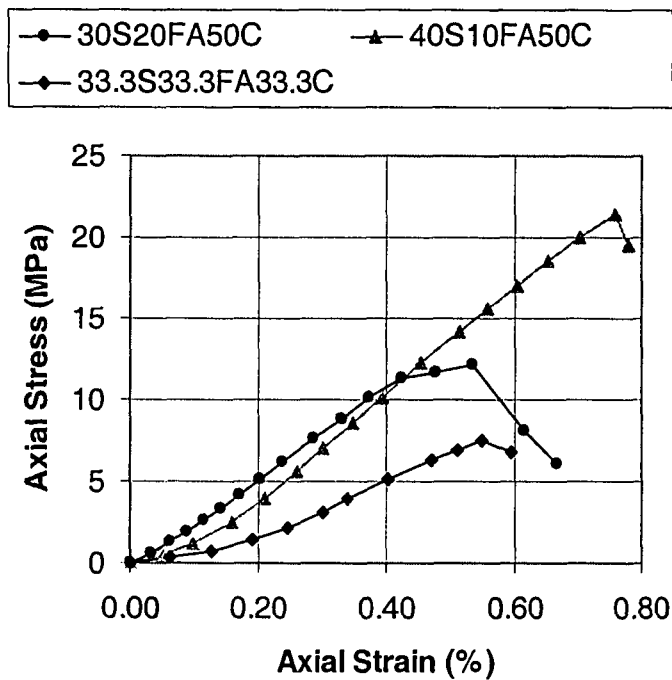


Figure 3.6 Stress-strain curves of coke, sulfur, and 10 to 33.3% fly ash mixes

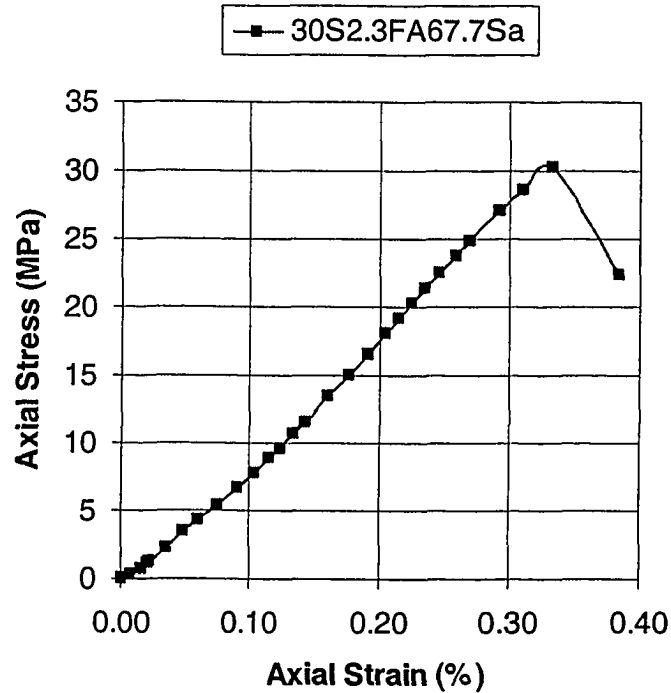


Figure 3.7 Stress-strain curve of tailing sand, sulfur, and fly ash mix

Table 3.3 gives the statistical values of the peak compressive strengths of all the mixes that were tested. It gives the minimum, maximum, mean and standard deviations of the triplicate samples of the different mix designs tested. Tables 3.4 also presents the same statistical data for the Young's modulus values. Peak compressive strength and Young's modulus of individual samples tested are presented in Tables A-2 and A-3 (Appendix A). The test results indicate that sulfur concrete is strong and stiff material. In fact it is much stronger and stiffer than presently used haul road construction materials at SUNCOR oil sands mines, like limestone and gravel.

Mix Type	Peak Strength (MPa)			
	Mean	Minimum	Maximum	Standard Deviation
30S70C	3.65	2.79	4.22	0.617
35S65C	4.57	3.92	5.3	0.567
40S60C	5.17	3.38	6.77	1.208
30S2.3FA67.7C	4.75	4.67	4.82	0.075
35S2.3FA62.7C	7.57	7.4	7.66	0.120
30S4.6FA65.4C	8.01	7.86	8.27	0.120
35S4.6FA60.4C	9.75	10.94	8.07	1.221
30S20FA50C	12.6	12.44	12.76	0.131
40S10FA50C	24.49	23.14	26.52	1.463
33.3S33.3FA33.3C	7.62	7.33	8.15	0.375
30S2.3FA67.7Sa	29.1	27.13	31.0	1.935

Table 3.3 Peak strength statistical data

Mix Type	Young's Modulus (MPa)			
	Mean	Minimum	Maximum	Standard Deviation
30S70C	850	750	950	81.65
35S65C	1133	950	1300	143.26
40S60C	1533	1350	1700	143.372
30S2.3FA67.7C	1300	1300	1300	0
35S2.3FA62.7C	1600	1550	1650	40.8
30S4.6FA65.4C	1500	1500	1500	0
35S4.6FA60.4C	2033	1800	2200	169.97
30S20FA50C	2750	2600	2850	108.01
40S10FA50C	3150	3050	3250	81.65
33.3S33.3FA33.3C	1900	1800	2000	81.65
30S2.3FA67.7Sa	9750	9300	10200	450

Table 3.4 Young's modulus statistical data

3.4 Sonic Velocity Measurement

Sonic velocities through the sulfur concrete samples were measured to determine elastic material properties such as: Young's modulus, bulk modulus, shear modulus and Poisson's ratio based on the knowledge of material's sound velocity and density. The velocities were measured using ultrasonic pulsed technique, where the sound velocity is obtained from the ratio of the ultrasonic path length to the pulse transit time in the material. The test was carried out on triplicate 76 mm x 152 mm samples of the different mix designs given in Table 3.1.

The ultrasonic pulsed wave transit time technique is a well established method for measuring the sound velocity in materials, as demonstrated by the existent ASTM E-494 "standard practice for measuring ultrasonic velocity in materials". As the name implies, it involves the transit time measurement of short wave pulses (by necessity less than sample propagation times) traveling over a known path through the bulk of the sample. The ratio of the path length to the transit time yields the velocity. The technique actually measures an average of the velocity over the path length taken by the pulse. Pulse durations on the order of, or less than microseconds with megahertz carrier frequencies are typical. High rate repetitive pulse techniques on the order of kilohertz allow for both rapid and accurate transit time measurements using time averaging techniques.

For short duration wave pulses with wavelengths much less than the sample dimensions, two normal modes of bulk wave propagation pertain to extended isotropic media. They are the longitudinal and shear modes with respective velocities V_L and V_S . Longitudinal waves, sometimes referred to as compression waves, alternately compress and dilate the material lattice (i.e., generate compressive and tensile strains) as they pass by. The resulting particle motion of the material is parallel to the direction of wave propagation. Shear waves, on the other hand, generate particle displacements perpendicular to the propagation direction, causing the material lattice to shear as the

waves pass by. From these two wave speeds and the density (ρ), all the elastic parameters of an isotropic material can be calculated: the Young's, bulk, and shear moduli, and Poisson's ratio. The relationships are (Blessing, G. V. 1990):

$$\text{Young's modulus} = \rho V_S^2 (3V_L^2 - 4V_S^2) / (V_L^2 - V_S^2)$$

$$\text{Bulk modulus} = \rho (V_L^2 - (4/3) V_S^2)$$

$$\text{Shear modulus} = \rho V_S^2$$

$$\text{Poisson's ratio} = (V_L^2 - 2V_S^2) / (2V_L^2 - 2V_S^2)$$

3.4.1 Test equipment and specimen

A terrametrics sonic velocity equipment model 55051600 was used for the test. The complete sonic velocity equipment consisted of a pulse generator with oscilloscope trigger, pulsing and sensing heads containing piezo electric crystals, cables for connection to an oscilloscope, calibration cylinders for periodic checking of the time constant of the heads, and an oscilloscope for displaying the pulses and measuring the travel time.

3.4.1.1 Sonic pulse generator

The pulse generator is designed to put out a voltage pulse with maximum amplitude of around 800 volts. The pulse is in the form of a rapid rise time with exponential decay. Because of the high energy output, the mechanical pulse produced by the pulsing head is easily picked up by the sensing head where it is transformed into an electrical signal which can be displayed on the scope without the need for pre-amplification.

The repetition rate of the output pulse is controllable and can be set between 30 and 120 pulses per second. Generally the best pulse rate is around 60 pulses per second, which produces a steady trace on the oscilloscope.

3.4.1.2 Pulsing and sensing heads

The pulsing and sensing heads are identical in every respect and are interchangeable. Pulsing and sensing heads are available in pairs, one type is designed to generate and sense compression waves, another type is designed to generate and sense shear waves.

The pulsing and sensing heads contain piezoelectric crystals to generate either compressional or shear waves. The transducers are housed in magnesium, which protects them from stray electromagnetic pick-up, and mechanical damage. The use of the magnesium improves the energy transmission across the face plate. The energy is further enhanced by pressurizing the crystal and by the use of phenol salicylate as a bonding agent between the head and the surface of the test sample. Resonant frequencies of the crystals are 600 kHz for the compression wave head and 800 kHz for the shear wave heads.

3.4.1.3 Test specimens

Test specimens require two flat parallel surfaces between which the travel times of the compression and shear waves will be measured. The faces should be flat ± 0.001 in. and parallel ± 0.005 in. per inch separation. The ratio between the pulse travel distance between parallel faces and the minimum lateral dimension should not exceed five, if reliable free medium velocities are required. Similarly the minimum lateral dimension of the test specimen should be at least ten times the wavelength of the compressive wave.

3.4.2 Test procedure

The diameter and height of test specimens were measured using a digital caliper. Diameter readings were taken at three locations, top and bottom ends and at the middle of the sample. At each location two measurements were taken at right angles to each other. Two sample height measurements were taken at right angles to each other. The average of these readings was used to calculate volume of sample. The weight of

the sample was taken by using laboratory scales with a precision of 0.1 g. Density of the specimens was then calculated from weight to volume ratio.

The pulsing and sensing heads were attached to the flat ends of the test specimen by means of molten phenol salicylate for strong bonding. The pulsing and sensing heads were connected to the pulse generator and to the oscilloscope by means of co-axial cables with MHV connectors. The trigger pulse on the pulse generator is also connected to the oscilloscope. The sonic velocity measurement test set up is shown in Figure 3.8.

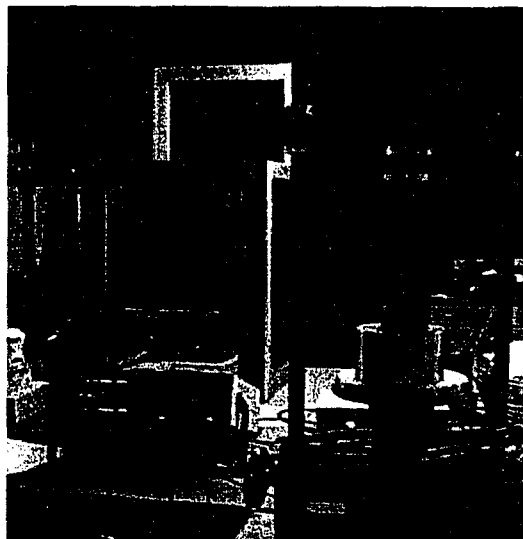


Figure 3.8 Sonic velocity measurement test set up

The trigger pulse was transmitted through the samples. Dual beam oscilloscopes were used to display both trigger pulse and output pulse. Pulse travel times were measured by using the delayed sweep controls on the oscilloscope. The first arrival of the compression wave was very easily determined since it is marked by the first deviation of the wave form from the initial horizontal straight line. Generally the polarity of the wave form is such that the wave will first deviate in a downward direction. The travel time measurement is then made from the start of the trace to the start of the first downward deviation. Actually, a minute portion of the travel time is not recorded due

to the fact that the scope triggers after about 1 μ seconds after the pulse is initiated. However, this small time is accounted for when the time delay involved in the waves passing through the pulsing heads is corrected for.

The first arrival time of shear waves are not so readily discernible because the shear plate type of piezo electric crystal will invariably generate some compression wave components which will arrive ahead of the shear waves. Some time after the compression wave has arrived at the sensing head; the shear wave arrives and causes a large upward sweep of the oscilloscope trace. The travel time of the shear wave is obtained simply by measuring from the start of the trace to the start of the strong upward sweep, which usually occurs at the bottom of a valley.

3.4.3 Test results

Summary of the sonic velocity measurement test is presented in Table 3.5. Results of individual samples tested are presented in Table A-4 (Appendix A).

Mix Type	Density (kg/m ³)	Young's Modulus (MPa)	Bulk Modulus (MPa)	Shear Modulus (MPa)	Poisson's Ratio
30S70C	1040	900	550	400	0.214
35S65C	1158	1250	800	500	0.237
40S60C	1220	1300	1150	500	0.280
30S2.3FA67.7C	1064	1400	1100	550	0.288
35S2.3FA62.7C	1193	1700	1800	650	0.342
30S4.6FA65.4C	1080	1550	1700	600	0.343
35S4.6FA60.4C	1217	1600	3500	600	0.393
30S20FA50C	1358	2900	3600	1050	0.367
40S10FA50C	1462	3200	4200	1150	0.375
33.3S33.3FA33.3C	1303	2000	1900	750	0.324
30S2.3FA67.7Sa	2170	10700	12000	3950	0.388

Table 3.5 Summary of the sonic velocity measurement test

3.5 Optimum Mix Designs

Based on uni-axial compression test and sonic velocity measurements results and production rate of the waste materials at SUNCOR Oil Sands mines, three optimum mix designs were selected for split tensile test, the freeze-thaw durability studies and geochemical investigation of the use of sulfur concrete in a road. The selected mixes were 30S2.3FA67.7C, 35S2.3FA62.7C, and 30S2.3FA67.7Sa. The first two mixes contained coke, sulfur and fly ash and the third one contained sand, sulfur and fly ash. Compressive stress - strain curves of samples prepared using the optimum mix designs are shown in Figure 3.9.

As shown in Figure 3.9, sulfur concrete made from coke is much weaker and deformable than the concrete made from tailing sand. This is mainly because individual coke particles are much weaker than the quartzite tailing sand particles. The dramatic decrease in stiffness is associated with the observation that coke sulfur concrete is porous with many open voids, whereas tailing sand sulfur concrete has fewer visible pores.

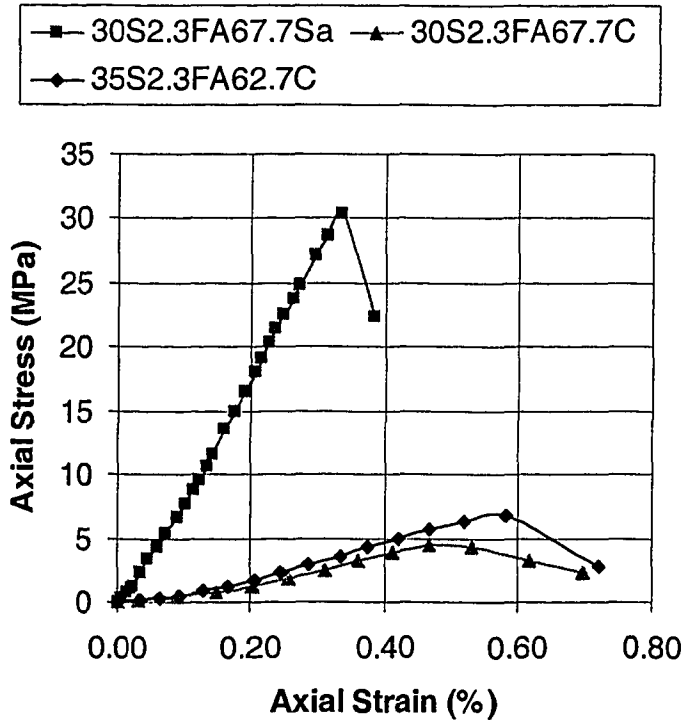


Figure 3.9 Stress-strain curves of optimum mix design samples

3.6 Split Tensile Test

The tensile strength of sulfur concrete specimens was investigated by using the split cylinder tensile test. The splitting tensile test rather than the direct tensile test was selected for investigating the tensile strength of sulfur concrete cylinders because the former test procedure is simpler.

3.6.1 Test procedure and equipments

ASTM C496 test procedure was followed during the entire test, as recommended by the ACI 548.2R (1988). Details of the testing procedure are given in Appendix B. The split tensile test consists of applying a diametric compressive force along the length of a cylindrical concrete specimen at a rate that is within a prescribed range until failure occurs. This loading induces tensile stresses on the plane containing the applied load and relatively high compressive stresses in the area immediately around the applied

load. Tensile failure occurs rather than compressive failure because the areas of load application are in a state of tri-axial compression, thereby allowing them to withstand much higher compressive stresses than would be indicated by the uni-axial compressive strength test results.

A displacement controlled screw type compression testing machine, Instron Universal Testing Instrument Model 4206 was used for applying the compression load on the samples tested. The machine was equipped with a built in load cell with a maximum load capacity of 150 KN. The loading rate was set to 1mm/min. Because the built in axial deformation measuring mechanism was found in error, LVDT differential transducers (used during the compression test) was used to measure deformations.

The split tensile test was carried out on duplicate 76 mm x 152 mm cylindrical test specimens, prepared based on the optimum mix designs. After the specimens were prepared and cured in air at room temperature, two perpendicular diametrical lines were marked on both faces of the cylinder in such a way that the lines at the opposite ends are on the same plane. Lines were drawn along the sides of the cylinder connecting the diametric lines on opposite faces to make a plane. The longitudinal lines were marked to locate the loading plane and LVDT differential transducers perpendicular to the loading plane, between cylinder ends. The test set up is shown in Figure 3.10.

The LVDT differential transducers were used to measure the displacement at failure. The specimens were wrapped at their ends by using plastic tapes to protect the transducers from potential damage caused by broken sample pieces at failure. The tape was wrapped very loosely so as not to have an effect on the test. The applied load was measured by using the same load cell used for compression test. The maximum load at failure was read from the Baldwin compression machine gauge.

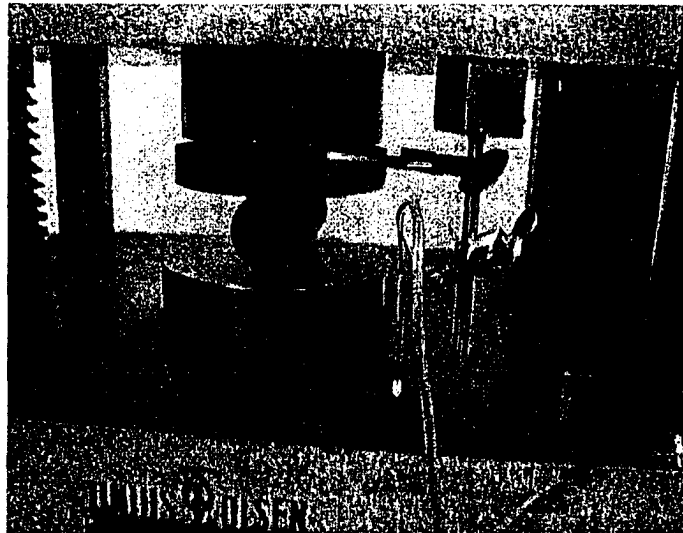


Figure 3.10 Split tensile test set up

3.6.2 Test results

The test results from duplicate samples are summarized in Table 3.6. Results of all the split tensile tests are included in Table A-5 (Appendix A). Split tensile stresses versus vertical strain curves are also plotted in Figures A-12 to A-14 (Appendix A).

Mix Type	Density (kg/m³)	Tensile strength (σ_t)(MPa)	Compressive strength (σ_c)(MPa)	Ratio of σ_t/σ_c (%)
30S2.3FA67.7C	1075	0.54	4.75	11.4
35S2.3FA62.7C	1191	0.88	7.57	11.6
30S2.3FA67.7Sa	2145	1.96	28	7.0

Table 3.6 Split tensile test summary

3.7 Freeze Thaw Durability Test

The resistance of sulfur concrete to multiple freeze thaw cycles is very important for its application as road construction material in northern locations, where large

temperature fluctuations throughout a year exist. Previous studies have shown that sulfur concrete prepared from unmodified sulfur has very poor durability when subjected to multiple freeze thaw cycles (Malhotra, 1973, Beaudoin and Sereda, 1974, Loov, 1975, Sullivan and McBee, 1976). ACI 548.2R (1988) recommended evaluating the freeze thaw durability of concrete subjected to multiple freeze thaw cycles according to ASTM C 666 test procedure A. Details of the testing procedure are given in Appendix B.

Procedure A involves freezing and thawing sulfur concrete samples in water. It is harsher than procedure B, which involves freezing in air and thawing in water, because the continual presence of water causes the available void spaces to be penetrated more rapidly in procedure A than in B. Furthermore, the relative dynamic modulus of elasticity must be determined at selected freeze thaw cycles in accordance with ASTM C215. If the measured relative dynamic modulus is less than 60% of the initial modulus before 300 freeze thaw cycles then the test should stop and the samples are assumed to have failed the test.

Although ASTM C666 is recommended by ACI 548.2R, it was not followed rigorously. Based on previous study (Cohen 1987) one can argue that the dynamic modulus of elasticity did not accurately represent the degree of deterioration of sulfur concrete during rapid freezing and thawing test. Therefore it was decided to perform a uni-axial compressive test thus measuring the static modulus of elasticity, compressive peak strength and compressive yield strength in order to evaluate the effect of multiple freeze thaw cycles on the strength and deformation properties of sulfur concrete.

3.7.1 Test procedure and equipments

The objective of the test was to evaluate the durability of sulfur concrete specimens subjected to rapid freeze thaw cycles by carrying out compression test instead of measuring the dynamic Young's modulus. From the compression test, the static

Young's modulus, the peak compressive strength, and the yield compressive stress were determined. They were then compared to the corresponding values of the original samples (before application of any freeze thaw cycle). The test was carried out on duplicate 76 mm x 152 mm cylindrical sulfur concrete samples prepared using the optimum mix designs.

Because compression test is destructive, the tested samples cannot continue to be used in the freeze thaw cycles. For this reason, four groups of samples, two per each mix type, were prepared for the test. Compression test was carried out on samples subjected to 50, 100, 200 and 300 freeze thaw cycles. All the samples started the freeze thaw cycle after two weeks of curing in air at room temperature (20°C).

An additional three samples, one from each mix, were prepared and a thermo-electrical transducer was inserted into the specimens at about the mid height to measure their temperature. The transducers were Omega Precision Interchangeable Thermistors model 44007, with a resistance of 5000 Ohms at 25°C. The thermistors were manufactured from oxides of nickel, manganese, iron, cobalt, magnesium, titanium, and other metals. They provide precise temperature information, and their accuracy was $\pm 0.2^{\circ}\text{C}$ in a working range of -80°C to 120°C . The temperature data of the thermistors were recorded using a data logger. The model of the data logger was Data Dolphin DD-124 manufactured by Optimum Instruments Inc. The reading precision of the device was about 1×10^{-7} Volts. The temperatures of the room and the heat transfer media (water or air) were verified by using regular mercury thermometers.

Procedure A of ASTM C666 requires that the samples must be in water during the freezing and thawing periods. Specimens were cast in plastic containers leaving a gap of approximately 3.5 mm around the cylinders. A twisted rubber band approximately 2 mm thick was placed around the top third of the specimens ensuring gap was maintained between the sample and the container. An O ring 2.5 mm thick and

approximately 50 mm in diameter was used at the bottom to support the sample leaving about 2.5mm gap between the sample and plastic mold.

The test requires alternately lowering sample temperature from $+4.4^{\circ}\text{C}$ to -17.8°C and raising it from -17.8°C to $+4.4^{\circ}\text{C}$ in cycles not less than 2 hours and no more than 5 hours duration. It also requires that not less than 25% of the time should be used for thawing. At the end of the cooling period, the temperature at the center of the specimens should be $-17.8 \pm 1.7^{\circ}\text{C}$, and at the end of the heating period, the temperature should be $4.4 \pm 1.7^{\circ}\text{C}$. During the entire experiment, the maximum and minimum temperature should be between 6.1 and -19.4°C , respectively.

The freeze thaw cycles were performed by moving the samples from freezer to cooler room and vice versa. Setting the temperatures of the freezer and cooler rooms keeping all the test requirements was not easy. After a week of trial and error, it was found that for the sand sulfur concrete specimens freezer room temperature of -19°C and cooler room temperature of 10°C was appropriate. For freezing, the samples were randomly placed in the freezer room in front of the cooling fans during every freezing period. It took approximately 1 hour for the sample temperature to reach about -16.5°C . For thawing, the plastic containers were randomly introduced into plastic tubs of water at 10°C , as shown in Figure 3.11. The samples took about 1.5 hours to thaw. Keeping the initial water temperature constant at 10°C for each thawing period was difficult because the time the water required to recover its initial temperature after used for thawing was longer than the time the samples were in the freezer. Therefore changing the water was required to keep the initial temperature to 10°C . During the thawing period the temperatures were monitored continuously to prevent the samples from reaching temperatures higher than the 6.1°C .

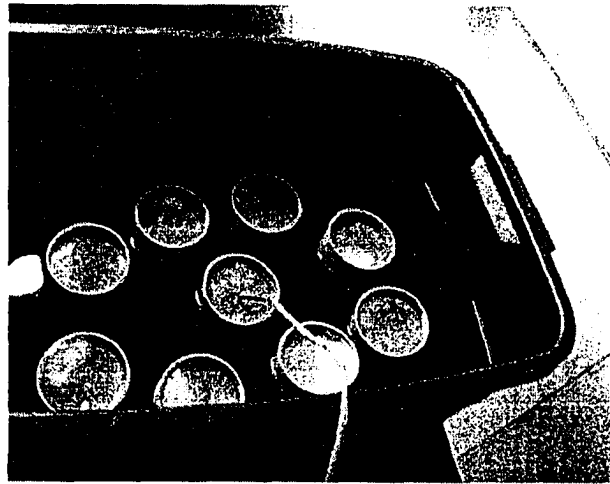


Figure 3.11 Sand sulfur concrete specimens during thawing in water

For the coke sulfur concrete specimens freezer room temperature of -19°C and cooler room temperature of 15°C was found appropriate. For freezing, the samples were randomly placed in the freezer room in front of the cooling fans during every freezing period. It took about 1.5 hours for the sample temperature to reach about -16.5°C . For thawing, the plastic containers were randomly placed in front of the cooling fans in the cooler room at 15°C . The samples took approximately 2 hours to thaw. During night times all the sand and coke concrete specimens were frozen to -19°C inside the freezer room.

The freeze thaw cycle was started at the same time on all the sand and coke concrete specimens. After 24 cycles pop-outs along the horizontal construction joints were observed in the coke concrete samples. The construction joints were created when the samples were prepared in multiple layers. The pop outs along the joints were followed by high degree of sample deterioration that led to sample disintegration. Consequently, it was determined that the coke samples had failed the freeze thaw test and they were abandoned. Failed specimens are shown in Figures 3.12 and 3.13. The main reason for the failure was that coke particles are porous so water surrounding the samples percolated into the pores and expanded during freezing breaking the particles apart. The test continued on the sand concrete specimens. Unconfined compression testing

was carried out on the sand sulfur samples after they were subjected to 50, 100, 200 and 300 freeze thaw cycles.

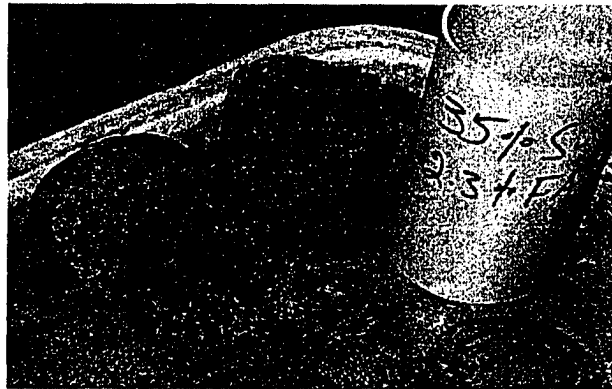


Figure 3.12 Construction joint on 35S2.3FA62.7C sample

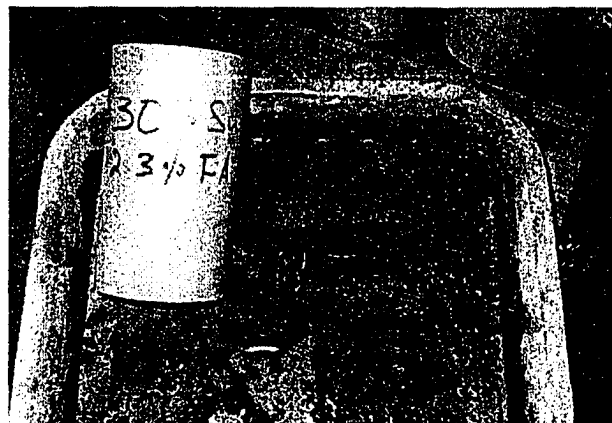


Figure 3.13 30S2.3FA67.7C sample failed after 24 cycles

3.7.2 Test results

A uni-axial compression test was carried out on the specimens at the end of each specified freezing and thawing periods. The test was performed only on the sand-sulfur concrete specimens, as the coke-sulfur samples failed before reaching the first 50 freeze thaw cycles. From the compression test, peak compressive strength, yield strength and Young's modulus were determined and compared with the values prior to any freeze-thaw cycle to evaluate the damage caused by the freeze-thaw cycle.

Number of freeze-thaw cycles	Young's modulus (MPa)	Peak strength (MPa)	Yield strength (MPa)
0	9750	29.5	25.5
50	6700	25	23
100	6350	23.5	21
200	5530	22	19.5
300	3925	17	16.5

Table 3.7 Rapid freeze-thaw test summary

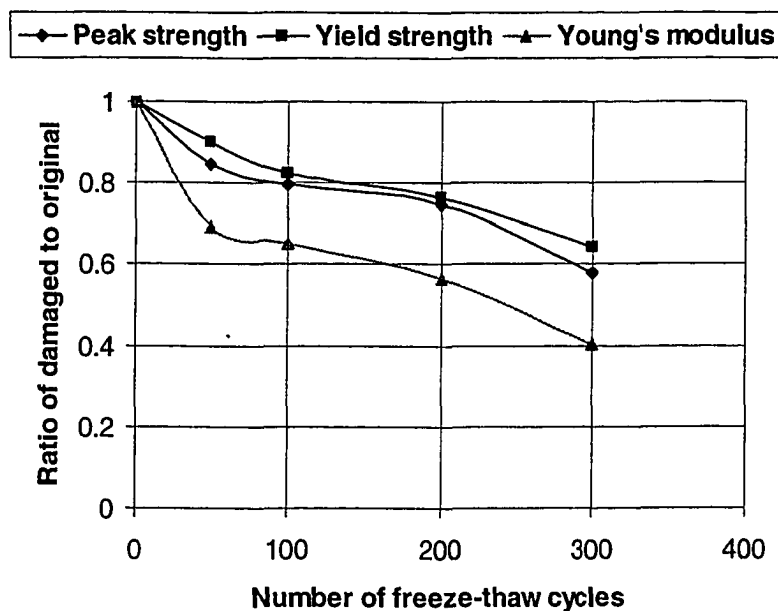


Figure 3.14 Effect of freeze thaw cycle on peak strength, yield strength and Young's modulus

Table 3.7 summarizes the rapid freeze-thaw test results. Figure 3.14 plots the variation of peak compressive strength, yield strength and Young's modulus with the number of freeze thaw cycles. The stress-strain curves are shown in Figures A-15 to A-19 (Appendix A). The test results showed that there is a considerable degradation of the material when subjected to multiple freeze thaw cycles. There is 42% reduction in peak strength, 36% reduction in yield strength and 60% reduction in Young's modulus after 300 freeze-thaw cycles. It is to be noted that even though the samples had

deteriorated, the strength and deformation characteristics after 300 freeze-thaw cycles indicated sand-sulfur concrete is still much better than the existing road building materials in crushed aggregate and limestone.

3.8 Geochemical Investigation

3.8.1 Potential geo-environmental impact associated with sulfur concrete haul roads

The geo-environmental impacts of sulfur in contact with atmosphere and water are primarily associated with the production of sulfuric acid due to microbial oxidation. The presence of elemental sulfur in and of itself is generally not detrimental to soil bacteria population (CPA 1990, Lau 2003). Soil acidification processes are likely to result in the following effects (Alberta Environment 1996, Maynard 1998, Lau 2003):

1. Leaching of cations which leads to reduced concentrations of calcium, magnesium and other base cations required for plant growth in soils,
2. Reduced availability and deficiency of major nutrients such as phosphorous and potassium,
3. Intolerance towards pH changes and impairment shown by vegetation, crops and soil microorganisms,
4. Decrease in the availability of molybdenum and increase in the availability of trace metals such as manganese, boron, zinc, copper, and iron for plants,
5. Increased solubility and thus mobilization of phytotoxic ions (e.g. aluminum), and
6. Greater contribution of acidity, nutrients and potentially hazardous ions to ground water and surface water.

In the context of potential environmental impacts around the haul roads where there is no vegetation in the active mine area or at the base of the reclaimed mine only issues 5 and 6 need to be addressed.

3.8.2 pH and electrical conductivity (EC) measurement

3.8.2.1 pH

pH measurement is one of the most commonly used and important measurements in both laboratory and industrial settings. In general, pH is a measure of the degree of acidity or alkalinity of a substance. It is related to the effective acid concentration (“activity”) of a solution and is defined by, $\text{pH} = -\log [\text{H}^+]$. The pH range includes values from 0 to 14. Values from 0 to 7 represent the acidic half of the scale. Values from 7 to 14 represent the alkaline or basic half of the scale. The pH value 7 is considered neutral, as it is neither acidic nor alkaline.

The pH value of a sample can be determined in several ways. The preferred and most accurate way is the potentiometric measurement, using a pH electrode, a reference electrode, and a pH meter. This method is based on the fact that certain electrodes, immersed in solution, produce a millivolt potential (i.e. voltage) that is related to the hydronium ion concentration or pH of a solution in a precise way.

The relationship between the electrode’s voltage and the solution pH is defined by the Nernst equation, $E_{\text{meas}} = E^* - (2.3RT/nF) \cdot (\text{pH})$. In this equation, E_{meas} is the voltage output of the electrodes, E^* is the total of all other voltages in the system including the reference voltage, R is the Gas Law constant, T is the temperature in Kelvin, n is the charge on the hydronium ion (+1), and F is the Faraday constant.

3.8.2.2 Electrical conductivity

Conductance is a quantity associated with the ability of primarily aqueous solutions to carry an electrical current, I , between two metallic electrodes when a voltage E is connected to them. Though water itself is a rather poor conductor of electricity, the presence of ions in the water increases its conductance considerably, the current being carried by the migration of the dissolved ions. The conductance of a solution is proportional to and a good, though non specific indicator of the concentration of ionic

species present, as well as their charge and mobility. It is intuitive that higher concentrations of ions in a liquid will conduct more current. Conductance derives from Ohms law, $E = IR$, and is defined as the reciprocal of the electrical resistance of a solution. $C = 1/R$, where C is conductance (siemens) and R is resistance (ohms).

In practice, conductivity measurements involve determining the current through a small portion of solution between two parallel electrode plates when an ac voltage is applied. Conductivity values are related to the conductance (and thus the resistance) of a solution by the physical dimensions – area and length – or the cell constant of the measuring electrode. By using cells with defined plate areas and separation distances, it is possible to standardize or specify conductance measurements. Thus comes, the term specific conductance or conductivity. The relationship between conductance and specific conductivity is, Specific conductivity, S.C. = (Conductance, C)*(Cell constant, K) = siemens * cm/cm² = siemens/cm. Conductivity measurements are reported as Siemens/cm, because the value is measured between opposite faces of a cell of known cubic configuration.

3.8.2.3 Test equipment

The equipment used for pH and electrical conductivity measurement during sulfur concrete weathering tests and long term geochemical stability of sulfur concrete mixtures was a Fisher Scientific product, accumet research AR50 pH meter, which is designed to measure pH, absolute mV, relative mV, ion concentration, or conductivity with a series of prompts on its screen. The AR50 pH meter kit consisted of a meter, an electrode (13-620-299), an automatic temperature compensation (ATC probe) (13-620-19), and a Conductivity probe (13-620-162).

AR50 pH meter provides microprocessor precision in a compact bench top design that is easy to use. In the pH mode, the meter measures in the range -2 to 20 with a relative accuracy of ± 0.002 . It has automatic and manual buffer recognition with five

calibration points. The conductivity mode has cell constant range of 0.1, 1.0, and 10 and measures conductivity in the range of 0 to 300 mS/cm with 0.5% accuracy.

3.8.3 Geo-chemical interaction studies

Study of geo-environmental impacts of sulfur concrete haul roads with the near surface environment focused on two important aspects, the short term interaction of sulfur concrete exposed at the surface during haul road construction and operation, and the long term interaction of the sulfur concrete following its burial with mine wastes in the mined out pits. These environmental interactions were studied separately to understand the potential environmental impact of using sulfur concrete for haul roads.

3.8.3.1 Sulfur concrete weathering tests

During haul road construction and operation there is a potential for chemical reactions involving sulfur in contact with atmospheric oxygen and water from both rain and snow melt. These reactions may release acids into the surface water thereby affecting the environment.

To provide an assessment of potential acid generation under field conditions a series of leaching studies were conducted on intact sulfur concrete samples. The chemical stability of sulfur concrete samples when alternately exposed to highly reactive deionized (DI) water and atmospheric oxygen at regular intervals was studied. The experiment was conducted to mimic operational conditions when the haul roads are in daily use with surface exposed to climatic variation. The test procedure is summarized as follows:

- Triplicate sets of sulfur concrete samples based on the optimum mix designs were prepared in 152 mm x 305 mm plastic cylinder molds.
- The hardened samples were covered with 15 cm of aggregate, which would normally act as wearing surface. The aggregate was saturated with water and the

water was drained off through an outlet installed through the cylinder, level with the sulfur concrete surface. By letting the water drain by gravity the aggregate was placed at the field moisture condition, which is the optimum moisture content for sulfur oxidation (Tan, 1982).

- The weight of the samples was measured before and after moisture addition to calculate the field moisture content of the aggregate.
- The containers were stored at room temperature (20⁰C) covered with a simple plastic cap to reduce moisture evaporation but allow atmospheric oxygen interaction through out the study.
- The samples were allowed to sit for six weeks so that geochemical reactions could occur. During this time the mass of water was maintained by replacing any water that evaporated on a weekly basis.
- After six weeks the aggregate was saturated with known volume of deionized water and was allowed to drain, the drained water was collected and analyzed for pH and electrical conductivity (EC). The test set up is shown in Figure 3.15. The test results are summarized in Table 3.8.

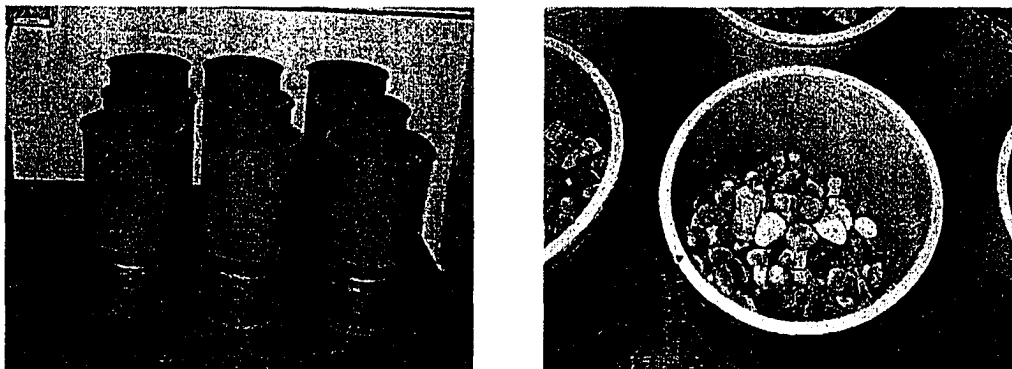


Figure 3.15 Weathering test set up

Deionized water with pH of 6.63 and EC value of 6.21×10^{-3} mS/cm was used to flush the samples. The results of weathering test are shown in Table 3.8. The test results show an insignificant change in pH of the drained water indicating that minimal

chemical reactions had occurred. The change in EC value is partly attributed to dissolved dust particles washed from the aggregate surface during the first flush. The same mass of deionized water was flushed through the same mass of aggregate as used in these experiments to determine the change in water chemistry as a result of the aggregate only. The pH of the drained water increased to 8.06 while the EC value increased to 0.44 mS/cm.

Mix design	pH	EC (mS/cm)
30S2.3FA67.7C - 1	6.62	0.58
30S2.3FA67.7C - 2	5.72	1.35
30S2.3FA67.7C - 3	6.23	1.18
35S2.3FA62.7C - 1	6.21	1.25
35S2.3FA62.7C - 2	6.84	1.17
35S2.3FA62.7C - 3	6.66	0.90
30S2.3FA67.7Sa - 1	6.64	1.06
30S2.3FA67.7Sa - 2	6.80	1.29
30S2.3FA67.7Sa - 3	7.09	1.06

Table 3.8 Weathering test results

In a longer duration test under operational condition of the haul road, microbial activity may be sufficient to increase the production of acid by the oxidation of elemental sulfur. Thus an operational test section of sulfur concrete haul road instrumented to measure and collect leachate is required to properly assess the geo-environmental impact of a sulfur concrete haul road.

3.8.3.2 Long term geochemical stability of sulfur concrete mixtures

In the long term, the haul roads constructed with sulfur concrete will be buried with mine wastes in the mined out pits when the oil sands mines are abandoned. Hence there might be potential diffusive release of contaminants from the buried sulfur concrete into the surrounding groundwater. The potential of diffusive release of

contaminants was examined by studying the chemical stability of sulfur concrete samples when submerged in the highly reactive deionized (DI) water, and in composite tailing (CT) release water, which is the most likely water type which will be in contact with the sulfur concrete when buried with the mine waste.

The experiment was conducted under controlled atmospheric and flow conditions to mimic anticipated future geochemical and hydro-geologic conditions. The tests were conducted under inert atmospheric conditions (in the absence of oxygen) to mimic the deep deposition of the materials when the sulfur concrete is disposed in the mined out pits, and under diffusive dissolution (no agitation or mixing of water during testing) conditions to mimic the anticipated hydro-geologic conditions. For low porosity sulfur concrete in still water the dissolved chemical mass released to the surrounding water is the result of dissolution from the surface of the material followed by diffusive transport within the water phase. The test procedure is summarized as follows:

- Triplet sets of sulfur concrete samples based on the optimum mix designs were prepared in 152 mm x 305 mm plastic cylinder molds.
- Porosity of the samples was determined through precise measurement of the mass of the constituents and sample dimensions. Porosity determination is shown in Table A-6 (Appendix A).
- The samples were then covered by a liter of DI or CT release water and stored in Nitrogen filled bags at room temperature (20 °C).
- pH and electrical conductivity (EC) of the water was measured on a weekly basis and water samples were taken at regular intervals. Test results are summarized in Figures 3.16 to 3.19.

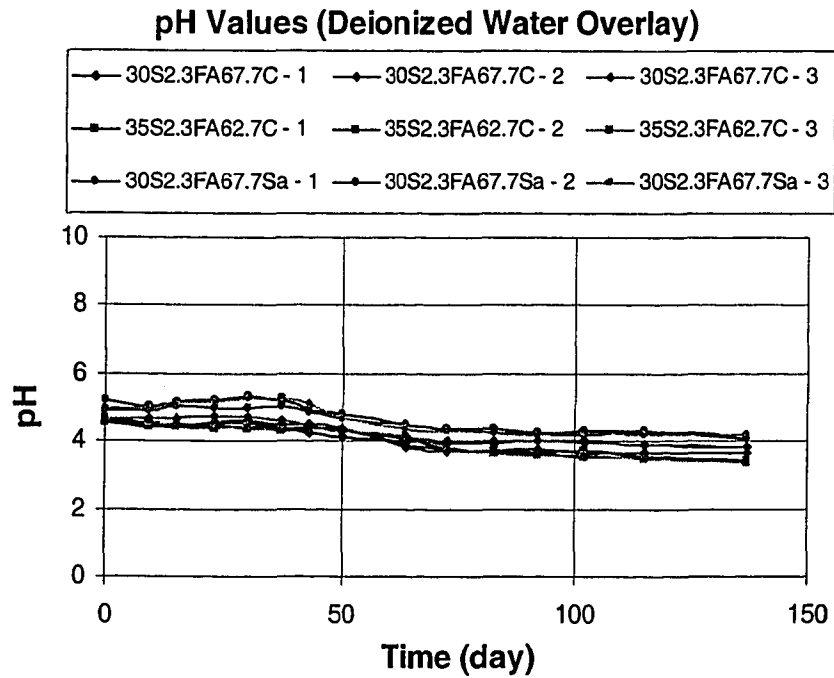


Figure 3.16 pH vs. time for DI water overlaid samples

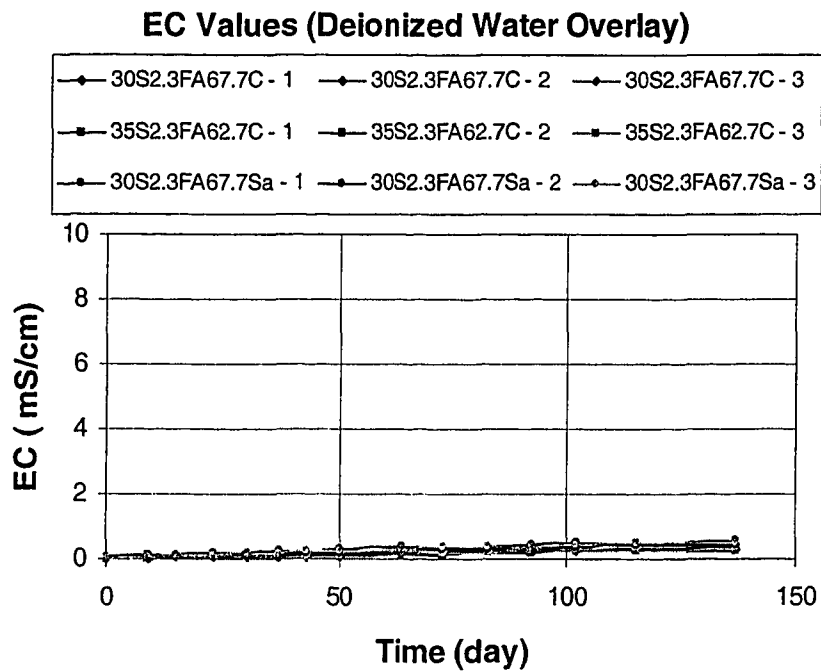


Figure 3.17 EC vs. time for DI water overlaid samples

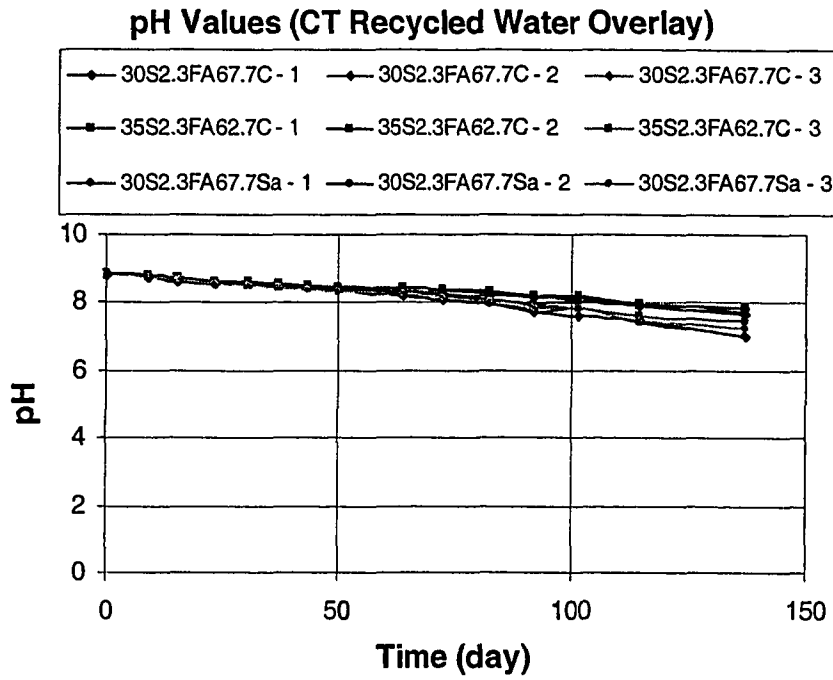


Figure 3.18 pH vs. time for CT recycled water overlaid samples

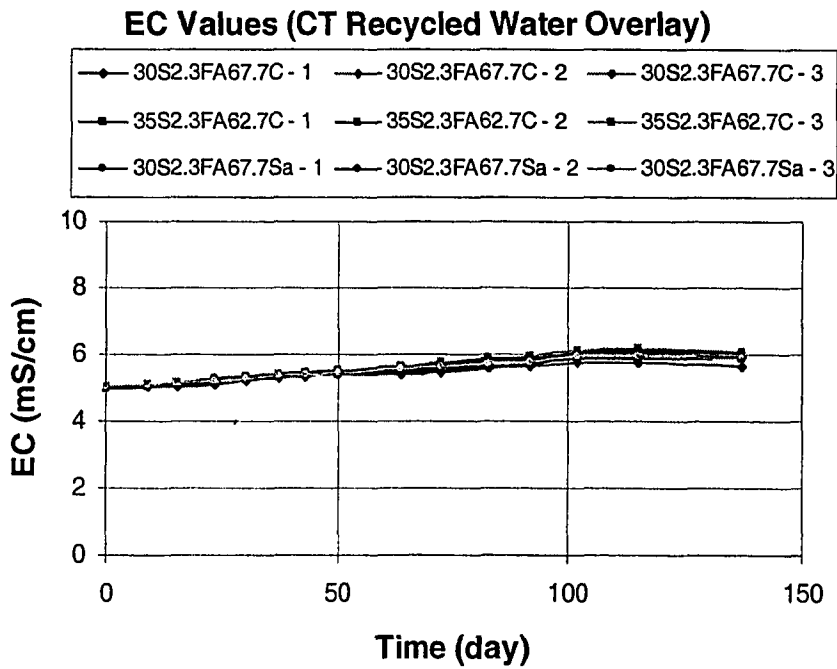


Figure 3.19 EC vs. time for CT recycled water overlaid samples

From Figures 3.16 to 3.19, the average change in pH value for DI water covered samples is 1.1 and for the CT release water covered samples is 1.2. The change in EC for DI water covered samples is 0.45 mS/cm and for the CT release water covered samples is 0.9 mS/cm. After about 140 days the change in pH and EC values of all the samples covered by DI water and CT release water are not significant indicating that minimal chemical reactions took place over this time duration. Thus the sulfur concrete samples are stable under the test conditions.

A longer term test is required to fully assess the geochemical interaction of CT release water with elemental sulfur for the long term storage of sulfur concrete in the mined out pits.

4 HAUL ROAD CROSS-SECTION DESIGN

A haul road cross section design has two main components, structural and geometric designs. The structural design of a haul road is basically the determination of the thickness of the pavement layers for a particular combination of construction materials and load configuration. The geometric design of haul road cross section deals with physical dimensions such as width, cross slope, side ditch height and safety berm height. The objectives of both designs are to provide a safe, efficient, smooth and vehicle friendly ride to the haul trucks and other vehicles without excessive maintenance through the design life. Some content of this chapter was summarized from guidelines for mine haul road design (Tannant and Regensburg, 2001).

4.1 Geometrical Cross Section Design Parameters

4.1.1 Road width

The width of haul roads on both straight and curved sections must be adequate to permit safe vehicle maneuverability and maintain road continuity. Because the size of equipment that travels on haul roads varies significantly from mine to mine, vehicle size rather than vehicle type or gross vehicle weight are best used to define road width requirements. In the past, for straight road segments, it was recommended that each lane of travel should provide clearance on each side of the vehicle equal to one-half of the width of the widest vehicle in use (AASHO 1965). For multiple lane roads, the clearance allocation between vehicles in adjacent lanes is generally shared. With the much larger and wider truck in use today, the guidelines regarding appropriate clearance may need to be reviewed.

Roads that are too narrow can drastically reduce tire life by forcing the truck operator to run on the berm when passing another vehicle. This will result in sidewall damage, uneven wear, and cuts. This is a particular problem when an operator adds new larger

trucks to an existing fleet but does not change the road layout to accommodate the wider trucks.

The minimum width of running surface for the straight sections of single and multi-lane roads can thus be determined from the following expression:

$$W = (1.5L + 0.5) * X \qquad \text{Equation (1)}$$

Where:

W = width of running surface (m), L = number of lanes, and X = vehicle width (m)

Additional road width in excess of the minimum determined from Equation (1) might be required locally along the road alignment, for example:

- to accommodate equipment larger than the primary road users, such as shovels
- to allow sufficient room for vehicles to pass on single lane roads, and
- if, on single lane roads, the sight distance is less than the stopping distance, sufficient space must be provided for moving vehicles to avoid collision with stalled or slow-moving vehicles.

Switchbacks or other areas on haul roads requiring sharp curves must be designed taking into consideration the minimum turning radius of the haul trucks. A wider road is required on curves to account for the overhang occurring at the vehicle front and rear.

4.1.2 Safety berm, side ditch and cross slope

The road width (at sub-grade level) should also account for safety berm and side ditches. Safety berms are typically constructed from mine spoil and are used to keep potential out of control vehicles on the road.

The height of the safety berm is generally about $\frac{2}{3}$ of the diameter of tire of the largest vehicle traveling on the road. The slopes of the sides of the safety berm can be as steep as 1H:1V, if the material stability permits. The safety berm is usually constructed with 1 to 2 m wide gaps spaced approximately every 25 m to facilitate surface drainage off the road.

A drainage ditch is excavated on each side of the road. The ditch depth is variable but a typical value is 0.5 m lower than the top of the sub-grade. The sides of the ditch should not be steeper than 3H:1V.

The cross slopes of the road should be enough to ensure proper drainage off the road. Normally a 2 % crowning is adequate.

4.2 Structural Design of Haul Road Cross-Section

A haul road cross-section generally consists of different layers. The sub-grade is the naturally occurring surface on which the haul road is built. It may be leveled by excavation or back-filled in some cases to provide a suitable surface. The sub-base, base course and surface course are layers of materials of increasing quality that are successively placed above the sub-grade to form the pavement.

Sub-grade: The sub-grade can consist of native insitu soil or rock, previously placed landfill or mine spoil, or other existing surface over which a road is to be placed. Where the sub-grade comprises hard, sound rock or dense, compact gravel, little or no fill may be necessary as haul trucks can travel on the sub-grade surface. At the other end of the spectrum, soft clays and muskeg will require substantial quantities of fill to help spread the heavy wheel loads and prevent rutting, sinking or overall road deterioration. Such adverse conditions, if allowed to occur, pose a serious threat to vehicular controllability and create unsafe haul road segments. If the sub-grade lacks

the required bearing capacity, then it needs to be altered through suitable measures such as compaction or the use of geotextiles.

Sub-base: Sub-base is the layer of a haul road just above the sub-grade and below the base course of the road. It usually consists of compacted granular material, either cemented or untreated. Run of mine and course rocks are the general components of this layer. Apart from providing structural strength to the road, it serves many other purposes such as minimizing effect of frost, accumulation of water in the road structure, and providing working platform for the construction equipment. The sub-base distributes vehicle load over an area large enough that the stresses can be borne by the natural, sub-grade material. The lower the bearing capacity of the ground, the thicker the sub- base must be.

Base course: The layer of haul road directly beneath the surface course of the road is called the base course. If there is no sub-base then the base course is directly laid over the sub-grade or roadbed. Usually high quality treated or untreated material with suitable particle size distribution is used for construction of this layer. Specifications for base course materials are generally considerably more stringent for strength, plasticity, and gradation than those for the sub-base. The base course is the main source of the structural strength of the road.

Surface course: The upper most layer of the haul road that comes directly in contact with tires is known as the surface course. A haul road surface is generally constructed with fine gravel with closely controlled grading to avoid dust problems while maintaining proper binding characteristic of the material. Apart from providing a smooth riding surface, it also distributes the load over a larger area thus reducing stresses experienced by the base course.

4.2.1 Haul road construction materials

Selection of both materials for construction and thickness of haul road cross section are critical issues for successful haul road design. At SUNCOR oil sand mines, presently haul roads are constructed using crushed limestone, gravel or lean oil sands as the major construction materials and they require thick road cross sections due to the low stiffness of these materials and the large truck loads that travel on the roads. Studies by Kumar (2000 and 2001) showed that a CAT 797 haul truck with more than 500 tons gross weight requires as much as 5 m thick cross section at the SUNCOR mine sites. Cameron et al (2001) summarized the haul road design approach at SYNCRUDE and indicated that haul roads in excess of 4 m thickness of compacted gravel are required for acceptable performance for their 300 to 400 tons payload trucks.

Kumar (2001) reported strength and deformation properties for materials used to construct haul roads by Mine Engineering at SUNCOR (Table 4.1)

Material	Density (Kg/m ³)	Young's Modulus (MPa)	Resilient modulus for design * (MPa)	Usage in road cross section
Gravel (minus 20mm)	2050	14	>200	Surface course
Sandy gravel	1930	70	175	Base course
Sandy till	1810	19	100	Base course
Lean oil sands	2050	10	30	Sub base
Interburden	2040	10	50	Sub base

Table 4.1 Strength and deformation properties of road building materials

Haul roads at SUNCOR are presently below desirable standards and are having a negative impact on mine productivity especially during the summer months (Kumar, 2001). The major symptoms of haul road deterioration are potholes, rutting and

settlement. Haul roads are deteriorated mostly due to precipitation/runoff, heavy traffic volume, spring breakup, poor compaction and vehicle spillage.

The construction materials used presently, shown in Table 4.1, have low strength and stiffness. To improve the quality of haul roads and reduce the required haul road cross section thickness, materials with better strength and stiffness must be used to construct the roads and/or the foundation soils beneath the haul road should be substantially improved. As is evident from Chapter 3, sulfur concrete produced from mine waste products such as sulfur, tailings sand, coke and fly ash, is much stronger and stiffer than the existing road building materials. Thus sulfur concrete capped with running surface course may be able to be used to build haul roads of higher quality, with reduced thickness, than current roads at SUNCOR's mine sites. Physical, mechanical and geochemical properties of sulfur concrete are presented in Chapter 3.

4.2.1.1 Surface course materials

The upper most layer of the haul road is known as the surface course. Surface course material selection is based on properties such as grain size distribution, strength, rigidity, and weathering characteristics. Surface course requires good quality material because it faces the greatest weathering and highest dynamic loads due to truck loads. Apart from these, surface course design should take care of operational requirements such as dust control, smoothness of ride, traction and rolling resistance.

Surface course material selection is usually based on local experience or guidelines related to unpaved public road construction. However, the unique service condition experienced by mine haul roads requires development of specifications tailored to those particular needs (Thompson and Visser, 2000).

Compacted natural gravel and crushed rock and gravel mixtures are widely used in surface mines for surface course construction. These materials can yield low rolling

resistance and high traction, and can be constructed and maintained at a relatively low cost. Other materials that can be used for surface course includes: asphaltic concrete and roller compacted concrete (RCC). The advantages and disadvantages of each material are summarized in Table 4.2.

Material	Advantages	Disadvantages
Compacted gravel & crushed rock	<ul style="list-style-type: none"> Relatively smooth, stable surface Relatively low construction cost Low deformation under load Ease of construction Low rolling resistance 	<ul style="list-style-type: none"> Frequent maintenance required Source material may require screening/crushing Dust problems in dry weather Erodible if flooded Potential frost action (fines > 10 %)
Asphaltic concrete	<ul style="list-style-type: none"> High coefficient of adhesion Minimal dust problems Smooth, stable surface Low rolling resistance Low maintenance cost High vehicle performance speeds Low deformation under load 	<ul style="list-style-type: none"> Ices easily in cold weather Needs base course with CBR = 80+ High construction cost Specialized construction Impractical for tracked vehicles
Rollcrete	<ul style="list-style-type: none"> High coefficient of adhesion Very low rolling resistance Minimal dust problems Smooth, stable surface Very low maintenance costs High vehicle speeds Very low deformation under load 	<ul style="list-style-type: none"> High construction costs Impractical for tracked vehicles

Table 4.2 Advantages and disadvantages of various road surface materials (after Monenco 1989)

Among these materials, the most commonly used and recommended one is compacted gravel and crushed rock

4.2.1.1.1 Compacted gravel and crushed rock

Generally surface course is constructed using high quality gravel crushed to minus 19 mm size with modulus about 330 MPa (Cameron & Lewko 1996). Thompson (1996) reported use of a 200 mm thick layer of material having resilient modulus in the range of 150-200 MPa compacted to 98% modified AASHTO for a 170 ton haul trucks. For larger trucks, thicker layers with material having higher modulus should be used as the surface course.

The American Association of State Highway and Transportation Officials (AASHTO): M147 (1993^a) gives the following guidelines for surface course aggregates for public unpaved roads:

- Coarse aggregate retained on the 2.0 mm (No. 10) sieve shall consist of hard, durable particles/fragments of stone or gravel. Materials that break up when alternately frozen and thawed or wetted and dried shall not be used.
- Coarse aggregate shall have a percentage of wear, by the Los Angeles Abrasion test, AASHTO T96, of not more than 50.
- Fine aggregate passing the 2.0 mm sieve shall consist of natural or crushed sand, and fine mineral particles passing the 0.075 mm (No.200) sieve.
- The fraction passing the 0.075 mm sieve shall not be greater than two-thirds of the fraction passing the 0.425 mm (No.40) sieve. The fraction passing the 0.425 mm sieve shall have a liquid limit not greater than 25 and a plasticity index not greater than 6.
- All the materials should be free from vegetable matter and lumps or balls of clay. The soil- aggregate material shall conform to the grading requirements of Table 4.3.

Sieve designation		Mass percent passing			
Standard (mm)	Alternate	Grading C	Grading D	Grading E	Grading F
25.0	1 in.	100	100	100	100
9.5	3/8 in.	50-85	60-100	-	-
4.75	No. 4	35-65	50-85	55-100	70-100
2.00	No. 10	25-50	40-70	40-100	55-100
0.425	No. 40	15-30	25-45	20-50	30-70
0.075	No. 200	5-15	5-20	6-20	8-25

Table 4.3 Grading requirements for soil aggregate materials for surface course (after AASHTO 1993a)

A satisfactory gradation for granular surface materials is provided in Table 4.4 (Monenco 1989). Roads subjected to freezing or prolonged inclement weather should not contain more than 10% fines (less than No. 200 US standard sieve size) to prevent muddy, slippery conditions when wet or thawing. The particles of the granular material should be clean, sound and durable. Gravels larger than 9.5 mm should have 30% or more fractured faces. Granular surfacing material should be placed in layers not exceeding 200 mm in thickness prior to compaction. Each layer should be uniform in gradation and moisture content, spread without causing particle segregation and compacted with a vibratory smooth drum roller weighing at least 15 tons to at least 98 % of Standard Proctor maximum dry density as determined in the laboratory.

ASTM sieve size	% by weight passing
76 mm	100
38 mm	70 – 100
25 mm	55 – 88
9.5 mm	40 – 70
#4	30 – 55
#10	22 – 42
#200	5 - 10

Table 4.4 Recommended grading for granular surface course (Monenco 1989)

Thompson and Visser (1997, 2000) presented results from haul road trafficability studies performed on roads in South Africa. They examined numerous functional performance indicators such as severity of potholes, corrugations, rutting, loose material, dustiness, loose and fixed stones, cracks, erosion, and skid resistance. These defects were correlated to surface material properties such as dust ratio, plasticity index, CBR, grading coefficient, shrinkage product as well as the maintenance cycle and daily tonnage hauled. Their research has led to the establishment of wearing course material specifications shown in Table 4.5 that are calibrated for mine haul roads. Figure 4.1 shows the ideal and recommended range of two important material properties for the surface course. The ideal range for the shrinkage product is 95 to 130 while the ideal range for the grading coefficient is 25 to 32. The impacts of material properties outside the recommended range are also depicted in Figure 4.1.

Property	Min.	Max.	Impact on functionality
Shrinkage product*	85	200	reduce slipperiness but prone to ravel & corrugations
Grading coefficient**	20	35	reduce erodibility but induce tendency to ravel
Dust ratio***	0.4	0.6	reduce dust generation but induces raveling
Liquid limit (%)	17	24	reduce slipperiness but prone to dust
Plastic limit (%)	12	17	reduce slipperiness but prone to dust
Plasticity index	4	8	reduce slipperiness but prone to dust
CBR at 98% Mod. AASHTO	80		resist erosion, improve trafficability
Max. particle size (mm)		40	ease maintenance, no tire damage

*Shrinkage product = bar linear shrinkage x P425

**Grading coefficient = $(P_{265} - P_2) \times P_{475} / 100$

***Dust ratio = P_{075} / P_{425} , Where: P075, P425, P2, P475, and P265 refer the percent by weight passing sieves of size 0.075, 0.425, 2.0, 4.75, and 26.5mm respectively.

Table 4.5 Recommended material properties for a haul road surface material (after Thompson & Visser 2000)

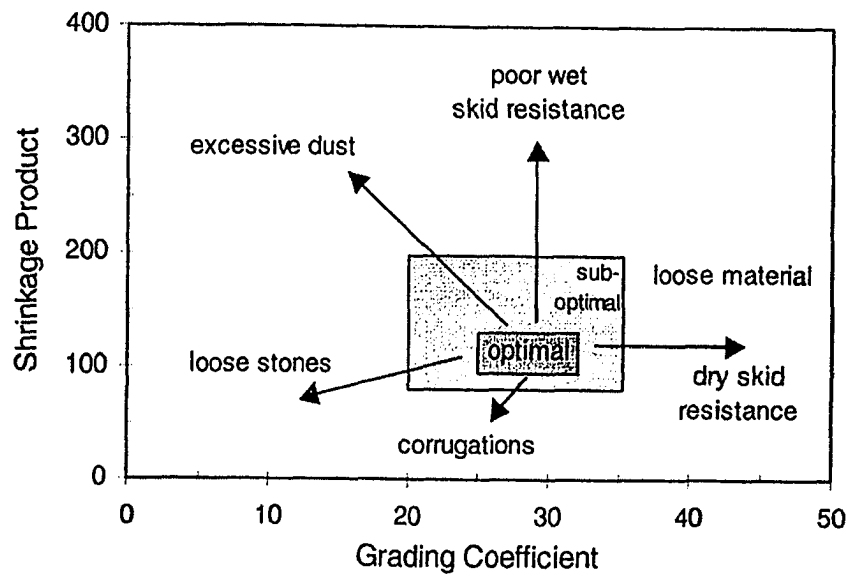


Figure 4.1 Optimal and sub-optimal range of values for the shrinkage product and grading coefficient for a granular surface course material (after Thompson & Visser 2000)

4.2.2 Cross section design

Kaufman and Ault (1977) did pioneering work on haul road design and construction for surface mines. The design procedure followed in their work was based on the CBR (California Bearing Ratio) analysis of the haul road construction material and the applied loads. The CBR design method is one of the most widely used methods for computing pavement layer thickness for road construction. This approach characterizes the bearing capacity of a given soil as a percentage of the bearing capacity of a standard-crushed rock, the ratio of capacities being referred to as the CBR for the given soil. Empirical design curves, known as CBR curves, relate the required fill thickness and applied wheel load to the CBR value. The CBR method is particularly useful for estimating the total cover thickness needed over the insitu sub-grade material. A weaker sub-grade requires thicker layers of road construction material. This moves the truck tires higher and away from the weak insitu material,

thus diminishing the stresses or strains to a level that can be tolerated by the sub-grade.

Wade (1989), Wieren and Anderson (1990) and many other authors modified CBR design procedures to suit changes in design parameters such as weight of the haul trucks and nature of the construction materials. But as haul truck size increased, the CBR-based design procedure failed to deliver optimum design criteria for haul roads. The method was denounced by authors such as Morgan et al. (1994) and Thomson and Visser (1997) due to the following reasons:

- The CBR method is based on the Boussinesq's semi-infinite single layer theory, which assumes a constant elastic modulus for different materials in the pavement. Various layers of a mine haul road consist of different materials each with its own specific elastic and other properties,
- The CBR method does not take into account the properties of the surface course material,
- The CBR method was originally designed for paved roads and airfield surfaces. Therefore the method is less applicable for unpaved roads, especially haul roads which experience much different wheel geometry and construction materials, and
- The empirical design curves were not developed for the high axle loads generated by large haul trucks and simple extrapolation of existing CBR design curves can lead to errors of under design, or even over design.

Thus haul road cross section design based on critical strain and resilient modulus, which provides a theoretical rather than an empirical design approach, was developed to deliver optimum design of haul roads. The method uses the fundamental engineering properties of the construction materials to estimate the stress and strains within the road cross section under realistic wheel loading conditions.

4.2.2.1 Cross-section design based on critical strain and resilient modulus

Morgan et al. (1994) and Thompson and Visser (1997) proposed a haul road design method based on elastic deformation of each layer in a haul road taking into account different moduli of elasticity for different layers. In this method the road cross section is treated as a composite beam and it is assumed that the road adequately supports haul trucks as long as the vertical strains in the pavement layers remain less than the critical strain limits, and the stress level in any layer of a haul road cross section does not exceed the bearing capacity of the material used in that layer. Based on field observations, maximum vertical strain limits have been established to be 1500-2000 micro-strain for typical haul roads. When the vertical strains in the pavement layers exceed the critical strain limit value, the road ceases to act as a composite beam and can no longer adequately support the haul truck.

For a given stress in a pavement layer, the induced strain is a function of the modulus of the material. The proponents of this design method (Morgan et al. 1994 and Thompson and Visser 1997) suggest the use of resilient modulus for describing the material properties of the pavement layer. The resilient modulus is determined from a cyclic loading test. It is like a tangent Young's modulus but it is measured after cyclic loading has compacted the test specimen. The cyclic stresses applied to the test specimen are less than its peak strength. Because the specimen is compacted during the cyclic loading, the stiffness increases as illustrated in Figure 4.2. Hence, the nature of the test required to determine the resilient modulus is similar to the cyclic loading experienced in a road. AASHTO (1993^b) T294 gives the laboratory test method to determine the resilient modulus of an unbound soil by repetitive loading of a soil sample in a tri-axial test cell.

Thompson (1996) estimated the resilient modulus by the falling weight deflectometer test. Alternatively, the Young's modulus of elasticity for a material can be determined by a compression test in laboratory. Figure 4.2 shows how the stiffness of a material increases with repetition of loading and thus the initial Young's modulus is lower than

the resilient modulus. The test to measure the Young's modulus is simple and very well understood and may give a reasonable lower estimate of the resilient modulus, albeit on the conservative side as there is no confining pressure and stiffening of soil due to repeated loading. Mohammad et al. (1998) describe yet another method for calculation of resilient modulus using a cone penetration test with continuous measurement of tip resistance and sleeve friction.

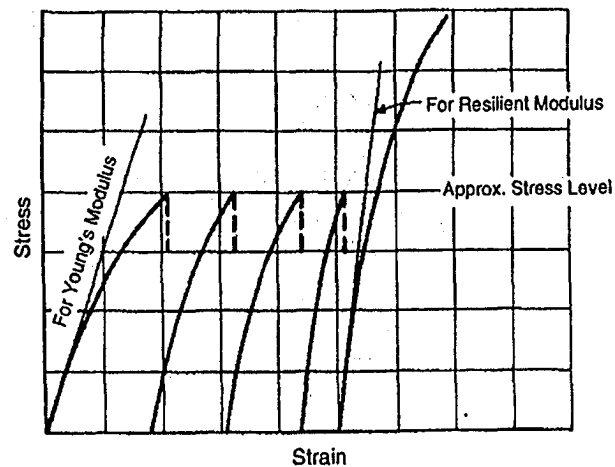


Figure 4.2 Method to obtain resilient modulus (after Bowles 1984)

4.2.2.1.1 Tire pressure and foot print area

The strains in a layer are a function of applied stress (tire load, size, and spacing) and the resilient modulus of the layer. Wheel loads for any haul truck can readily be computed from the manufacturer's specifications. Note that haul trucks are frequently loaded above their rated weight capacity and this should be taken into consideration in the road design. By dividing the loaded vehicle weight over each axle by the number of tires on that axle, the maximum load for any wheel of the vehicle can be established. In every case, the highest wheel load should be used in the design computations.

Haul trucks used in surface mines have grown significantly in terms of size and capacity. In 1989, the largest trucks available had about 218 tons payload capacity, but by 1999, the payload capacity has risen to more than 300 tons. Correspondingly, the load per tire has increased to more than 85 tons. Considering the fact that increases in the size of haul trucks were virtually at a stand still during the early half of the decade, (due to the inadequacy of tire technology for larger trucks), this recent increase in haul truck size is significant. Larger haul trucks are being designed, produced, and accepted by the industry for one most important reason: economy of scale.

Two important elements of tires that affect haul road design are foot print area and tire pressure. Tire pressure has gone up to 690 kPa from 551 kPa in recent years, although the new low profile truck tires (55/80R63) have an inflation pressure of 586 kPa. The increase in tire pressure has placed greater stresses on the road surface. The bearing capacity of materials used for the surface course should be greater than the tire pressure. Due to the large tire foot print areas, the stress bulb below a tire can extend deep into the road cross-section, resulting in the need for well designed pavement cross section with sufficient bearing capacity and stiffness.

The shape of the tire footprint can be approximated as a rounded rectangle. The footprint is longer for low profile, low-pressure tires or for tires operating below their recommended inflation pressure. The pressure distribution beneath a tire is non-uniform, especially for bias ply tires. However, an assumption of uniform pressure distribution on a circular area for the purpose of stress analysis in haul road layers gives reasonably satisfactory results (Kumar, 2000). Specifications of selected Michelin tires are summarized in Table 4.6.

Tire	Truck Payload	Footprint Area (m ²)	Load per Tire	Tire Pressure (kPa)
Standard Tire 40.00R57	218 ton	1.11	63 ton	689
Retrofit Tire 44/80R57	218 ton	1.13	63 ton	586
Low Profile 55/80R63	327 ton	1.68	93 ton	586

Table 4.6 Michelin radial tire specifications (after Doyle, 1999)

4.2.2.1.2 Design procedure

Figure 4.3 presents a flow chart summary of the road design method based on the resilient moduli of the various layers in the road cross section. The method is based on the criteria that the vertical strain at any point within the haul road should be less than a critical strain limit. The critical strain limit is dependent on the traffic density and design life of the haul road, which defines the number of load repetitions during the design life of the road. Generally, this limit falls between 1500 and 2000 micro-strain for typical haul road.

Resilient modulus is the major input for calculating the vertical strain. It can be determined either by a resilient modulus test (AASHTO 1993b, T294) or by a falling weight deflectometer test. The Young's modulus of a material gives a conservative estimate of the resilient modulus.

Once the critical strain limit has been established and the layer moduli at various depths below the tires are measured or estimated, the next step is to determine the vertical stresses that act below the tire. Various methods can be used to calculate the stress distribution although numerical stress analysis programs are probably the easiest technique to use.

Initially, the thickness of each layer should be estimated based on past experience or designs at other mines with similar conditions. The least vertical strain will occur if

the stiffest material is placed at the top, the next stiffest underneath it, and so on. For modeling strain, other material properties such as Poisson's ratio of each material are also required. The increase in strain due to interaction of adjacent tires should also be considered. If the strain in any layer is more than the critical strain limit, then the thickness and/or the stiffness of the layer above that material should be increased. On the other hand, if the strain in any layer is much less than the critical strain limit, then the thickness of the layer above can be decreased. The amount by which the thickness should be increased or decreased depends on the difference between the vertical strain and the critical strain limit. In both cases the modeling should be repeated to ensure that the strain at all points remains less than the critical strain limit as the road cross-section is determined.

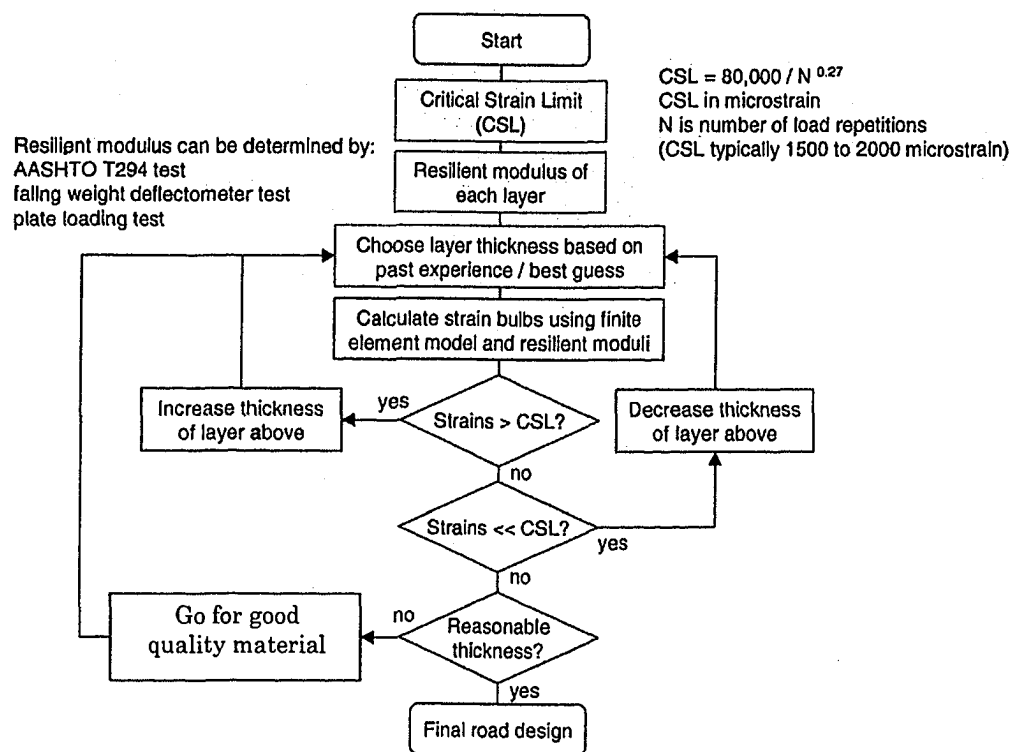


Figure 4.3 Major steps of the resilient modulus haul road design method (modified from Kumar 2000)

The layer thickness determined by this method depends on the resilient (Young's) modulus of the haul road construction material. A low modulus construction material may result in a very thick layer, which may be unacceptable for economic or operational reasons. Then it becomes essential to investigate the use of improved compaction methods and/or better quality materials to build the road section with reduced thickness. Strain modeling should be performed again to ensure that the vertical strain at all points within the cross-section is less than the critical strain limit.

4.2.2.1.3 Critical strain limit

The important criterion for haul road design is establishing the critical strain limit for each pavement layer. A road cannot adequately support haul trucks when the vertical strain exceeds the critical strain limit as the road ceases to act as a composite beam. Morgan et al. (1994) found that the critical strain limit was about 1500 micro-strain at the top of the sub-grade while Thompson and Visser (1997) noted that the limit was around 2000 micro-strains at the road surface. Somewhat different critical strain limits may be used for design depending on the design life of the road and traffic density. The strain limit depends on the anticipated number of haul trucks using the road over its working life. One empirical equation for estimating the critical strain limit is given by Knapton (1988). This equation was developed for heavy loading conditions found on docks at container ports. A modified version of the equation for haul roads show that same functional relationship between the critical strain limit and the design life of the road and traffic density:

$$E = 80000 / N^{0.27} \qquad \text{Equation (2)}$$

Where: E = allowable strain limit in micro-strains

N = number of load repetitions (number of haul trucks using the road over its working life).

This equation has been developed for semi-permanent and permanent haul roads. A critical strain of 2000 micro-strain is obtained for about 800,000 load repetitions,

which would be typical for a permanent haul road carrying 400,000 loaded trucks over its life span. If the number of load repetitions increases to 2.5 million, then the critical strain limit drops to about 1500 micro-strain. Semi-permanent or temporary roads will typically experience roughly less than 500,000 load cycles and hence a critical strain limit larger than 2000 micro-strain would be appropriate. Equation (2) gives a reasonable critical strain limits for load repetition numbers ranging between 50,000 and 5,000,000. However, it should be noted that Equation (2) needs further calibration for mine haul roads and may change in the future (Tannant and Regensburg, 2001). A strain limit value of 1500 to 2000 micro-strain is used for typical haul road design.

4.2.2.1.4 Resilient modulus test

Resilient modulus is the major input for modeling vertical strain within haul roads. The resilient modulus of sand-sulfur concrete mixtures for constructing haul roads was determined from tri-axial cyclic load tests in laboratory. The nature of the test simulates the cyclic loading experienced in a road subjected to moving wheel loads. The test procedures are summarized as follows:

- Testing was carried out on 102 mm x 203 mm sand-sulfur concrete samples (prepared from 67.7 % tailings sand, 30 % sulfur, and 2.3 % fly ash by weight) inside a tri-axial cell at room temperature.
- Confining pressure of 10 kPa (approximate confining pressure at field condition) and cyclic deviatoric stress of 600 kPa, which is equivalent to inflation tire pressure of the design haul truck (CAT 797), was applied on the test sample.
- The cycle time was 3.08 seconds composed of 0.45 seconds loading and 2.63 seconds resting time.
- The applied cyclic stress and corresponding axial deformations were continuously measured during the test and the results are shown in Figures 4.4 and 4.5.

From Figure 4.5 it can be observed that all the axial deformation that occurred in the specimen during loading was recovered during unloading. No plastic strain accumulation was observed in the specimen. This was because the applied cyclic stress, 600 kPa, was much lower than the failure strength of the material which is approximately 29 MPa; it fell well within elastic range of the material leading to only recoverable elastic deformations. Thus the resilient modulus is nearly the same as the Young's modulus of the material. So Young's modulus value obtained in section 3.3.2 was used for modeling associated with selection of the pavement cross section.

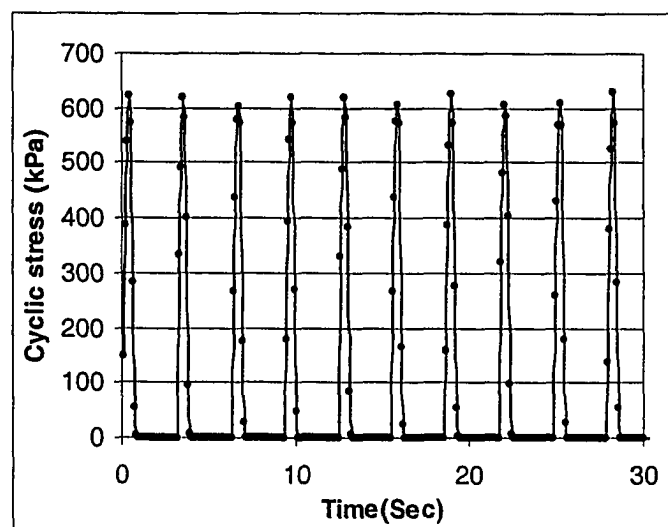


Figure 4.4 Cyclic stress vs. time plot

Kumar 2001 has reported resilient modulus values of road construction materials available at SUNCOR mine sites at Fort McMurray. The resilient modulus of the insitu sub-grade material, lean oil sand, is about 30 MPa whereas the surface course material, gravel minus 20mm, has resilient modulus > 200 MPa.

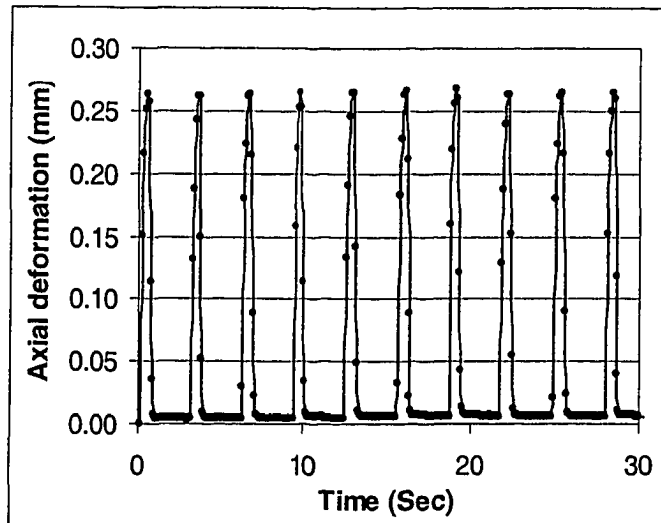


Figure 4.5 Axial deformation vs. time plot

4.2.2.1.5 Finite element analysis

For designing haul roads it is imperative to understand the stress and strain distributions in the haul road cross section induced by the haul truck tires. Finite element stress and deformation analysis was carried out using a two dimensional finite element program for calculating stresses and strains, Sigma/W version 5.12 (2002), which is product of GEO SLOPE International Ltd.

The objective of the modeling was to analyze vertical stress and strain distributions in the pavement layers for different combinations of pavement layer thicknesses and modulus of materials. A haul road cross section is adequate if the stress at any point is less than the bearing capacity of the material and the vertical strain is less than the critical strain limit, established to be between 1500 to 2000 micro-strains. The adequacy of the haul road cross-section for the design truck load was then examined using these stress and strain criteria for the different models.

The load distribution on the road surface beneath a haul truck tire was assumed to be uniform over a circular area (Kumar 2000). The design haul truck used in the analysis was CAT 797, the biggest haul truck presently used at SUNCOR mine sites in Fort

McMurray. It has an inflation tire pressure of 600 kPa with tire foot print area of 1.68 m² (0.73 m radius for circular load modeling). Typical sub-grade material at SUNCOR mine sites, lean oil sand, has a resilient modulus of 30 MPa (Kumar 2001). The sand-sulfur concrete (67.7 % tailing sand, 30 % sulfur, and 2.3 % fly ash by weight) to be used as the structural element of the pavement has Young's modulus of 9750 MPa. The Young's modulus decreased to 3925 MPa when the sulfur concrete is subjected to 300 freeze-thaw cycles (Section 3.7.2). The haul road cross section selected consists of sand-sulfur concrete layer, which is placed on top of the sub-grade. 0.3 m thick surface gravel with a resilient modulus of 300 MPa was placed on top of the sulfur concrete layer to act as a wearing course.

The axisymmetric option was selected in the Sigma/W analysis as it allows modeling a circular load, whereas the plane strain option simulates a strip load (of infinite length). A circular stress distribution on the road surface is a better approximation of a tire and how it loads the road than a strip load. A typical axisymmetric model which was used to analyze stress and strain distributions in a pavement layer induced by haul trucks is shown in Figure 4.6. Here the cross section consisted of 0.9 m thick sulfur concrete, $E = 9750$ MPa, covered by 0.3 m thick gravel surface course, $E = 300$ MPa.

The assumptions used in generating the models are:

- Type of model used - axisymmetric
- Analysis type - Load deformation
- Size of half model - 15 m (width) x 12 m (depth),
- Type of material - Linear elastic
- Element type – 4 node quadrilaterals
- Number of elements = 1520
- Number of nodes = 1599
- Poisson's ratio = 0.35

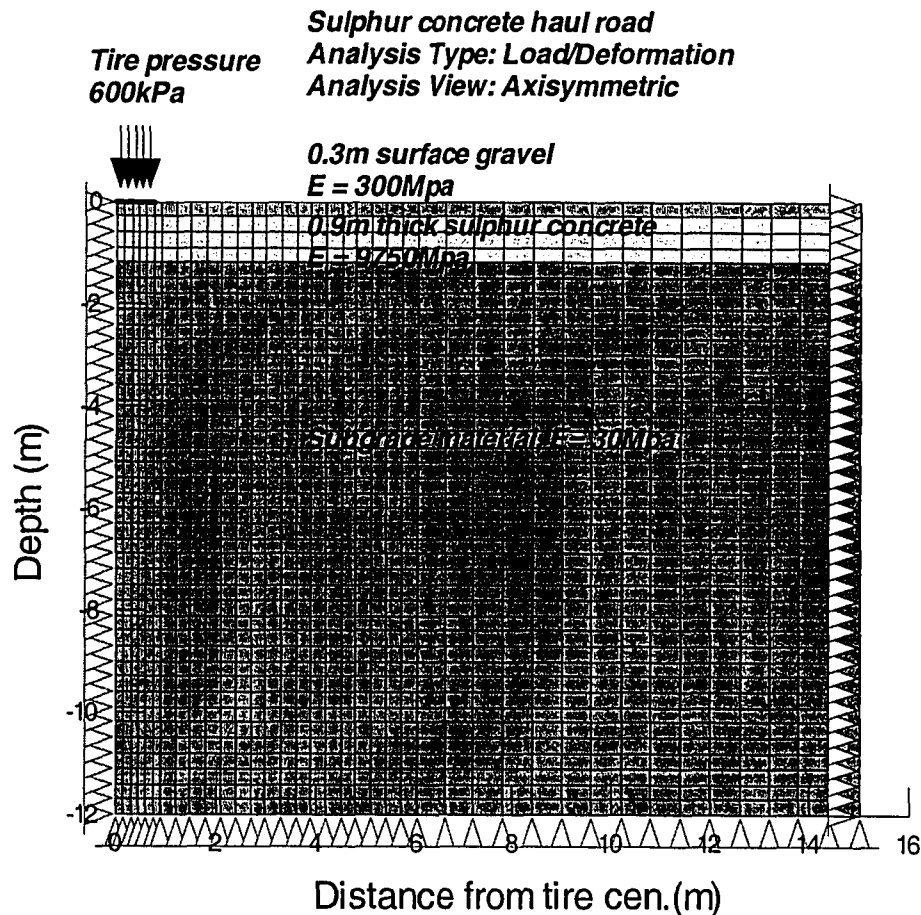


Figure 4.6 Typical axisymmetric model used in a Sigma/W analysis

The axis of rotation is at $x = 0$ (x and y are horizontal and vertical axes, respectively). The tire pressure is applied between the points $(0,0)$ and $(0.75,0)$. The boundary of the model (at $y = 0$) represents the surface of the haul road and thus is a free boundary. The vertical boundaries of the model (at $x = 0$ and $x = 15$) are restrained in x direction allowing the material at the boundary to move only in vertical (y) direction. The lower boundary of the model (at $y = -12$) is restrained in y direction. The right and lower boundaries are chosen to be at a reasonable distance from the tire, so that the boundary conditions do not affect the stresses and strains beneath the tire. The top layer (between $y = 0$ and $y = -0.3$) represents the surface course material. The sulfur concrete layer is placed underneath the surface course between $y = -0.3$ and $y = -1.2$ for the case shown in Figure 4.6. The layer below $y = -1.2$ represents the sub-grade or

insitu material. The thickness of the sulfur concrete layer was varied for different models until the stress and strain design criteria are satisfied.

An axisymmetric model allows only one circular load (tire) at a time in the model. So the effect of stress/strain bulb interaction from multiple tires couldn't be studied directly using the Sigma/W program. However, the principle of superposition allows superposition of elastic stresses and strains. Therefore, the axisymmetric model was used to generate the vertical strain distribution below a single tire and the results were then numerically superimposed to simulate strains beneath multiple tires. The most critical case was the back axle of the truck shown in Figure 4.7, which has four tires; the front axle has only two tires. Moreover, there is very little interaction between the front and back tires of the truck due to the axial spacing.

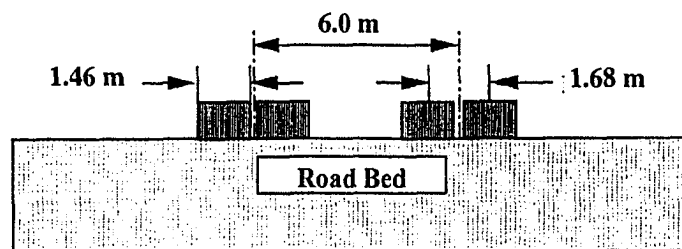


Figure 4.7 Schematic diagram for positions of tires on back axle of CAT 797 haul truck

Stress/strain bulbs for single tire load were generated using the axisymmetric model. The stress/strain data was queried at a grid of 0.3 m horizontally and vertically. The data was mirrored along the $X = 0$ line to generate full stress/strain bulbs for one tire, as an axisymmetric model generates only half of the space. Then the stress/strain values at grid points were staggered by a horizontal distance of 1.68 m (to get the data for the adjacent tire) and added to generate stress/strain values at various grid points to represent vertical stress/strain generated by two adjacent tires. The result obtained by the above procedure was staggered again by a horizontal distance of 6.0 m (to get data for the tires at the other end of the axle) and added to generate values of vertical

stress/strain at grid points representing stress/strain generated by all four tires along the back axle of a truck. The data generated for the three cases (one tire, two tires and four tires) were plotted using Sigma Plot version 8.02 software.

The analysis was performed on different models by varying the thickness of sulfur concrete layer. After many trial and errors, pavement consisting of 0.9 m thick sulfur concrete layer with modulus of 9750 MPa covered by 0.3 m thick gravel surface course with modulus of 300 MPa was found to satisfy the strain limit and bearing capacity criteria.

Figures 4.8 to 4.10 shows the vertical strain distributions beneath the single tire, two adjacent tires and all four tires on the back axle of the haul truck, respectively. Examination of the figures reveals that interaction between adjacent tires affects the vertical strain levels in the sub-grade layer. The maximum strain level in the sub-grade increased from 400 to 750 micro strain and from 400 to 900 micro strain when two and four tires were considered, respectively. The effect is not significant in the surface course and sulfur concrete layers because the strain bulbs are not sufficiently wide enough to interact in those layers.

Figure 4.11 shows the vertical stress distribution beneath four tires of the back axle of CAT 797 haul truck. The maximum stress level in the sub-grade due to the single tire load was 15 kPa and it increased to 27 kPa when two tires were considered (not shown). The maximum stress level in the sub-grade, sulfur concrete layer and surface course is 33 kPa, 970 kPa and 600 kPa, respectively when all four tires in the back axle were considered.

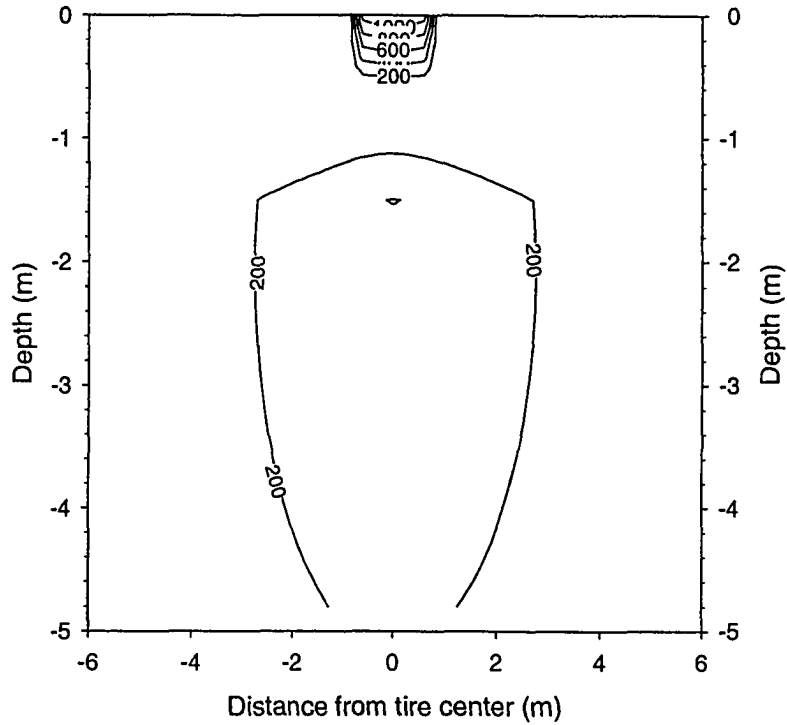


Figure 4.8 Vertical strains beneath single tire (in micro-strain) using $E = 9750 \text{ MPa}$

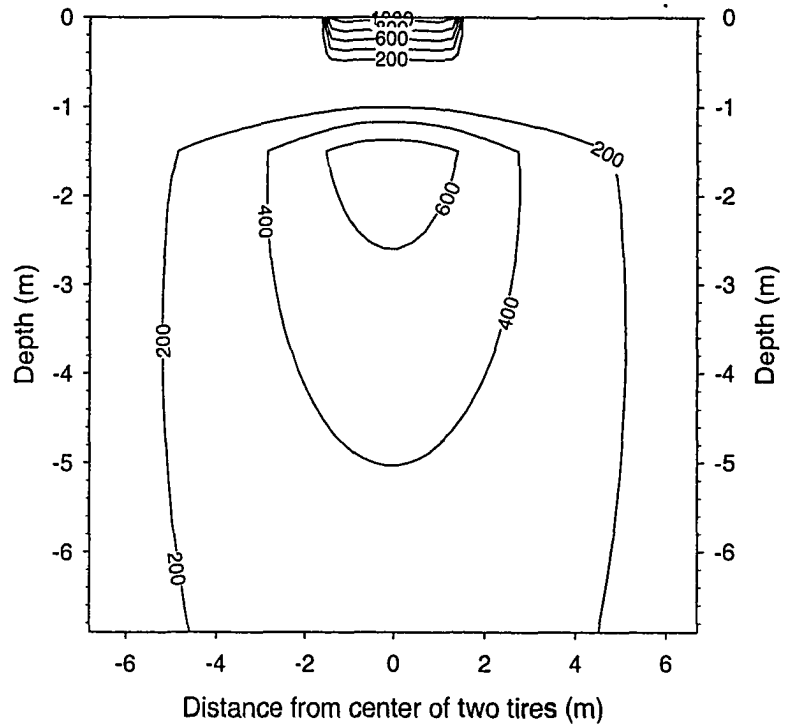


Figure 4.9 Vertical strains beneath two adjacent tires (in micro-strain) using $E = 9750 \text{ MPa}$

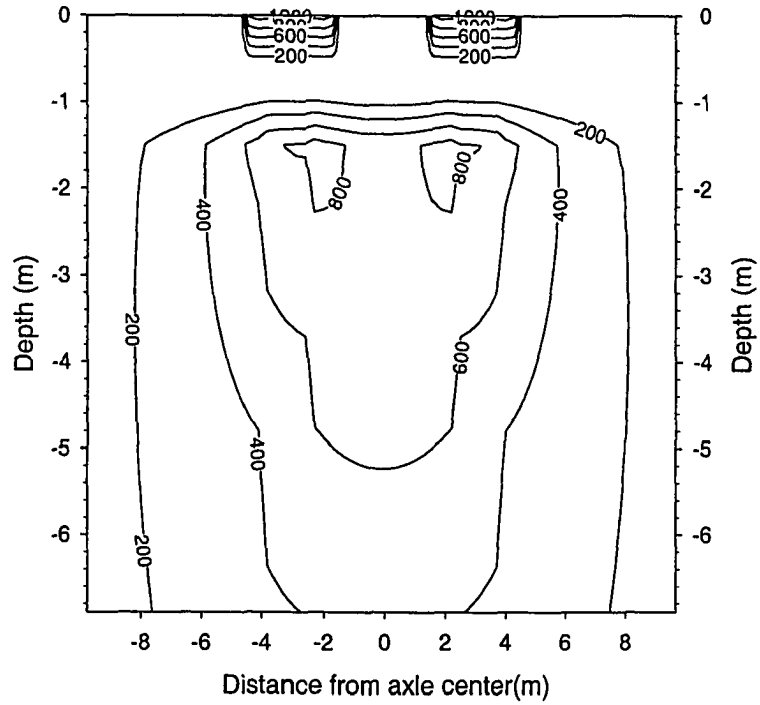


Figure 4.10 Vertical strains beneath four rear tires (in micro-strain) using $E = 9750 \text{ MPa}$

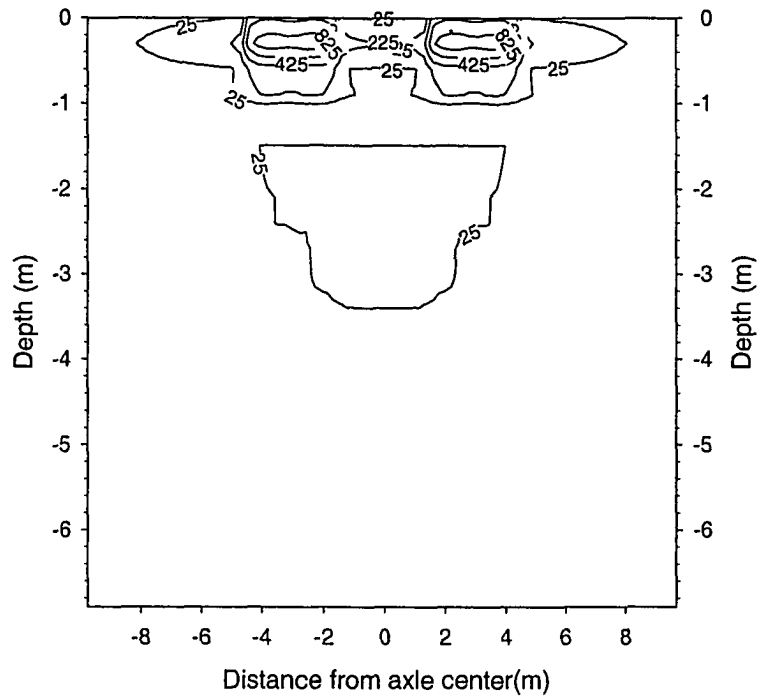


Figure 4.11 Vertical stress distribution beneath four rear tires (in kPa) using $E = 9750 \text{ MPa}$

The Sigma/W analysis was also performed on different models using modulus of 3925 MPa for sulfur concrete (reduced modulus value obtained after 300 freeze-thaw cycles). After many trial and errors it was found that 1.2 m thick sulfur concrete covered by 0.3 m gravel surface course with modulus of 300 MPa was required to satisfy the strain limit and bearing capacity design criteria.

Figures 4.12 to 4.14 shows the vertical strain distributions beneath the single tire, two adjacent tires and all four tires on the back axle of the haul truck, respectively. Examination of the figures reveals that interaction between adjacent tires affects the vertical strain levels in the sub-grade layer. The maximum strain level in the sub-grade increased from 450 to 800 micro strain and from 450 to 950 micro strain when two and four tires were considered, respectively. The effect is not significant in the surface course and sulfur concrete layers because the strain bulbs are not sufficiently wide enough to interact in those layers.

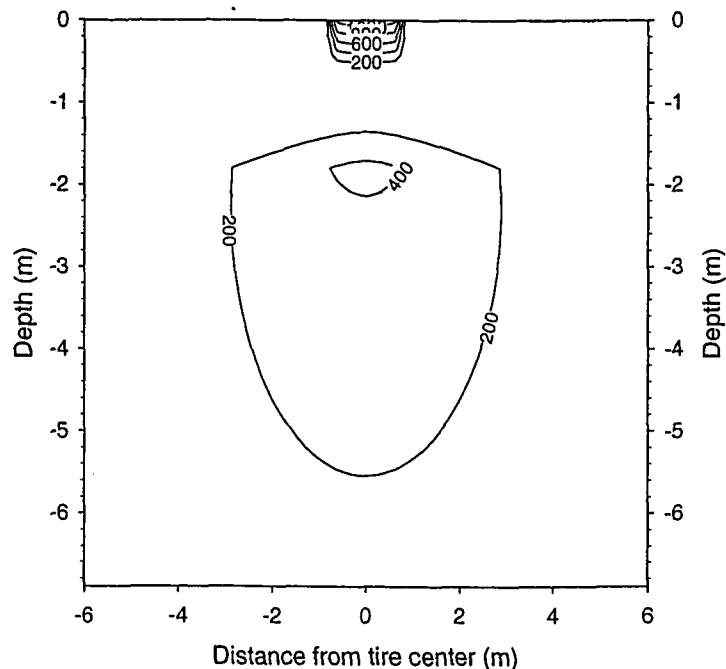


Figure 4.12 Vertical strains beneath single tire (in micro-strain) using $E = 3925$ MPa

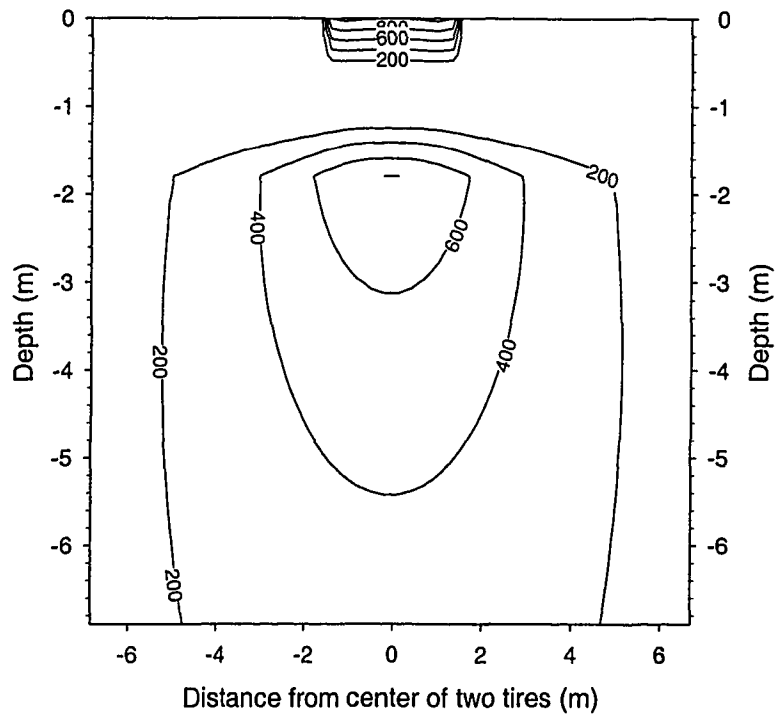


Figure 4.13 Vertical strains beneath two adjacent tires (in micro-strain) using $E = 3925 \text{ MPa}$

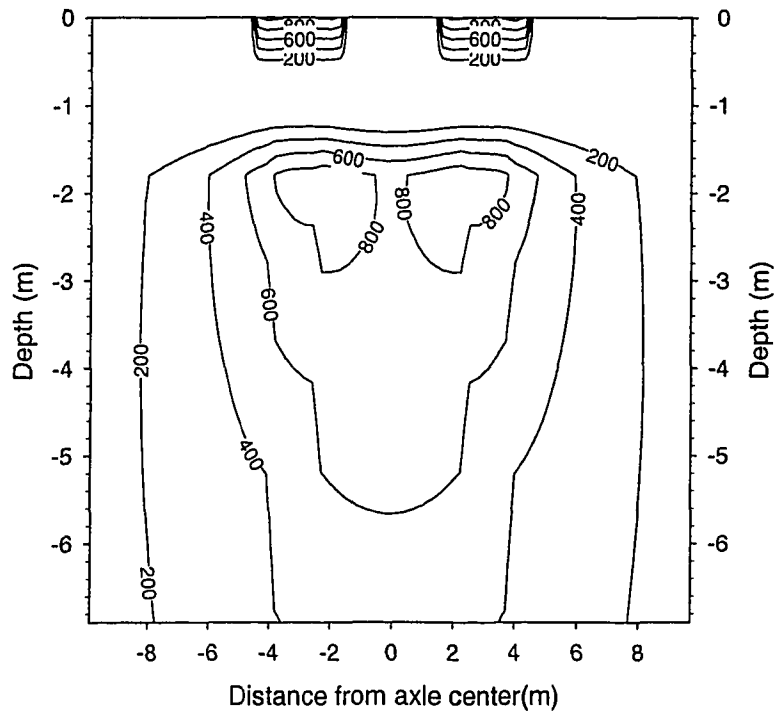


Figure 4.14 Vertical strains beneath four rear tires (in micro-strain) using $E = 3925 \text{ MPa}$

Figure 4.15 shows the vertical stress distribution beneath four tires of the back axle of CAT 797 haul truck. The maximum stress level in the sub-grade due to the single tire load was 17 kPa and it increased to 28 kPa when two tires were considered (not shown). The maximum stress level in the sub-grade, sulfur concrete layer and surface course is 35 kPa, 750 kPa and 600 kPa, respectively when all four tires in the back axle were considered.

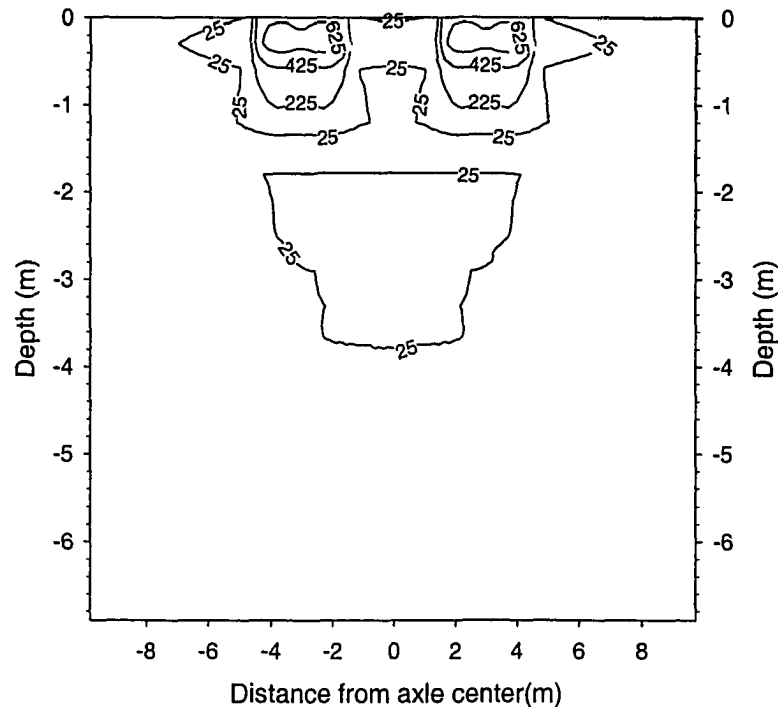


Figure 4.15 Vertical stress distribution beneath four rear tires (in kPa) using $E = 3925$ MPa

The Sigma/W analysis carried out showed that haul road constructed from 0.9 m thick sand sulfur concrete with modulus of 9750 MPa, or 1.2 m thick sand sulfur concrete with modulus of 3925, covered by 0.3 m thick surface gravel with modulus 300 MPa, on a sub-grade with modulus of 30 MPa, satisfies both the bearing capacity and strain limit criteria. Therefore, haul roads can be constructed with 0.9 m to 1.2 m thick sand sulfur concrete layers covered by 0.3 m surface gravel course depending on their design life (number of freeze-thaw cycles they will be subjected to).

5 CONCLUSION AND RECOMMENDATION

This thesis investigated the technical feasibility of construction of mine haul roads using sulfur concrete prepared from the mine wastes (sulfur, coke, fly ash and tailing sand) that are readily available at SUNCOR Oil Sands mines. This was achieved by conducting an extensive laboratory testing program to evaluate the physical, mechanical and chemical properties of different mix designs of sulfur concrete and by carrying out preliminary design evaluation of a haul road test section.

5.1 Summary of Findings

Two mixing techniques were used to produce sulfur concrete specimens for laboratory testing: the open hot mix and the dry post heating mix. Because of the simplicity of the equipment required, the open hot mix process was opted to produce the test specimens, which requires the sulfur to be molten and the aggregates to be heated before mixing. This process produces toxic gases such as Hydrogen Sulfide (H_2S) and Sulfur Dioxide (SO_2). However, as long as the temperature of the mix is maintained below about $149^{\circ}C$, the concentrations of these gases remain below the Maximum Allowable Concentrations (MAC) suggested by the American Conference of Governmental Industrial Hygienists (ACGIH).

As clearly seen in Figure 3.4, the strength and deformation properties of the sulfur concrete prepared from coke and sulfur improved with an increase in sulfur content. This is because the coke particles are porous and absorb molten sulfur requiring additional sulfur to provide strong bonding between individual particles. Figures 3.5 and 3.6 depict that fly ash contributes to improved strength and stiffness with the coke aggregate in the sulfur concrete by acting as fine grained pore filler. Its addition to the coke improved the grain size distribution of the aggregates allowing the sulfur to properly coat and cement the particles together resulting in a stronger and stiffer material. Tables 3.3 and 3.4 show that sulfur concrete produced from sulfur, fly ash

and tailings sand is much stronger and stiffer than concrete produced from sulfur, fly ash and coke.

The sulfur concrete mixtures tested in this research program had relatively linear stress-strain curves. The coke concrete specimens show higher axial strain at failure than the tailing sand concretes. However, in almost all the specimens tested, the post peak response ended with a sudden loss of load behaving in a brittle manner.

Three optimum mix designs, namely, 30S2.3FA67.7C, 35S2.3FA62.7C and 30S2.3FA67.7Sa, were selected for detailed investigation of sulfur concrete for its use in haul road construction. The first two mixes contained coke, sulfur and fly ash and the third one contained sand, sulfur and fly ash. The compressive stress - strain curves of these specimens (Figure 3.9) showed sulfur concrete made from coke is much weaker and more deformable than that made with tailing sand. This is mainly because individual coke particles are much weaker than the quartzite tailing sand particles. The dramatic decrease in stiffness is because coke sulfur concrete is porous with many open voids, whereas tailing sand sulfur concrete has fewer pores.

Coke sulfur concrete specimens failed when subjected to only 24 freeze-thaw cycles, when pop-outs occurred along the horizontal construction joints. The construction joints were created when the samples were prepared in multiple layers. The pop outs along the joints were followed by high degree of sample deterioration that led to sample disintegration. This failure was because coke particles are porous, water percolated into the pores and expanded during the freezing cycle breaking the particles apart.

The sand sulfur concrete specimens also showed strength deterioration when subjected to multiple freeze-thaw cycles. The sulfur concrete made from 30 % sulfur, 2.3 % fly ash and 67.7 % tailings sand by weight showed 42 % reduction in peak strength, 36 % reduction in yield strength and 60 % reduction in Young's modulus after 300 freeze-

thaw cycles. Figure 3.14 plots the variation of peak compressive strength, yield strength and Young's modulus with the number of freeze thaw cycles. The test results showed that there is a considerable degradation of the material when subjected to multiple freeze thaw cycles. However, it is to be noted that even though the samples have deteriorated, the strength and deformation characteristics after 300 freeze-thaw cycles indicated sand-sulfur concrete is still much better than the existing road building materials made of crushed aggregate and limestone.

Potential geo-environmental impacts of sulfur concrete haul roads with the near surface environment were studied using weathering and diffusion tests. The weathering test simulated the short term interaction of sulfur concrete exposed at the surface during haul road construction and operation, while the diffusion testing simulated the long term interaction of sulfur concrete following its burial with mine wastes in mined out pits. The test results showed that for the 5 months duration in which the test was conducted, there was very little interaction between the sulfur concrete and the environment, suggesting that sulfur concrete can be used as haul road construction material in a safe manner with no detrimental effect to human health or the environment.

The laboratory test results showed that, with the materials available from the oil sands industry such as sulfur, fly ash and tailings sand, competent construction materials can be produced. The sulfur concrete tested is much stronger and stiffer than the existing haul road building materials at SUNCOR Oil Sands mines, thus improved haul roads can be built with reduced pavement thicknesses.

The Sigma/W analysis carried out on the sand sulfur concrete haul road cross section showed that a 0.9 m thick sand sulfur concrete with modulus of 9750 MPa, or 1.2 m thick sand sulfur concrete with modulus of 3925, covered by 0.3 m thick surface gravel with modulus 300 MPa, on a sub-grade with modulus of 30 MPa, satisfies both the bearing capacity and strain limit criteria and is thus adequate to sustain CAT 797

haul trucks. Therefore, haul roads should be able to be constructed with 0.9 m to 1.2 m thick sand sulfur concrete sections covered by 0.3 m surface gravel course at SUNCOR oil sands mine sites depending on their design life (number of freeze-thaw cycles they will be subjected to).

5.2 Recommendations

5.2.1 Sample preparation

The fabrication of sulfur concrete specimens following the procedures given in ACI 548.2R (1988) resulted in construction joints in the specimens, which were clearly observed during the freeze-thaw cycles. The construction joints were formed when the sulfur concrete was cast in multiple layers. Thus, to avoid these construction joints, it is recommended to use smaller molds, approximately 38 mm x 76 mm, to cast sulfur concrete in a single layer.

5.2.2 Sulfur concrete placement during construction

The pop out of test specimens along the weak planes (construction joints) during the freeze-thaw test alerts on the method of placement of sulfur concrete during road construction. A construction procedure which secures a strong bond between the successive layers of sulfur concrete should be implemented. One alternative is using sheepsfoot compacters during placement of sulfur concrete to produce interlocking between successive layers. Another possible option is to spray a thin layer of very hot sulfur/sulfur concrete on top of the compacted layer before placing the subsequent layer. This way, a better bond between the different layers could be formed.

5.2.3 Geochemical interaction studies

Elemental and ionic constituent concentrations in the drained water samples collected from the short term weathering test must be measured to provide a chemical signature of the components dissolved from the sulfur concrete. These data will establish the

acid formation reaction rates from the surface of the sulfur concrete and multi species dissolution rates. The data can also be incorporated into a reactive transport path geochemical model to predict the potential changes in geochemistry for water in contact with the particular sulfur concrete during the operational life of the haul roads.

The elemental and ionic constituents and their concentrations in the sampled waters collected from the long term diffusion test must be measured to provide a chemical signature of the components solubilized from the sulfur concrete. This will allow the mass rate of diffusion flux for individual elements and ionic compounds released from the sample into the water to be determined. These diffusion rates can be incorporated into a one dimensional reactive transport model to predict the potential changes in geochemistry for water in contact with the particular sulfur concrete during its long term burial with the mine wastes.

5.2.4 Future work

Because sulfur concrete is a new material for haul road construction, it is recommended to build an instrumented haul road test section and monitor the truck-haul road interactions and geochemical interactions of sulfur concrete with the environment under varying climatic conditions prior to implementing wide spread use of sulfur concrete haul roads.

REFERENCES

- Abdel-Jawad, Y. and Al-Qudah, M. 1993. The Combined Effect of Water and Temperature on The Strength of sulfur Concrete. Cement and Concrete Research, Vol. 24, pp. 165 – 175.
- AASHTO 1965. A policy on Geometric Design of Rural Highways. American Association of State Highway and Transportation Officials, Association general Offices, Washington D.C.
- AASHTO 1993a. *Standard Specifications for Transportation Materials and Methods of Sampling and Testing, Part-I Specifications, Sixteenth Edition*. American Association of State Highway and Transportation Officials. Washington D.C. USA.
- AASHTO 1993b. *Standard Specifications for Transportation Materials and Methods of Sampling and Testing, Part-II Tests, Sixteenth Edition*. American Association of State Highway and Transportation Officials. Washington D.C. USA.
- ACI 548.2R-88 1988. Guide for Mixing and Placing Sulfur Concrete in Construction, reported by ACI Committee 548. ACI Materials Journal, July-August, pp 314-325.
- Bacon, R. F. and Davis, H. S. 1921. Recent Advances in The American sulfur Industry. Chemical and Metallurgical Engineering, Vol. 24, No. 2, pp. 65-72.
- Beaudoin, J. J. and Sereda, P. J. 1973. The Freeze Thaw Durability of Sulfur Concrete. Building Research Notes, Division of Building Research, National Research council, Ottawa. 53p.
- Blessing, G. V. 1990. The Pulsed Ultrasonic Velocity Method for Determining Material Dynamic Elastic Moduli. Dynamic Elastic Modulus Measurements in Materials, ASTM STP 1045, Philadelphia, PA, pp. 47-57.
- Blight et al. 1978. Preparation and Properties of Modified Sulfur Systems. New Uses of Sulfur-II, Advances in Chemistry Series 165, Am Chem Soc, pp 13-30.
- Bordoli, B. K. and Pearch, Eli M. 1978. Plastic Sulfur Stabilization by Copolymerization of Sulfur with Dicyclopentadiene. New Uses of Sulfur-II, Advances in Chemistry Series 165, Am Chem Soc, pp 31-53.
- Bowels, J. E 1984. **Physical and Geotechnical Properties of Soils**. Second Edition, Mc-Graw-Hill Book Company, New York, USA.
- Cameron, R., Lewko, R. 1996. Predictive Relative Surface and Subgrade Deflection Versus Total Granular Thickness for Various Combinations of Fills and Sizes of Heavy Hauler. Internal Report. Syncrude Canada Limited.

- Cameron, R., Lewko, R. and Golden, M., 2001. Deflection (Strain) Based Haul Road Design. Proceedings of 54th Canadian Geotechnical Conference, September 16-19, Calgary, Alberta, pp. 1320 – 1327.
- Cohen, M.D. 1987. Damage Mechanism of Cyclic Freezing -Thawing in Sulfur Concrete. Cement and Concrete Research, Vol. 17, pp. 357-360
- Crick, S. M. and Whitmore, D. W. 1998. Using Sulfur Concrete on a Commercial Scale. Concrete International, American Concrete Institute, Detroit, Michigan, February, pp. 83-86.
- Crow, L. J. and Bates, R. C. 1970. Strength of Sulfur – Basalt Concretes. U.S. Bureau of Mines Investigation Report 7439, Mining Research Laboratory, Bureau of Mines, Spokane, Washington, 21 pp.
- Czarnecki, B. and Gillot, J. E. 1989. Effect of Different Admixtures on the Strength of Sulfur Concrete. Cement, Concrete and Aggregates, CCAGDP, Vol. 11, No.2, pp. 109-118.
- Czarnecki, B. and Gillot, J. E. 1989. Stress – Strain Behavior of Sulfur Concrete made with Different Aggregates and Admixtures. Quarterly Journal of Engineering Geology, London, Vol. 22, pp.196 – 206.
- Czarnecki, B. and Gillot, J. E. 1990. The Effect of Mix Design on the properties of Sulfur Concrete. Cement, Concrete and Aggregates, CCAGDP, Vol. 12, No.2, Winter 1990, pp. 79-86.
- Dale, J. M. and Ludwig, A. C. 1966. Feasibility Study for Using Sulfur-aggregate Mixtures as a Structural Material. Technical Report NO, AFWL-TR-66-57, Southwest Research Institute, San Antonio, Sept., 40p
- Dale, J. M. and Ludwig, A. C. 1968. Advanced Studies of the sulfur-Aggregate Mixtures as a Structural Material. Technical Report NO, AFWL-TR-68-21, Southwest Research Institute, San Antonio, Oct., 68p
- Deme, I. 1974. Processing of Sand-Asphalt-Sulfur Mixes. Presented at the Annual Meeting of the Association of Asphalt Paving Technologists, Williamsburg, Virginia, February.
- Deuel, L. E., and Saylak, D. 1981. Environmental and Safety Aspects of the Use of Sulfur in Highway Pavements: Part II – Weathering and In-Service Considerations. Proceedings of SULFUR-81 and International Conference on Sulfur, Calgary, May, pp. 681-709.

- Diehl, L. 1976. Dicyclopentadiene Modified Sulfur and Its Uses as an Example. Proc New Uses for Sulfur and Pyrites, May 17-19, Madrid. The Sulfur Institute, Washington D.C., pp. 202-214.
- Duecker, W. W. 1934. Admixtures Improve Properties of Sulfur Cements. Chemical and Metallurgical Engineering, Vol. 41, No. 11, pp. 583-586.
- Duecker et al. 1948. Studies of Properties of Sulfur Jointing Compounds. Journal of Am Waterworks Association, Vol. 7, pp. 715-728.
- Funke, R. H., Jr. and McBee, W. C. 1982. An Industrial application of Sulfur Concrete. ASC Symposium Series No 183, American Chemical Society, Washington, D.C., pp. 195-208.
- Gamble, B. R. and Shrive, N. G. 1978. Creep in Sulfur. Proceedings of the International Conference on Sulfur in Construction, CANMET, Energy, Mines and Resource Canada, Sept. 12-15, Ottawa, pp. 503-518.
- Garcia, J. F. 2002. A Sulfur Concrete Retaining Wall. Unpublished M.Sc Thesis Department of Civil & Environmental Engineering, University of Alberta
- Gillott et al. 1980. Sulfur Concretes, Mortars and the Like. U.S. Patent No. 4, 188,230, Feb. 12
- Gillott et al. 1982. Studies of Sulfur Concrete Made With Different Aggregates. Proceedings of SULPHUR-82, International Sulfur Conference, London, England, pp. 45-49.2
- Gillott et al. 1983. Effect of Different Aggregates on the Durability of Sulfur Concretes. Durability of building materials, Vol. 1, pp. 255-273.
- Gregor, R. and Hack, A. 1978. A new Approach to Sulfur Concretes. New Uses of Sulfur-II, Advances in Chemistry Series 165, Am Chem Soc, pp. 54-78.
- Izatt, J. O. 1977. Sulfur-Extended Asphalt Paving Project Highway US 93-95, Boulder City, Nevada – A Construction Report. Prepared for the Sulfur Institute, January.
- Johnston, C. D. 1978. Preparation, Proportioning and Properties of Sulfur Concrete. Proceedings of the International Conference on Sulfur in Construction, CANMET, Energy, Mines and Resource Canada, Sept. 12 – 15, Ottawa, pp. 413-432
- Kaufman, W.W. and Ault, J. C. 1977. Design of Surface Mining Haulage Roads – a Manual. U.S Department of Interior, Bureau of Mines, Information Circular 8758.
- Kemp et al. 1971. UV Light Accelerates Acid Build in Wet Sulfur. Alberta Sulfur Research Quarterly Bull, 7:4:29-31.

- Knapton J. 1988. The Structural Design of Heavy Duty Pavements for Ports and Other Industries. British Ports Federation
- Kobbe, W. H. 1924. New Uses for Sulfur in Industry. J Ind and Eng Chem, 16:10:126.
- Kumar, V. 2000. Design and Construction of Haul Roads Using Fly Ash. Unpublished M.Sc Thesis, School of Mining and Petroleum Engineering, Department of Civil & Environmental Engineering, University of Alberta.
- Kumar, V. 2001. Haul Road Design. Internal Engineering Report, Mine Engineering SUNCOR Energy Inc., pp. 1-24
- Laishly, E. J. and Tyler, M. C. 1978. Biological Oxidation of Sulfur Construction Materials. Proceedings of the International Conference on Sulfur in Construction, CANMET, Energy, Mines and Resource Canada, Sept. 12-15, Ottawa, pp. 171-180
- Lau, C. S. 2003. Geo-environmental Issues for Waste Sulfur Storage and Disposal. Department of Civil and Environmental Engineering, University of Alberta
- Lee D. Y. and Klaiber, F. W. 1976. Fatigue Behavior of Sulfur Concrete. New Horizons in Construction Materials, pp 363, Envo Publishing Co., Lehigh Valley, PA
- Lee D. Y. and Klaiber, F. W. 1981. Fatigue Behavior of Plasticized Sulfur Concrete. SULPHUR-81, International Conference on Sulfur, Calgary, May.
- Lee D.Y. et al. 1978. Fatigue Behavior of Improved Sulfur Concrete. Proceedings of the International Conference on Sulfur in Construction, CANMET, Energy, Mines and Resources Canada, Sept. 12-15, Ottawa, pp. 489-502.
- Leutner, B. and Diehl, L. 1977. Manufacture of Sulfur Concrete. U.S. Patent No 4,025,352, May 24.
- Litvan, G. G. 1976. Frost Action in Cement in the Presence of Deicers. Cement and Concrete Research, 6,3, pp. 351-356.
- Loov, R. E. 1975. Sulfur Concrete – State of the Art in 1974. Research Report No. CE 75-2, Department of Civil Engineering, University of Calgary, 10 pp.
- Malhotra, V. M. 1973. Mechanical Properties and Freeze-Thaw Resistance of Sulfur Concrete. Division Report IR 73-18, Energy, Mines and Resources Canada, 33 pp.
- Malhotra, V. M. 1974. Effect of Specimen Size on Compressive Strength of Sulfur Concrete. Division Report IR 74-25, Energy, Mines and Resource Canada

- Malhotra, V. M. 1979. Sulfur Concrete and Sulfur Infiltrated Concrete: Properties, Applications and Limitations. CANMET Report 79-28. Energy, Mines, and Resources Canada, Ottawa, 26p.
- Malhotra et al. 1978. Editors, Proceedings, International Conference on Sulfur in Construction, Ottawa, Sept., V.2, 555 pp
- McBee W. C., and Sullivan, T. A. 1979. Development of Specialized Sulfur Concretes. BuMines Report No RI 8346, U.S. Bureau of Mines, Washington D.C., 21 p.
- McBee W. C., and Sullivan, T. A. 1982. (assigned to US Department of Commerce). Modified Sulfur Cement. U.S. Patent No 4,311,826, Jan 19
- McBee W. C., and Sullivan, T. A. 1982, (assigned to US Department of Commerce). Concrete Formulations Comprising Polymeric Reaction Products of Sulfur/Cyclopentadiene, Oligomer/Dicyclopentadiene. U.S. Patent No 4,348,313, Sept. 7
- McBee, W.C., Sullivan, T.A., and Fike, H. F. 1986. Corrosion Resistant Sulfur Concretes. Corrosion and Chemical Resistant Masonry materials Handbook, Noyes Publications, Park Ridge, pp. 392-417
- McBee, W.C., Sullivan, T.A., and Jong, B.W. 1981. Modified Sulfur Concrete Technology. Proceedings, SULFUR-81 International Conference on Sulfur, Calgary, May. Pp. 367-388
- McBee, W.C., Sullivan, T.A., and Jong, B.W. 1983. Industrial Evaluation of Sulfur Concrete in Corrosive Environments. BuMines Report No RI 8786, U.S. Bureau of Mines, Washington, D.C., 15 pp.
- McBee, W.C., Sullivan, T.A., and Jong, B.W. 1983. Corrosion Resistant Sulfur Concretes. BuMines Report No 8758, U.S. Bureau of Mines, Washington, D.C., 28 pp.
- McKinney, P. V. 1940. Provisional Methods for Testing Sulfur Cements. ASTM Bulletin 96-107, Oct., pp. 27-30.
- Mohammed, L. N., Titi, H.H. and Herath, A. 1998. Intrusion Technology: An Innovative Approach to Evaluate Resilient Modulus of Sub-grade Soils, Application of Geotechnical Principles in Pavement Engineering, American society of Civil Engineers, Geotechnical Special publication Number 85: 39-58.
- Monenco 1989. Design Manual for Surface Mine Haul Roads. Draft report by Monenco Consultants Limited, Calgary, Alberta.

- Morgan, J.R., Tucker, J.S. and McInnis, D.B. 1994. A Mechanistic Design Approach for Unsealed Mine Haul Roads. *Pavement Design and Performance in Road Construction* 1412: 69-81.
- Nimer, F. L., and Campbell, R. W. 1983. Sulfur Cement-Aggregate-Organosilane Composition and Methods for Preparing. U.S. Patent No 4,376,830, Mar. 15
- Okamura, H. A. 1998. Early Sulfur Concrete Installations. *Concrete International*, American Concrete Institute, January, pp. 72-75
- Payne, C. R. and Duecker, W. W. 1940. Chemical Resistance of Sulfur Cements. *Trans Am Inst Eng*, 36:1:91-111.
- Pickard, Scott S. 1983. Sulfur Concrete at AMAX Nickel Project Case History. *Proceedings, International Symposium on New Materials for Building and Civil Engineering*, National institute for Applied Sciences, Rennes, Sept., pp. 244-270.
- Powers, T. C. 1975. Freezing Effects in Concrete. American Concrete Institute, Special publication No SP-47, pp. 1-11
- Raymont, M. E. D. 1978. Sulfur Concretes and Coatings. Sulfur Development Institute of Canada, Calgary, Alberta, 43 pp.
- Rennie, W. J. 1978. Sulfur Asphalts: The Pronk S/A Emulsion Binder System, 2nd Edition. *New Uses for Sulfur Technological Series No 3 SUDIC*, Calgary, Alberta
- Rybezynski et al. 1974, Sulfur Concrete and Very Low Cost Housing. *Canadian Sulfur Symposium*, pp. 1-9.
- Saylak, D. et al. 1980. Environmental and Safety Aspects of the Use of Sulfur in Highway Pavements. Final Report No FHWA-RD-80/191, Texas A&M University, August
- Saylak, D., Deuel, L. E., and Zahray, R. 1981. Environmental and Safety Aspects of the Use of Sulfur in Highway Pavements: Part I – Mix Preparation and Construction. *Proceedings of: SULFUR-81 and International Conference on Sulfur*, Calgary, May, pp. 651-679.
- Schneider, R. A. and Simic, M. 1981. Plasticized Sulfur Composition. U.S. Patent No 4,308,072, Dec. 29.
- Sego, D.C. et al., 2003. Draft Research Proposal on Haul Road Improvement at SUNCOR. School of Mining and Petroleum Engineering, Department of Civil & Environmental Engineering, University of Alberta.

- Shrive et al. 1977. Basic properties of Some Sulfur Bound Composite Materials. *Material Science and Engineering*, Vol. 30, No 1, pp. 71-79
- Shrive et al. 1977. A Study of Durability in Temperature Cycles and water resistance of Sulfur Concretes and Mortars. *Journal of Testing and Evaluation*, Vol. 5, No 6, pp. 484-493
- Shrive et al. 1981. Freeze/Thaw Durability of Sulfur Concretes. *Proceedings of SULFUR-81 an International Conference on Sulfur*, Calgary, May, pp. 185-194.
- Sullivan, T. A. 1986. *Corrosion Resistant Sulfur Concretes Design Manual*. The Sulfur Institute, Washington, D.C., 44 p
- Sullivan, T. A., McBee, W. C and Blue, D.D. 1975. Sulfur in Coatings and Structural Materials. *Advances in Chemistry Series No 140*, American Chemical Society, Washington, D.C., pp. 55-74
- Sullivan, T. A., and McBee, W. C. 1976. Development and Testing of Superior Sulfur Concretes. *BuMines Report No. RI 8160*, U.S. Bureau of Mines, Washington DC, 30p.
- Tan, K. H., 1982. **Principles of Soil Chemistry**. Marcel Dekker Inc.
- Tannant, Dwayne D. and Regensburg, Bruce, 2001. *Guidelines for Mine Haul Road Design*. School of Mining and Petroleum Engineering, Department of Civil & Environmental Engineering, University of Alberta.
- Terzaghi, K. 1943, **Fundamentals of Soil Mechanics**. John Wiley and Sons Inc., New York, USA
- Thompson R. J. 1996. *The Design and Management of Surface Mine Haul Roads*. Ph.D. thesis, Faculty of Engineering, University of Pretoria.
- Thompson R. J. and Visser, A. T. 1997. A Mechanistic Structural Design Procedure for Surface Mine Haul Roads. *International Journal of Surface Mining, Reclamation and Environment* 11: 121-128
- Thompson R. J. and Visser, A. T. 1997. The Evaluation of Mine Haul Road Wearing Course Material Performance. *Surface Mining – Braunkohl & Other Minerals*, 52(4), 409-415.
- Vroom, A. H. 1977. Sulfur Cements, Process for Making Same and Sulfur Concretes Made Therefrom. U.S. patent No 4,058,500, Nov. 15
- Vroom, A. H. 1981. Sulfur Cements, Process for Making Same and Sulfur Concretes Made Therefrom. U.S. patent No 4,293,463, Oct. 6

- Wade, N. H. 1989. Design Manual for Surface Mine Haul Roads. Monenco Consultant Limited, Calgary, Alberta.
- Wieren, L. W. V. and Anderson, H. M. 1990. An Overview of Haul Roads at Syncrude Canada Limited. Course Notes for Mine Planning and Equipment Selection.
- Woo, G. L. 1983. Phosphoric Acid Treated Sulfur Cement Aggregate Compositions. U.S. Patent No 4,376,831, Mar. 15.
- Wright, A. H. 1859. U.S. Patent 25,074.
- Yarbrough, R. L. 1983. Specialized Construction Practices for Sulfur Concretes. Presented at the ACI Annual Convention., Los Angeles, Mar., 15 pp. (Unpublished).

APPENDIX A LABORATORY TEST RESULTS

This appendix presents laboratory test results of the unconfined compression test, sonic velocity measurement test, split tensile test, resistance to rapid freezing and thawing test and geochemical interaction test carried out on different mix designs of sulfur concrete specimens prepared from oil sands industry mine wastes like sulfur, fly ash, coke and tailings sand.

Mix design	Density (kg/m ³)	Statistics		
		Mean	Range	Standard Deviation
30S70C-1	1036	1040.3	9	3.68
30S70C-2	1045			
30S70C-3	1040			
35S65C-1	1187	1158	58	23.68
35S65C-2	1129			
35S65C-3	1158			
40S60C-1	1214	1221.7	55	23.1
40S60C-2	1198			
40S60C-3	1253			
30S2.3FA67.7C-1	1078	1063.7	38	16.86
30S2.3FA67.7C-2	1073			
30S2.3FA67.7C-3	1040			
30S4.6FA65.4C-1	1060	1080.3	33	14.52
30S4.6FA65.4C-2	1088			
30S4.6FA65.4C-3	1093			
35S2.3FA62.7C-1	1205	1193	72	30.59
35S2.3FA62.7C-2	1151			
35S2.3FA62.7C-3	1223			
35S4.6FA60.4C-1	1250	1217.3	98	46.18
35S4.6FA60.4C-2	1152			
35S4.6FA60.4C-3	1250			
30S20FA50C-1	1310	1358.3	76	34.3
30S20FA50C-2	1386			
30S20FA50C-3	1379			
40S10FA50C-1	1493	1462.3	62	25.32
40S10FA50C-2	1463			
40S10FA50C-3	1431			
33.3S33.3FA33.3C-1	1290	1303.3	34	16.78
33.3S33.3FA33.3C-2	1293			
33.3S33.3FA33.3C-3	1327			
30S2.3FA67.7Sa-1	2079	2170	182	91
30S2.3FA67.7Sa-2	2261			

Table A-1 Density of sulfur concrete mixes

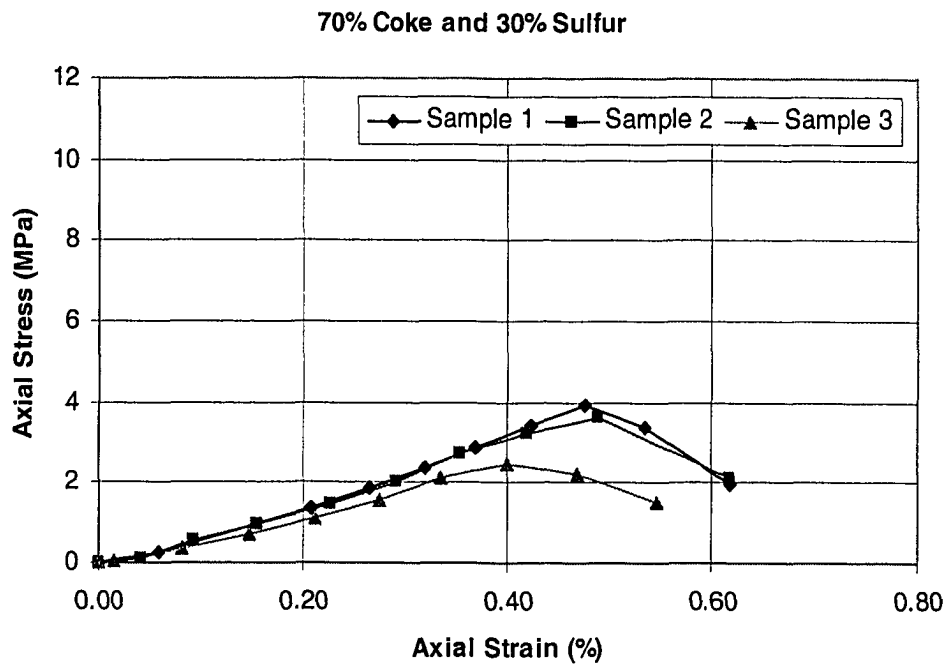


Figure A-1 30S70C stress-strain curve

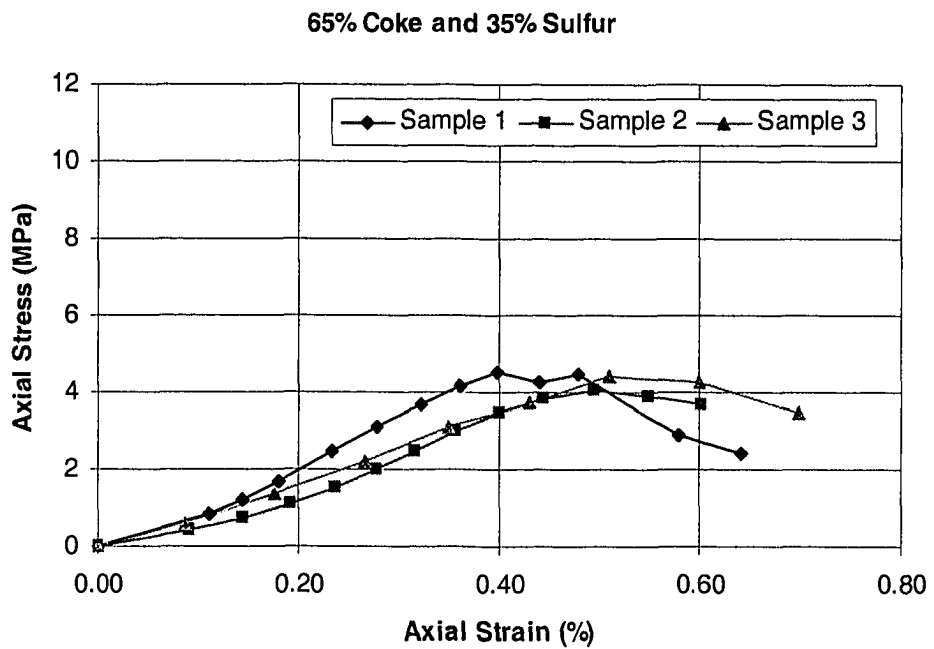


Figure A-2 35S65C stress-strain curve

60% Coke and 40% Sulfur

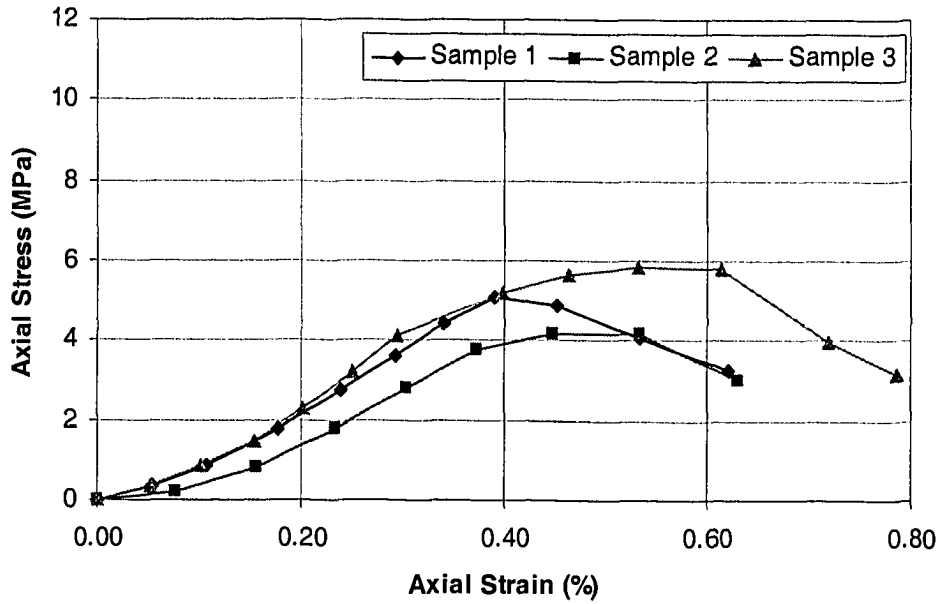


Figure A-3 40S60C stress-strain curve

67.7% Coke, 30% Sulfur, and 2.3% Fly Ash

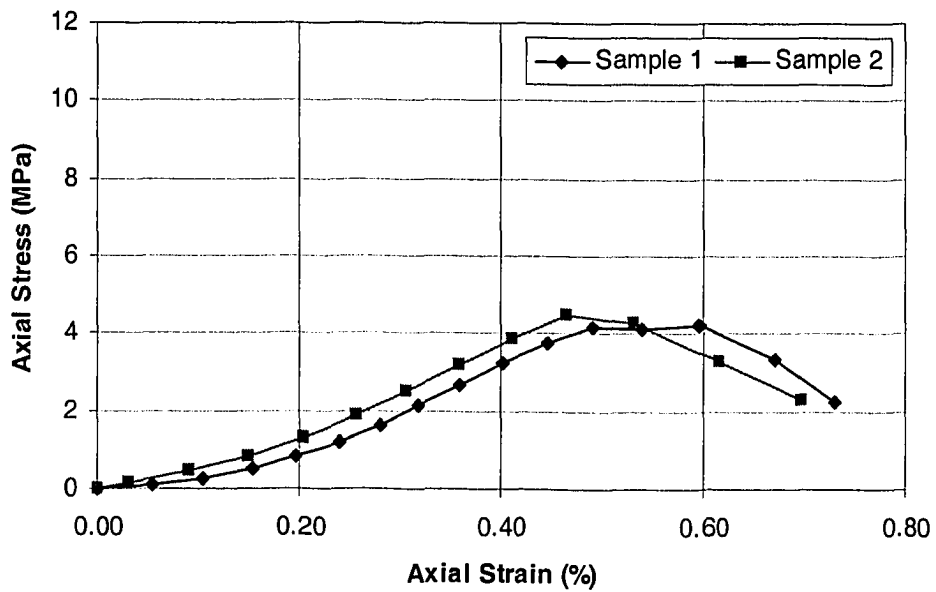


Figure A-4 30S2.3FA67.7C stress-strain curve

65.4% Coke, 30% Sulfur, and 4.6% Fly Ash

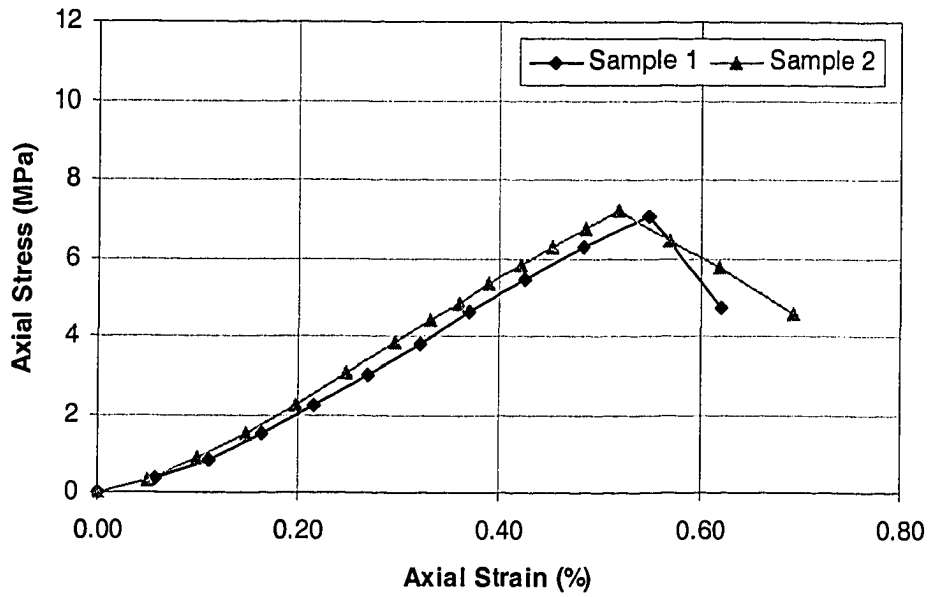


Figure A-5 30S4.6FA65.4C stress-strain curve

62.7% Coke, 35% Sulfur, and 2.3% Fly Ash

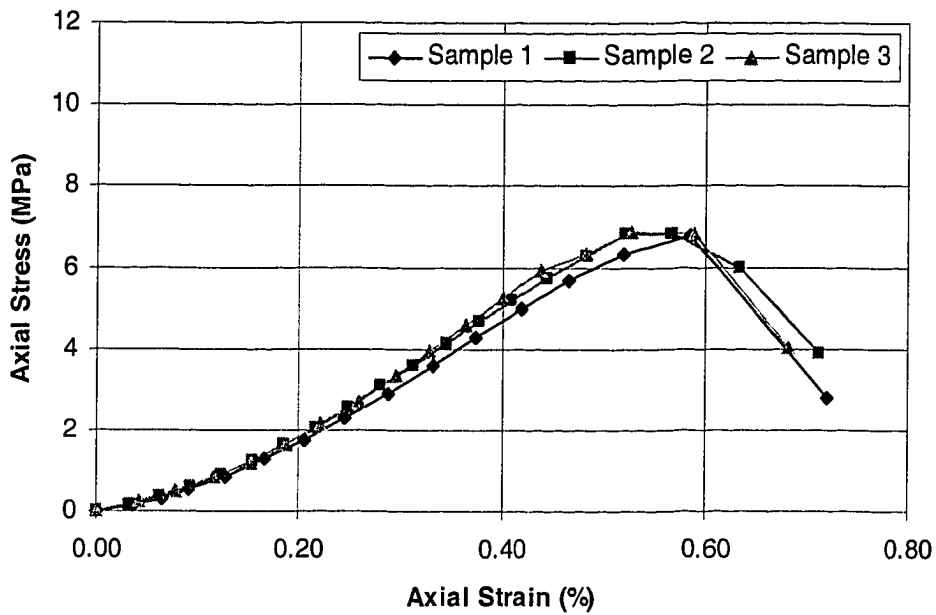


Figure A-6 35S2.3FA62.7C stress-strain curve

60.4% Coke, 35% Sulfur, and 4.6% Fly Ash

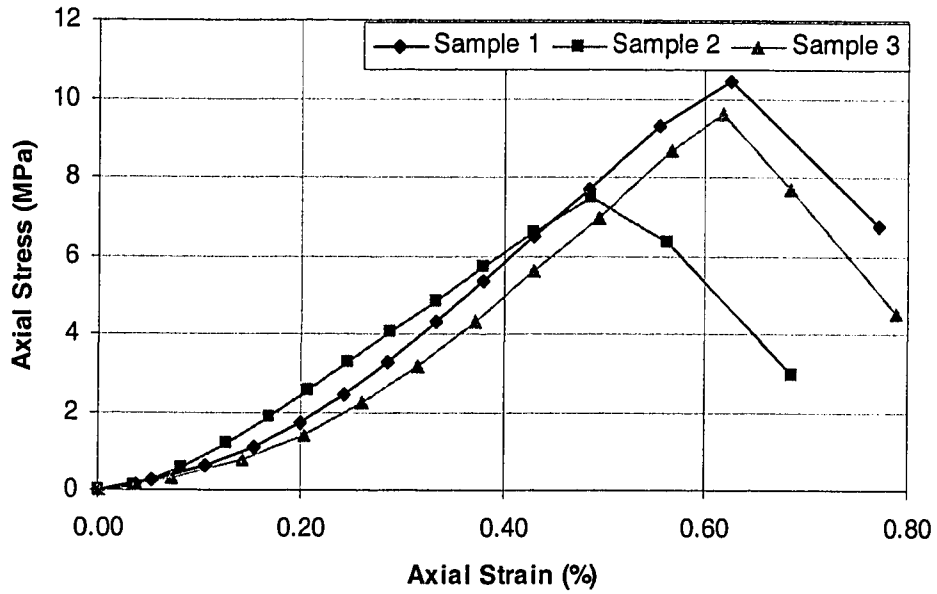


Figure A-7 35S4.6FA60.4C stress-strain curve

50% Coke, 30% Sulfur, and 20% Fly Ash

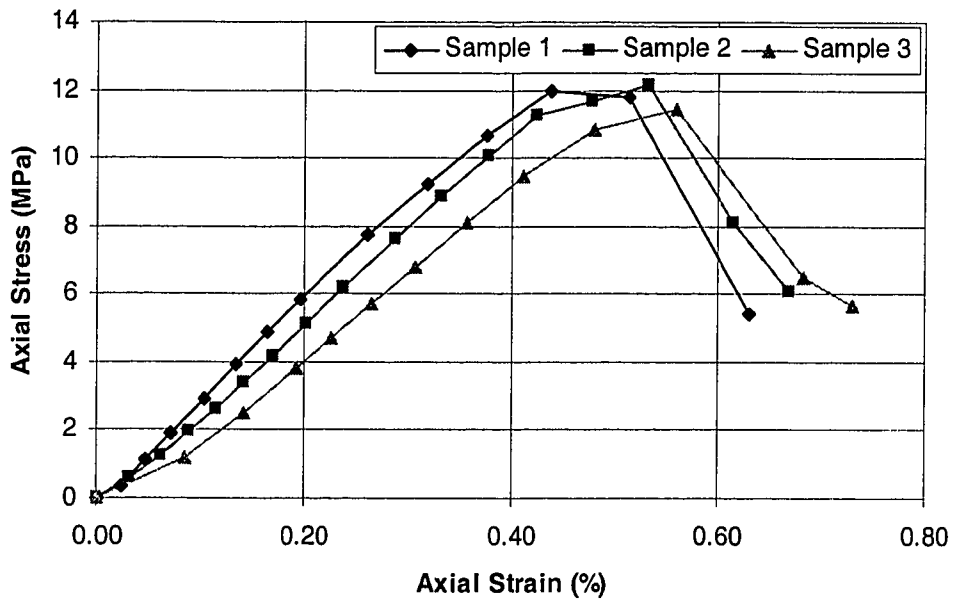


Figure A-8 30S20FA50C stress-strain curve

50% Coke, 40% Sulfur, and 10% Fly Ash

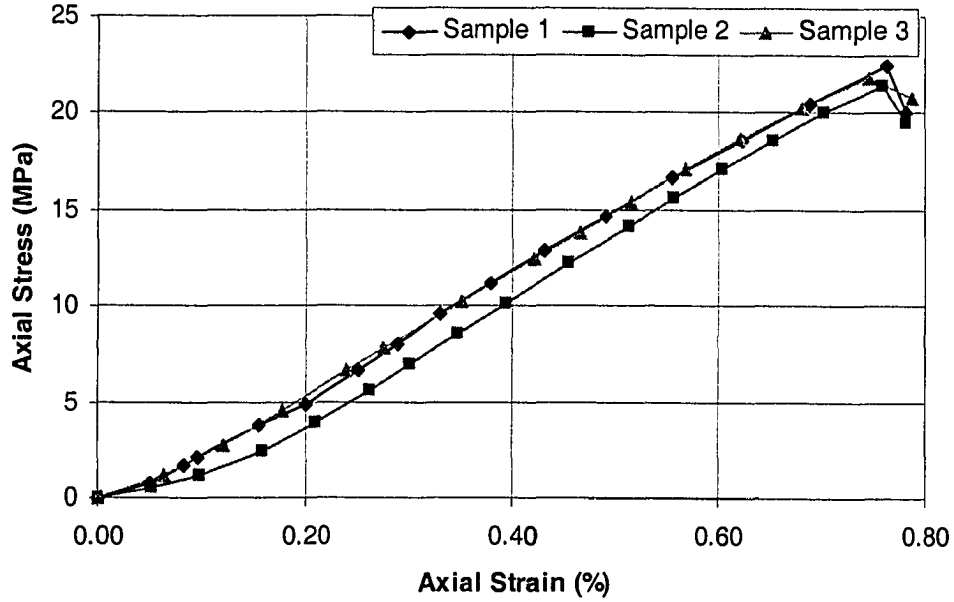


Figure A-9 40S10FA50C stress-strain curve

33.3% Coke, 33.3% Sulfur, and 33.3% Fly Ash

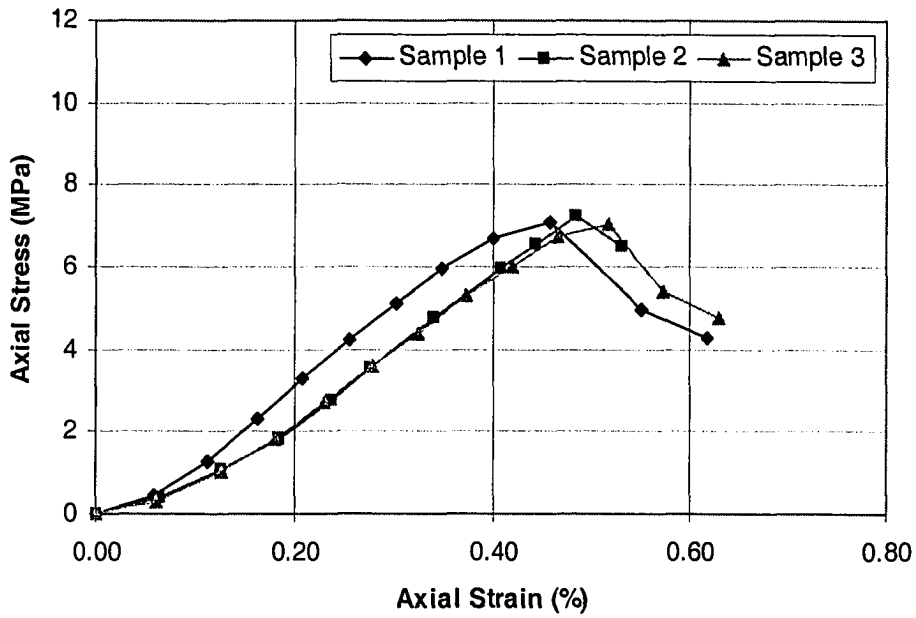


Figure A-10 33.3S33.3FA33.3C stress-strain curve

67.7% Tailing Sand, 30% Sulfur, and 2.3% Fly Ash

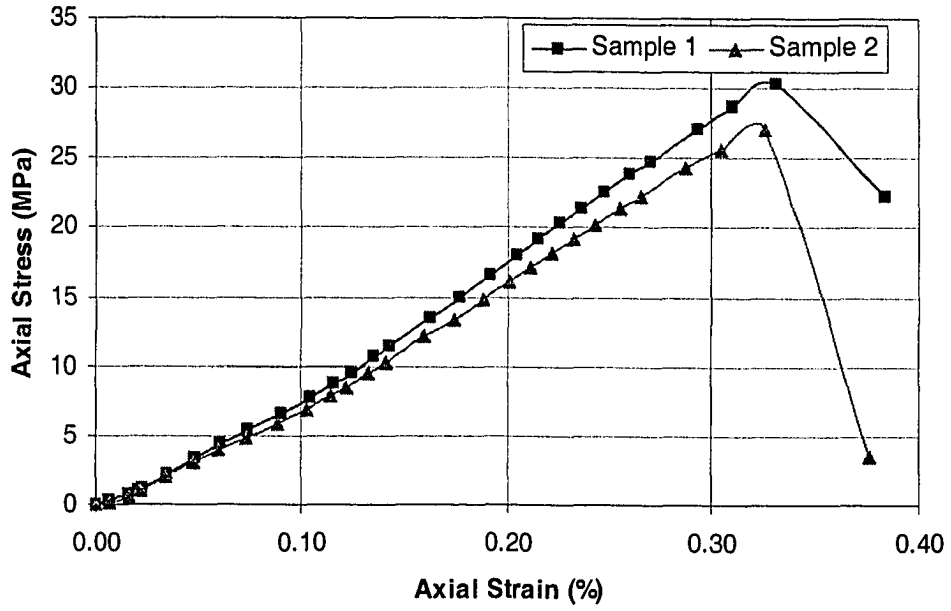


Figure A-11 30S2.3FA67.7C stress-strain curve

Mix design	Peak strength (MPa)	Statistics		
		Mean	Range	Standard Deviation
30S70C-1	4.22	3.65	1.43	0.62
30S70C-2	3.93			
30S70C-3	2.79			
35S65C-1	4.48	4.57	1.38	0.57
35S65C-2	3.92			
35S65C-3	5.30			
40S60C-1	5.35	5.17	3.39	1.21
40S60C-2	3.38			
40S60C-3	6.77			
30S2.3FA67.7C-1	4.82	4.75	0.15	0.08
30S2.3FA67.7C-2	4.67			
30S2.3FA67.7C-3	-			
30S4.6FA65.4C-1	7.90	8.01	0.41	0.19
30S4.6FA65.4C-2	8.27			
30S4.6FA65.4C-3	7.86			
35S2.3FA62.7C-1	7.66	7.57	0.26	0.12
35S2.3FA62.7C-2	7.65			
35S2.3FA62.7C-3	7.40			
35S4.6FA60.4C-1	10.94	9.75	2.87	1.22
35S4.6FA60.4C-2	8.07			
35S4.6FA60.4C-3	10.23			
30S20FA50C-1	12.44	12.6	0.32	0.13
30S20FA50C-2	12.76			
30S20FA50C-3	12.61			
40S10FA50C-1	26.52	24.49	3.38	1.46
40S10FA50C-2	23.14			
40S10FA50C-3	23.8			
33.3S33.3FA33.3C-1	7.33	7.62	0.82	0.38
33.3S33.3FA33.3C-2	8.15			
33.3S33.3FA33.3C-3	7.38			
30S2.3FA67.7Sa-1	31	29.1	3.87	1.9
30S2.3FA67.7Sa-2	27.13			

Table A-2 Peak compressive strength of sulfur concrete mixes

Mix design	Young's Modulus (MPa)	Statistics		
		Mean	Range	Standard Deviation
30S70C-1	950	850	200	81.65
30S70C-2	850			
30S70C-3	750			
35S65C-1	1300	1133.3	350	143.37
35S65C-2	1150			
35S65C-3	950			
40S60C-1	1550	1533.3	350	143.37
40S60C-2	1350			
40S60C-3	1700			
30S2.3FA67.7C-1	1300	1300	0	0
30S2.3FA67.7C-2	1300			
30S2.3FA67.7C-3	-			
30S4.6FA65.4C-1	1500	1500	0	0
30S4.6FA65.4C-2	-			
30S4.6FA65.4C-3	1500			
35S2.3FA62.7C-1	1550	1600	100	40.8
35S2.3FA62.7C-2	1600			
35S2.3FA62.7C-3	1650			
35S4.6FA60.4C-1	2200	2033.3	400	169.97
35S4.6FA60.4C-2	1800			
35S4.6FA60.4C-3	2100			
30S20FA50C-1	2850	2750	250	108.01
30S20FA50C-2	2800			
30S20FA50C-3	2600			
40S10FA50C-1	3150	3150	200	81.65
40S10FA50C-2	3250			
40S10FA50C-3	3050			
33.3S33.3FA33.3C-1	2000	1900	200	81.65
33.3S33.3FA33.3C-2	1900			
33.3S33.3FA33.3C-3	1800			
30S2.3FA67.7Sa-1	10200	9750	900	450
30S2.3FA67.7Sa-2	9300			

Table A-3 Young's modulus of sulfur concrete mixes

Mix design	Density (kg/m ³)	P-Speed (m/s)	S-Speed (m/s)	Young's Modulus (MPa)	Bulk Modulus (MPa)	Shear Modulus (MPa)	Poisson's Ratio
30S70C - 1	1036	-	-	-	-	-	-
30S70C - 2	1045	994	599	911	531	375	0.214
30S70C - 3	1040	-	-	-	-	-	-
35S65C - 1	1187	-	-	-	-	-	-
35S65C - 2	1129	1147	673	1266	803	512	0.237
35S65C - 3	1157	-	-	-	-	-	-
40S60C - 1	1214	1398	699	1580	1580	593	0.333
40S60C - 2	1198	1234	656	1345	1136	516	0.303
40S60C - 3	1253	-	-	-	-	-	-
30S2.3FA67.7C - 1	1078	-	-	-	-	-	-
30S2.3FA67.7C - 2	1072	1299	709	1388	1093	539	0.288
30S2.3FA67.7C - 3	1040	-	-	-	-	-	-
35S2.3FA62.7C - 1	1205	-	-	-	-	-	-
35S2.3FA62.7C - 2	1151	1523	747	1723	1813	642	0.342
35S2.3FA62.7C - 3	1224	-	-	-	-	-	-
30S4.6FA65.4C - 1	1060	-	-	-	-	-	-
30S4.6FA65.4C - 2	1088	-	-	-	-	-	-
30S4.6FA65.4C - 3	1093	1494	730	1564	1665	582	0.343
35S4.6FA60.4C - 1	1250	1804	767	2041	3086	734	0.390
35S4.6FA60.4C - 2	1152	1925	700	1608	3517	565	0.424
35S4.6FA60.4C - 3	1250	-	-	-	-	-	-
30S20FA50C - 1	1310	1962	900	2901	3626	1061	0.367
30S20FA50C - 2	1386	-	-	-	-	-	-
30S20FA50C - 3	1379	1769	855	2718	2972	1008	0.348
40S10FA50C - 1	1493	1892	870	3091	3839	1132	0.366
40S10FA50C - 2	1463	1984	888	3172	4219	1154	0.375
40S10FA50C - 3	1431	1809	910	3152	3103	1185	0.331
33.3S33.3FA33.3C-1	1290	1711	789	2194	2702	804	0.365
33.3S33.3FA33.3C-2	1293	1494	762	1987	1885	750	0.324
33.3S33.3FA33.3C-3	1327	1615	667	1650	2674	590	0.397
30S2.3FA67.7Sa - 1	2079	3293	1411	11494	17028	4142	0.388
30S2.3FA67.7Sa - 2	2261	2764	1322	10679	12003	3950	0.352

Table A-4 Sonic velocity measurement results

Sample ID	Density (kg/m ³)	Tensile strength (σ_t)(MPa)	Compressive strength (σ_c)(MPa)	Ratio of σ_t/σ_c (%)	Vertical strain at failure (%)
30S2.3FA67.7C - 1	1076	0.54	4.82	11.20	0.38
30S2.3FA67.7C - 2	1074	0.55	4.67	11.78	0.42
35S2.3FA62.7C - 1	1195	0.86	7.40	11.62	0.52
35S2.3FA62.7C - 2	1186	0.88	7.65	11.50	-
30S2.3FA67.7Sa - 1	2125	2.00	30.00	6.67	0.22
30S2.3FA67.7Sa - 2	2165	1.88	26.50	7.09	0.27

Table A-5 Split tensile test results

67.7% Coke, 30% Sulfur, and 2.3% Fly Ash

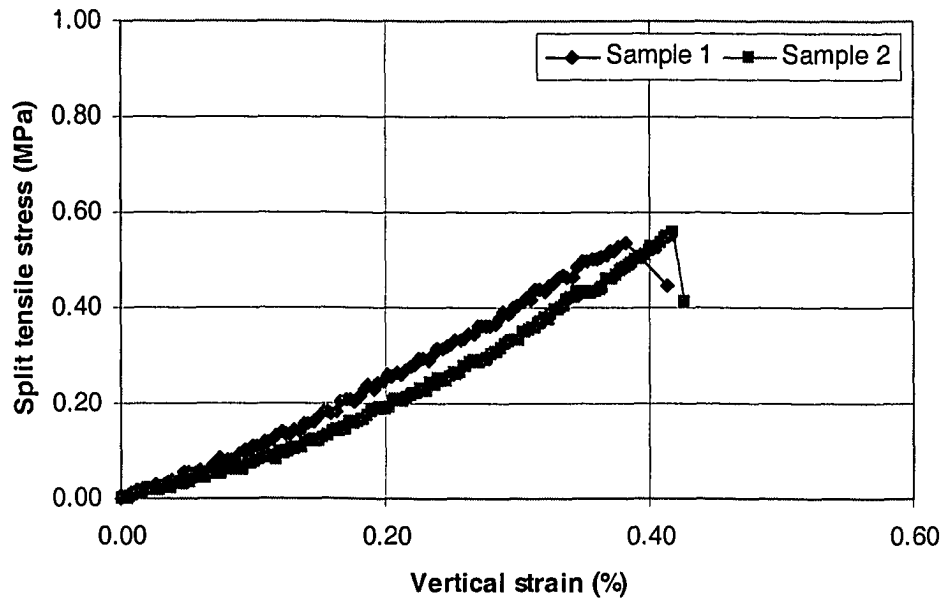


Figure A-12 30S2.3FA67.7C tensile stress-vertical strain curve

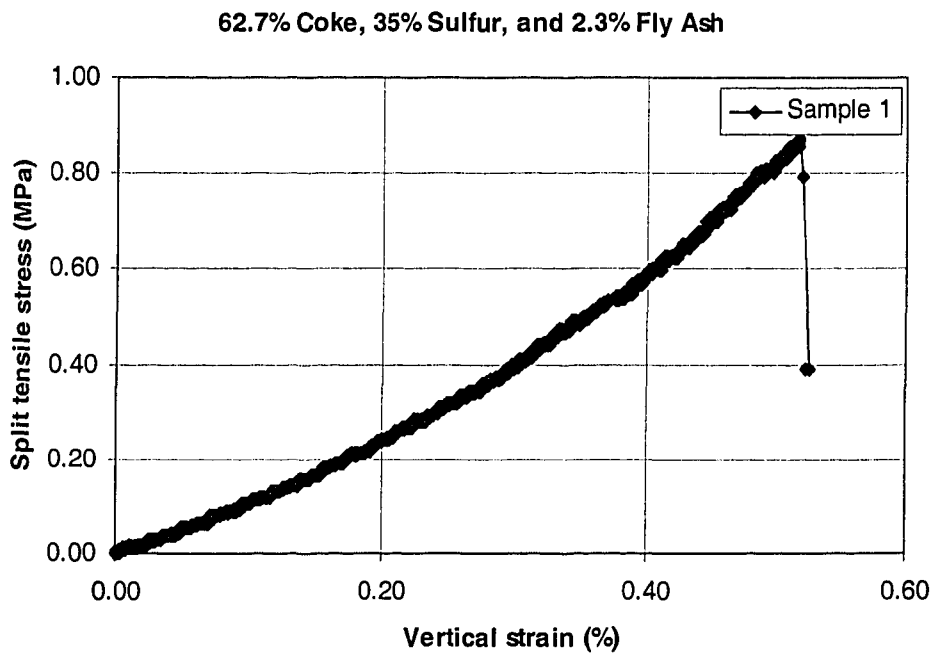


Figure A-13 35S2.3FA62.7C tensile stress-verticle strain curve

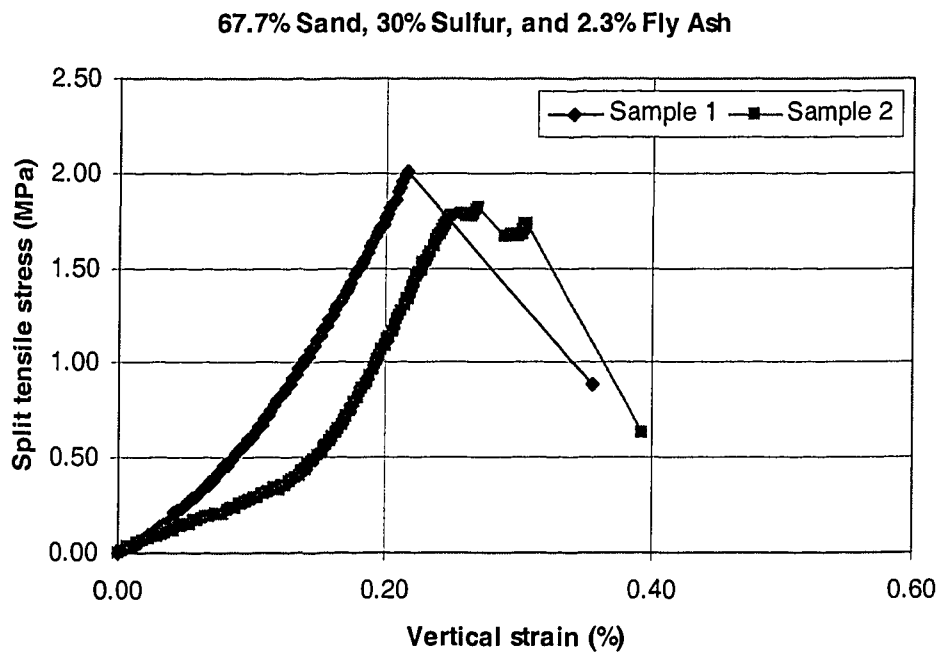


Figure A-14 30S2.3FA67.7Sa tensile stress-verticle strain curve

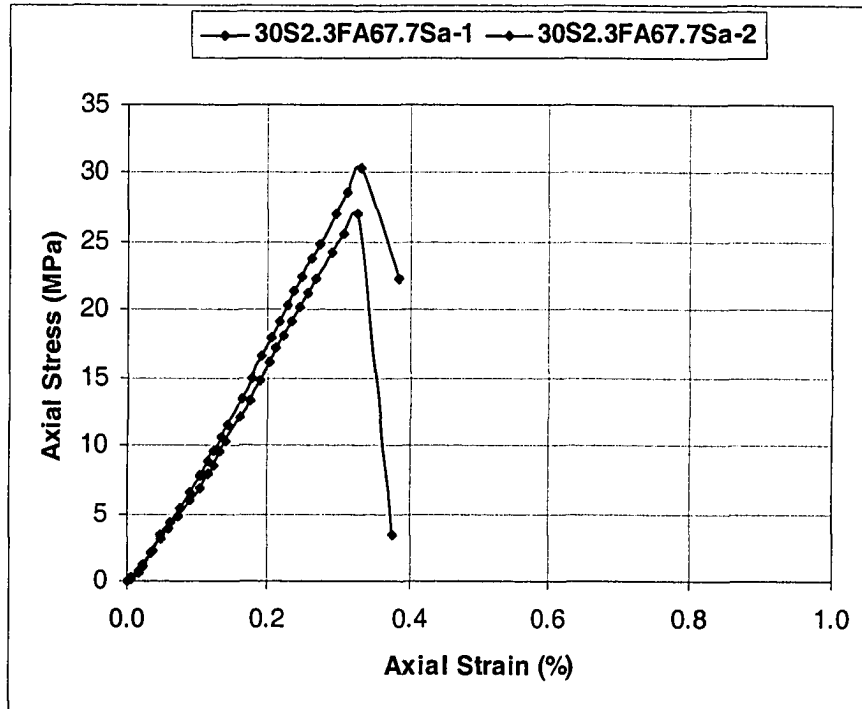


Figure A-15 Compressive stress-strain curve of original sample (0 freeze-thaw cycle)

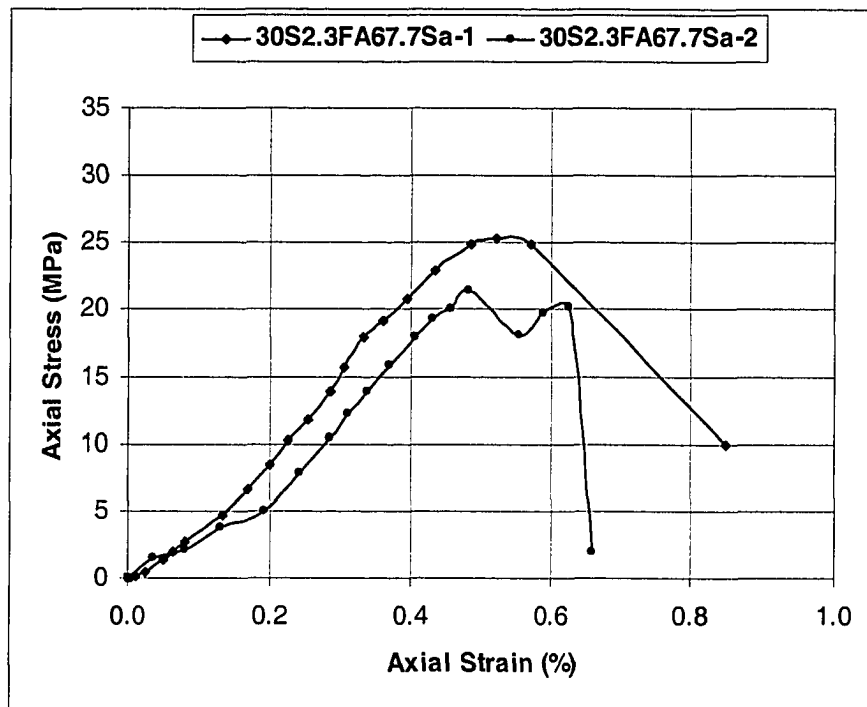


Figure A-16 Compressive stress-strain curve after 50 freeze-thaw cycles

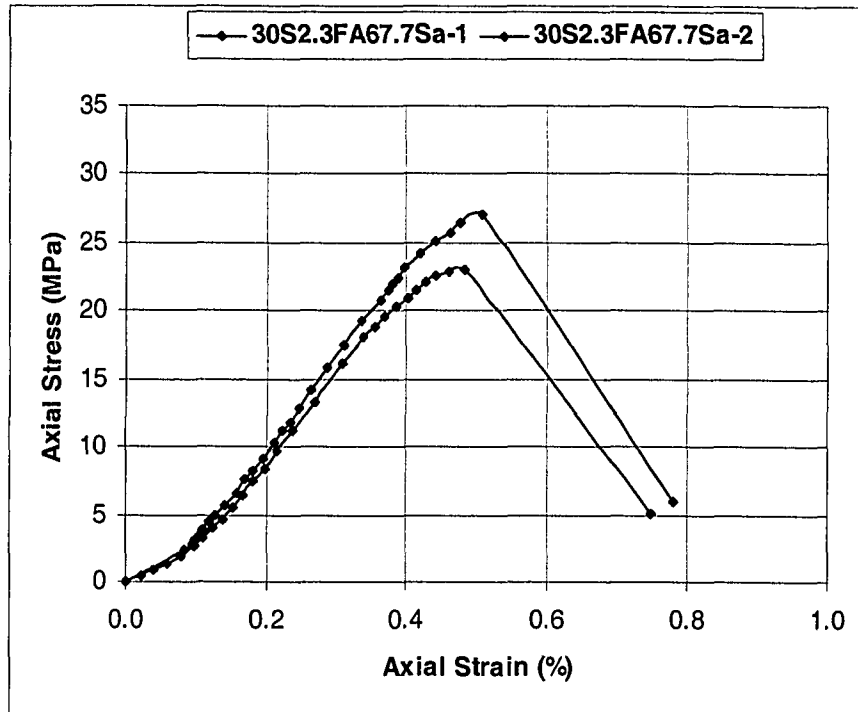


Figure A-17 Compressive stress-strain curve after 100 freeze-thaw cycles

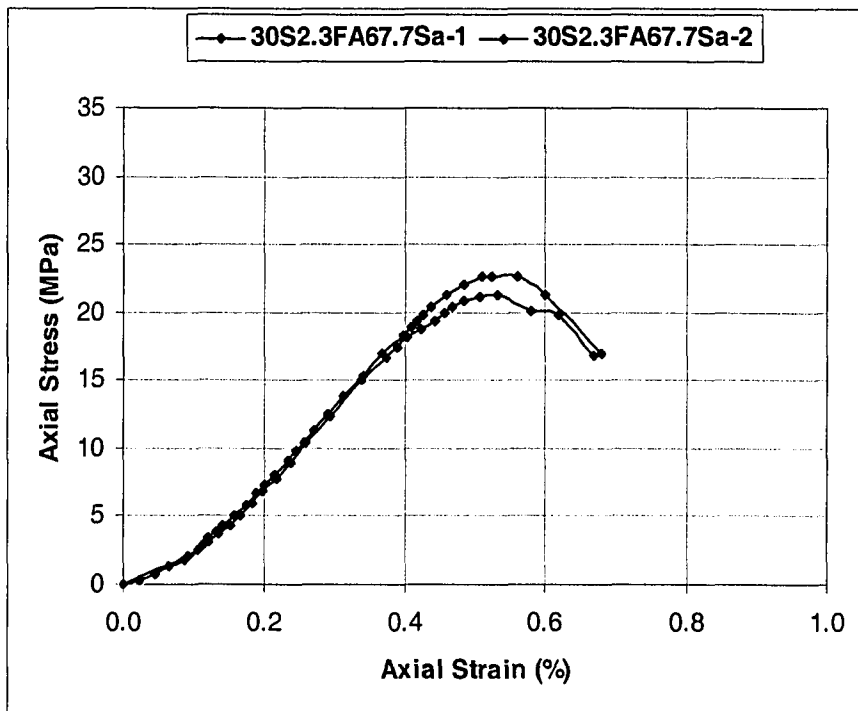


Figure A-18 Compressive stress-strain curve after 200 freeze-thaw cycles

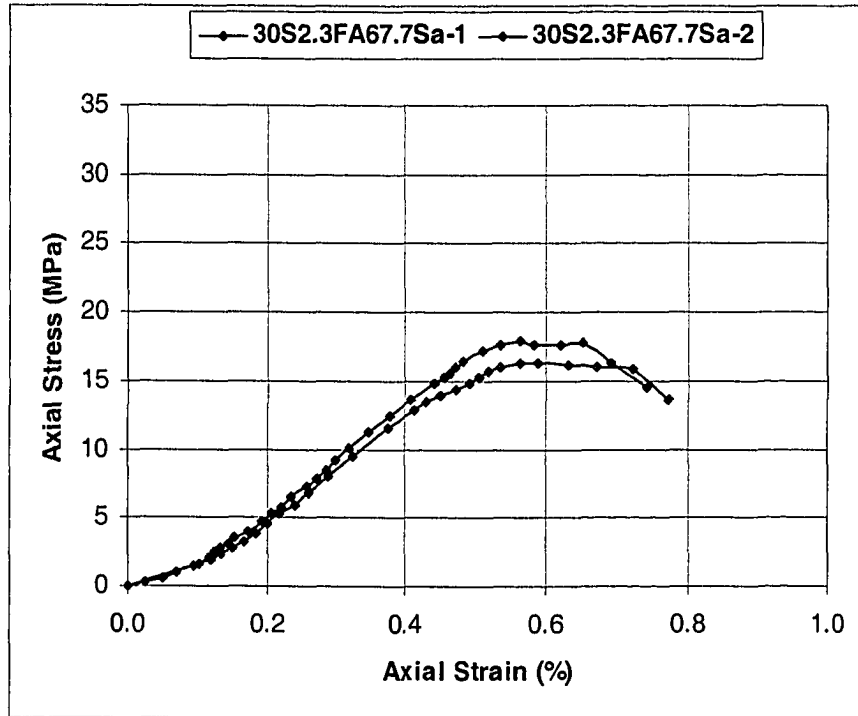


Figure A-19 Compressive stress-strain curve after 300 freeze-thaw cycles

Mix design	Coke (g)	Sulfur (g)	Fly Ash (g)	Theoretical (calculated) volume (cm ³)	Measured volume (cm ³)	Porosity (%)	Average porosity (%)
30S2.3FA67.7C - 1	762	338	26	751	908	17.28	17.53
30S2.3FA67.7C - 2	797	353	27	786	945	16.80	
30S2.3FA67.7C - 3	803	356	27	792	981	19.35	
30S2.3FA67.7C - 4	804	356	27	793	1000	20.66	
30S2.3FA67.7C - 5	802	355	27	791	927	14.67	
30S2.3FA67.7C - 6	818	363	28	807	927	12.91	
30S2.3FA67.7C - 7	793	351	27	782	1018	23.19	
30S2.3FA67.7C - 8	813	360	28	802	981	18.31	
30S2.3FA67.7C - 9	818	362	28	806	945	14.66	

35S2.3FA62.7C - 1	788	440	29	822	945	13.02	15.20
35S2.3FA62.7C - 2	812	453	30	847	981	13.73	
35S2.3FA62.7C - 3	777	434	29	811	1000	18.92	
35S2.3FA62.7C - 4	803	448	29	838	1000	16.19	
35S2.3FA62.7C - 5	799	446	29	834	963	13.43	
35S2.3FA62.7C - 6	807	450	30	842	981	14.24	
35S2.3FA62.7C - 7	824	460	30	859	1018	15.58	
35S2.3FA62.7C - 8	784	437	29	817	963	15.15	
35S2.3FA62.7C - 9	814	454	30	849	1018	16.62	

30S2.3FA67.7Sa - 1	1413	626	48	856	950	9.82	10.13
30S2.3FA67.7Sa - 2	1457	646	50	883	1002	11.85	
30S2.3FA67.7Sa - 3	1463	648	50	887	984	9.91	
30S2.3FA67.7Sa - 4	1452	644	49	880	967	8.98	
30S2.3FA67.7Sa - 5	1471	652	50	891	984	9.47	
30S2.3FA67.7Sa - 6	1472	652	50	892	993	10.19	
30S2.3FA67.7Sa - 7	1458	646	50	884	984	10.24	
30S2.3FA67.7Sa - 8	1461	647	50	885	1002	11.63	
30S2.3FA67.7Sa - 9	1451	643	49	879	967	9.05	

Table A-6 Sulfur concrete porosity calculation

APPENDIX B LABORATORY TEST PROCEDURES

B.1 Standard Test Method for Measuring Compressive Strength, Young's Modulus and Stress - Strain Curves of Cylindrical Concrete Specimens.

Scope and Summary of Test Method

The ASTM C 39 covers determination of compressive strength of cylindrical concrete specimens such as molded cylinders and drilled cores. It is limited to concrete having a unit weight in excess of 800 kg/m^3 . The test method consists of applying a compressive axial load to molded cylinders or cores at a rate which is within a prescribed range until failure occurs. The compressive strength of the specimen is calculated by dividing the maximum load attained during the test by the cross-sectional area of the specimen.

The standard indicates that care must be exercised in the interpretations of the significance of compressive strength determined by this test method since strength is not a fundamental or intrinsic property of concrete made from the given materials. The ASTM C 39 also points out that the values obtained depend on the size and shape of the specimens, the batching, the mixing procedures, and the methods of sampling, molding, and fabrication and the age, temperature, and moisture conditions during curing. But the compressive strength of sulfur concrete specimens do not vary significantly with age and the moisture condition during curing is obviously not applicable because the sulfur concrete cylinders are cured in air at room temperature (20°C) in contrast with portland cement concrete that is cured in a moisture room maintained at 100% relative humidity.

Apparatus

The testing machine shall have sufficient capacity and capable of providing the following rates of loading: for testing machines of the screw type, the moving head

shall travel at a rate of approximately 1 mm/minute when the machine is running idle. For hydraulically operated machines, the load shall be applied at a rate of movement (platen to crosshead measurement) corresponding to a loading rate on the specimen within the range of 150 to 350 kPa/s. The designated rate of movement shall be maintained at least during the latter half of the anticipated loading phase of the testing cycle. The machine must be power operated and must apply the load continuously rather than intermittently, and without shock. The calibration of the testing machine must be verified within 18 months, preferably in 12 months interval.

The accuracy of the testing machine shall be in accordance with the following provisions: the percentage of error for the loads within the proposed range of use of the testing machine shall not exceed + 1.0 % of the indicated load and the accuracy of the testing machine shall be verified by applying five test loads in four approximately equal increments in ascending order. The difference between any two successive test loads shall not exceed one third of the difference between the maximum and minimum test loads.

The testing machine shall be equipped with two steel bearing blocks with hardened faces (with Rockwell hardness of not less than 55 HRC), one of which is a spherically seated block that will bear on the upper surface of the specimen, and the other a solid block on which the specimen shall rest. Bearing faces of the blocks shall have a minimum dimension at least 3 % greater than the diameter of the specimen to be tested. Except for the concentric circles described below, the bearing faces shall not depart from a plane by more than 0.02 mm in any 150 mm of blocks 150 mm in diameter or larger, or by more than 0.02 mm the diameter of any smaller block; and new blocks shall be manufactured within one half of this tolerance. When the diameter of the bearing face of the spherically seated block exceeds the diameter of the specimen by more than 13 mm, concentric circles not more than 0.8 mm deep and not more than 1 mm wide shall be inscribed to facilitate proper centering.

Specimens

Specimens shall not be tested if any individual diameter of a cylinder differs from any other diameter of the same cylinder by more than 2 %. Neither end of compressive test specimens when tested shall depart from perpendicularity to the axis by more than 0.5° (approximately equivalent to 3 in 300 mm). The ends of compression test specimens that are not plane within 0.050 mm shall be sawed or ground to meet that tolerance, or capped in accordance with either Practice C 617 or Practice C 1231. The diameter used for calculating the cross-sectional area of the test specimen shall be determined to the nearest 0.25 mm by averaging two diameters measured at right angles to each other at about mid-height of the specimen. The length shall be measured to the nearest 0.05 D when the length to diameter ratio is less than 1.8, or more than 2.2, or when the volume of the cylinder is determined from measured dimensions.

Calculation

Compression strength is calculated by dividing the maximum load carried by the specimen to the average cross sectional area and expressing the results to the nearest 0.1MPa. The procedure for calculating the Young's modulus was adopted from Brown (1981). The axial strain is calculated from $\epsilon_a = \Delta l / l_0$, where l_0 is the original axial length and Δl is the change in measured axial length. The stress strain curve is obtained by plotting the axial strain versus the axial stress from zero up to the failure stress of the specimen.

In addition, the calculation of Young's modulus (E), or modulus of elasticity, followed Brown (1981), and is defined as the ratio of the axial stress change to the axial strain produced by the stress change. Engineering practice uses three methods to calculate the modulus. In this thesis, the average Young's modulus is adopted (E_{av}) and is

determined from the average slope of the more or less straight line portion of the axial stress- axial strain curve.

B.2 Standard Test Method for Splitting Tensile Strength of Cylindrical Concrete Specimens

Scope and Summary of Test method

The ASTM C 496 covers the determination of the splitting tensile strength of cylindrical concrete specimens, such as molded cylinders and drilled cores. The test method consists of applying a diametric compressive force along the length of a cylindrical concrete specimen at a rate that is within a prescribed range until failure occurs. This loading induces tensile stresses on the plane containing the applied load and relatively high compressive stresses in the area immediately around the applied load. Tensile failure occurs rather than compressive failure because the areas of load application are in a state in a state of tri-axial compression, thereby allowing them to withstand much higher compressive stresses than would be indicated by the uni-axial compressive strength test results.

Apparatus

The testing machine shall conform to the requirements of ASTM C 39. If the diameter of the largest dimension of the upper bearing face or the lower bearing block is less than the length of the cylinder to be tested a supplementary bearing bar or plate of machined steel shall be used. The surfaces of the bar or plate shall be machined within 0.025 mm of planeness, as measured on any line of contact of the bearing area. It shall have a width at least 51 mm, and a thickness not less than the distance from the edge of the spherical or rectangular bearing block at the end of the cylinder. The bar or plate shall be used in such manner that the load will be applied over the entire length of the specimen.

Two bearing strips of nominal size 3.2 mm thick plywood, free of imperfections, approximately 25mm wide, and of a length equal to or slightly longer than the specimen shall be provided for each specimens. The bearing strips shall be placed between the specimen and both the upper and lower bearing blocks of the testing machine or between the specimen and supplemental bars or plates if used. Bearing strips shall not be reused.

Specimens

The test specimen shall conform to the size, molding, and curing requirements set in C 192. The moisture condition during curing is obviously not applicable because the sulfur concrete cylinders are cured in air at room temperature (20⁰C) in contrast with portland cement concrete that is cured in a moisture room maintained at 100% relative humidity.

Test procedure

The proper execution of this test requires marking the specimens by drawing diametric lines on each end of the specimens by using a suitable device that will ensure that they are in the same axial plane.

The diameter of the test specimens must be obtained to the nearest 0.25 mm by averaging three diameters measured near the ends and the middle of the specimen and lying on the plane containing the lines marked on the two ends. The length of the specimen must be determined by averaging at least two measurements taken in the plane containing the lines marked on two ends.

The marked lines guide the proper positioning of the specimens in the test apparatus. Place a plywood strip along the center of the lower bearing block. Then place the

specimen on top of the strip and align so that the lines marked on the ends of the specimen are vertical and centered over the plywood strip. Place a second plywood strip lengthwise on the cylinder, centered on the lines marked on the ends of the cylinder. The positioning must ensure that the projection of the plane of the two lines marked on the ends of the specimen intersects the center of the upper bearing plate.

Apply the load continuously and without shock, at a constant rate within the range 689 to 1380 kPa/min splitting tensile stress until the specimen fails. Record the maximum applied load indicated by the testing machine at failure. The splitting tensile strength (T) is calculated as $T = 2P / \pi ld$, where T is splitting tensile strength in kPa, P is the maximum applied load in KN, l is the specimen length in meter, and d is the specimen's diameter in meter.

B.3 Standard Test Method for Resistance of Concrete to Rapid Freezing and Thawing

Scope and Summary of Test Method

The ASTM C 666 covers the determination of the resistance of concrete specimens to rapidly repeated cycles of freezing and thawing in the laboratory by two different procedures: Procedure A, rapid Freezing and Thawing in Water, and Procedure B, Rapid Freezing in Air and Thawing in Water. Both procedures are intended for use in determining the effects of variations in the properties of concrete on the resistance of the concrete to the freezing and thawing cycles specified in the particular procedure. Neither procedure is intended to provide a quantitative measure of the length of service that may be expected from a specific type of concrete.

It is assumed that the procedures will have no significantly damaging effects on frost resistant concrete which may be defined as 1) any concrete not critically saturated with water (that is, not sufficiently saturated to be damaged by freezing) and 2) concrete

made with frost resistant aggregates and having an adequate air void system that has achieved appropriate maturity and thus will prevent critical saturation by water under common conditions. No relationship has been established between the resistance to cycles of freezing and thawing of specimens cut from hardened concrete and specimens prepared in the laboratory.

Apparatus

The freezing and thawing apparatus shall consist of a suitable chamber or chambers in which the specimens may be subjected to the specified freezing and thawing cycle. The apparatus must be capable of producing continuously and automatically reproducible cycles within the specified temperature requirements. In the event that the equipment doesn't operate automatically, provisions shall be made for either its continuous manual operation on a 24 hour basis or for the storage of all specimens in a frozen condition when the equipment is not in operation.

Procedure A requires that the specimens shall be surrounded by not less than 1 mm nor more than 3 mm of water at all times while it is being subjected to freezing and thawing cycles. Also the bottom of the specimen should not be in direct contact with the bottom of the container in order to avoid substantially different conditions from the remainder areas of the sample. A flat spiral of 3 mm wire placed in the bottom of the container has been found adequate for supporting specimen. Rigid containers which have a potential to damage specimens are not permitted for use.

The temperature measuring equipment consists of thermometers, resistance thermometers, or thermocouples capable of measuring the temperature at various points within the specimen chamber and at the center of the specimen to within 1.1 °C.

Freezing and Thawing Cycle

Base conformity with the requirements for the freezing and thawing cycle on temperature measurements of control specimens of similar concrete to the specimens under test in which suitable temperature measuring devices have been imbedded. Change the position of these control specimens frequently in such a way as to indicate the extremes of temperature variation at different locations in the specimen cabinet.

The nominal freezing and thawing cycle for both procedures shall consist of alternately lowering the temperature of the specimens from 4.4 to -17.8 °C and raising it from -17.8 to 4.4 °C in not less than 2 nor more than 5 hours. Procedure A requires not less than 25% of the time shall be used for thawing. at the end of the cooling period the temperature at the center of the specimens shall be -17.8 ± 1.7 °C and at the end of the heating period the temperature shall be 4.4 ± 1.7 °C with no specimen at any time reaching a temperature lower than -19.4 °C nor higher than 6.1 °C. the time required for the temperature at the center of any single specimen to be reduced from 2.8 to -16.1 °C shall be not less than one half of the length of the cooling period, and the time required for the temperature at the center of any single specimen to be raised from -16.1 to 2.8 °C shall be not less than one half of the length of the heating period. The difference between the temperature at the center of the specimen and the temperature at its surface shall at no time exceed 27.8 °C. The period of transition between the freezing and thawing phases of the cycle shall not exceed 10 minute.

Test Procedure

Freezing and thawing tests should be started by placing the specimens in the thawing water at the beginning of the thawing phase of the cycle. Specimens should be removed from the apparatus, in a thawed condition, at intervals not exceeding 36 cycles of exposure to the freezing and thawing cycles for testing the fundamental transverse frequency. The specimens should be returned to the freeze thaw apparatus

either to random positions or according to some predetermined rotation scheme to ensure that all specimens are subjected to the conditions at all parts of the freezing apparatus. The test should continue until the samples have been subjected to 300 freeze thaw cycles or until their relative dynamic modulus of elasticity deteriorates to 60% of the initial modulus. When it is anticipated that the specimens may deteriorate rapidly, they should be tested for fundamental transverse frequency at intervals not exceeding 10 cycles when initially subjected to the freeze thaw cycles.